

Copyright

by

Douglas Karl Pudleiner

2016

**The Thesis Committee for Douglas Karl Pudleiner
Certifies that this is the approved version of the following thesis:**

**Design Considerations Based on Size Effects of Anchored Carbon Fiber
Reinforced Polymer (CFRP) Systems**

**APPROVED BY
SUPERVISING COMMITTEE:**

Supervisor:

Wassim Ghannoum

James O. Jirsa

**Design Considerations Based on Size Effects of Anchored Carbon Fiber
Reinforced Polymer (CFRP) Systems**

by

Douglas Karl Pudleiner, B.S.C.E

Thesis

Presented to the Faculty of the Graduate School of

The University of Texas at Austin

in Partial Fulfillment

of the Requirements

for the Degree of

Master of Science in Engineering

The University of Texas at Austin

May 2016

Dedication

To my fiancé and family, for all of their love and support throughout my education.

They all continue to play instrumental parts in my life and without them this would not
have been possible.

Acknowledgements

I would first like to thank God for all his blessing and provision. It is for Him that we exist.

To my family, you have raised me to be the person I am today. Your continual support and ever pushing me to be my best is one of the reasons I have completed this thesis.

To my fiancé, who decided to move half way across the country with me and has always been there with me throughout this process. I look forward to spending a lifetime with you and continuing to help each other strive to be better.

To my supervising professors, Dr. Wassim Ghannoum and Dr. James Jirsa. I have learned a great deal from both of you and much appreciate all of you guidance.

I would like to acknowledge the members of my project team, Nawaf Alotaibi, Changhyuk Kim, and especially William Shekarchi for teaching and training me in the ways of Ferguson Structural Engineering Laboratory (FSEL). All of you help along the way has been a blessing.

The countless other students who are too many to name and have both helped me numerous times as well as made FSEL an enjoyable place to work. In particular Alex Katz and Jessica Salazar for their friendship

The assistance and technical support from both lab technicians and administrative staff including Blake Stasney, David Braley, Dennis Phillip, Deanna Mueller, Michelle Damvar, John Bacon, and Joel Arredondo is greatly appreciated.

Last but not least, I would like to express my gratitude towards TX-DOT who graciously funded the research and allowed me the opportunity to complete this thesis.

Abstract

Design Considerations Based on Size Effects of Anchored Carbon Fiber Reinforced Polymer (CFRP) Systems

Douglas Karl Pudleiner, M.S.E

The University of Texas at Austin, 2016

Supervisor: Wassim Ghannoum

Due to their high strength, limited architectural impact, and speed of installation, externally applied carbon fiber reinforced polymer (CFRP) materials are gaining use in infrastructure rehabilitation. To be effective, CFRP materials must be adequately anchored to develop their full capacity. Many anchorage materials and systems have been proposed for CFRP strips and laminates. CFRP spike anchors can develop the full tensile strength of CFRP strips and offer several advantages over other anchorage methods. Namely, they are easy to install, flexible, which allows them to overcome geometric complications, and resilient to environmental and corrosive factors.

However, only a limited number of studies have been conducted on CFRP strips anchored using CFRP anchors. These studies identified clear size effects that influence the strength of CFRP anchors and strips. However, past research was conducted on relatively small anchor and strip systems that are on the low end of practical sizes for infrastructure retrofit and repair applications.

The objectives of this study were to investigate size effects in anchored CFRP systems and provide design guidelines for CFRP anchors. Twelve tests were conducted on

concrete beams reinforced in flexure with anchored CFRP strips up to 10-in. wide. The primary parameters investigated were: width of CFRP strip, number of layers of fabric in CFRP strips, number of anchors per strip width, ratio of anchor to strip cross-sections, anchor fan overlap length, and chamfer radius of the anchor hole. The full distribution of strains at the surface of the anchored CFRP strips was monitored using an optical measurement system. These measurements helped evaluate the effectiveness of various anchor details in distributing strains across strips.

The experimental program confirmed the size effects uncovered in previous studies. CFRP anchors were able to fracture CFRP strips at stresses above the expected and design stresses provided by the manufacturer. However, the larger the CFRP strip area developed per anchor, the lower the stress at fracture of that strip. In addition, the anchor-hole chamfer radius was found to influence both anchor strength and the strain distribution in CFRP strips. Guidelines for designing and detailing CFRP anchors are given based on experimental results.

Table of Contents

List of Tables	xii
List of Figures.....	xiii
Chapter 1: Introduction	1
1.1 Motivation.....	1
1.2 Objectives and Scope	2
1.3 Organization.....	2
Chapter 2: Background Information	4
2.1 FRP Materials	4
2.2 FRP in retrofit and strengthening.....	5
2.3 Past studies on FRP anchorage systems.....	8
2.3.1 Overview	8
2.3.2 Deformable Anchorage	8
2.3.3 U-jackets with Full-Depth Threaded Anchor Rods	10
2.3.4 CFRP Anchor Bolts	10
2.3.5 U-Anchors.....	12
2.3.6 CFRP Rope	13
2.4 Spike Fiber Reinforced Anchors.....	14
2.4.1 Overview	14

2.4.2 Anchor Hole Details	16
2.4.3 Geometry of Anchor Fan	22
2.4.4 Width of Strip per Anchor (Anchor Tributary Width).....	24
2.4.5 Anchor Material Ratio	25
2.4.6 FRP Patch Details	25
2.5 Size Effects in CFRP Strips and Anchors.....	27
2.5.1 Size Effects on Anchor Strength.....	27
2.5.2 Size Effects on Strip Strength	27
Chapter 3: Experimental Program	29
3.1 Overview of Experimental Program	29
3.2 Specimen Design, Details, and Construction.....	31
3.2.1 Construction.....	34
3.3 Typical Specimen Preparation and Strengthening.....	38
3.3.1 Specimen Preparation	38
3.3.2 Preparation of CFRP Anchors	40
3.3.3 Installation of CFRP Strips and Anchors.....	42
3.4 Material properties	47
3.4.1 CFRP	47
3.4.2 Concrete	48
3.5 Test Matrix Details	48

3.5.1 Primary Test Parameters	48
3.5.2 Other Test Parameters.....	52
3.5.3 Test Matrix and Specimen Nomenclature.....	54
3.6 Data Collection and Processing	56
3.6.1 Instrumentation	56
3.6.2 Data Processing.....	59
Chapter 4: Test Results	64
4.1 Typical Test	64
4.2 Failure Modes and Implications.....	67
4.3 Test Results.....	71
4.3.1 Effects of the Anchor Fan Overlap Length.....	72
4.3.2 Effects of the Chamfer Radius of Anchor Hole.....	74
4.3.3 Effects of CFRP Strip Thickness or Number of Fabric Layers ..	77
4.3.4 Effects of Strip Width and Anchor Tributary Width	78
4.3.5 Effects of the Anchor Material Ratio (AMR)	83
4.4 Size Effect Relations.....	85
Chapter 5: Design of Anchored Carbon Fiber Reinforced Polymer (CFRP)	
Systems.....	89
5.1 Design Approach	89
5.2 Design Guidelines.....	91

5.2.1 Notations and Definitions	91
5.2.2 Sizing CFRP Anchors	93
5.2.3 Anchor Fan Details	96
5.2.4 Anchor Hole Details	97
5.2.5 Anchor Patch Geometry.....	99
5.3 Design Example	99
Chapter 6: Summary and Conclusions	104
6.1 Summary	104
6.2 Conclusions.....	105
6.3 Future Work	106
References	108
Vita	115

List of Tables

Table 2-1: Typical tensile properties of fibers used in FRP systems (ACI 440.2R)	4
Table 2-2: Tensile properties of FRP laminates with fiber volumes of 40 to 60% (ACI 440.2R).....	4
Table 3-1: Fiber material properties	47
Table 3-2: Epoxy material properties	48
Table 3-3: Test parameters.....	55
Table 4-1: Summary of strength performance measures	72
Table 4-2: Effects of the number of strip layers on the ultimate stress in 5-in.wide strips	77
Table 4-3: Effect of strip width.....	78
Table 4-4: Strip strain comparisons with respect to anchor tributary width.....	83
Table 4-5: Strip strain comparisons with respect to AMR	85

List of Figures

Figure 2-1: Typical material properties of grade 60 steel and CFRP	5
Figure 2-2: Anchoring GFRP against CMU wall (adapted from Hall et al., 2002).9	
Figure 2-3: Detailed drawing of anchorage system (Hall et al., 2002).....9	
Figure 2-4: Types of U-jackets (adapted from Deifalla and Ghobarah, 2006).....10	
Figure 2-5: Details of DMA and SDMA systems (adapted from Ortega et al., 2009)	11
Figure 2-6: Cut-away section of U-Anchor installed at web flange junction (Khalifa et al., 1999)	12
Figure 2-7: Drawing of U-Anchor (Khalifa et al., 1999).....	12
Figure 2-8: CFRP rope test specimens (El-Saikaly et al., 2015)	14
Figure 2-9: FRP anchor parameters	16
Figure 2-10: Test Setup for direct pullout tests (Akyuz and Ozdemir, 2004)	18
Figure 2-11: Inclined anchor pull-out (Ozbakkaloglu and Saatcioglu, 2009).	19
Figure 2-12: Stress distributions around the anchor bend	19
Figure 2-13: Anchor fan details (Kobayashi et al., 2001).....	23
Figure 2-14: Anchor fan stresses (Kobayashi et al., 2001).....	24
Figure 2-15: Bi-directional CFRP patches.....	26
Figure 3-1: Large beam specimens before CFRP installation	29
Figure 3-2: CFRP system loading in a three point load beam test.....	30
Figure 3-3: CFRP system loading in a shear strengthened concrete beam with inclined cracking.....	30
Figure 3-4: Detailed drawings of concrete specimen	31
Figure 3-5: Detailed drawings of concrete specimen with CFRP.....	32
Figure 3-6: Beam Specimen Failure	33

Figure 3-7: Typical steel reinforcing cage	33
Figure 3-8: Diagram of forces and reinforcing bar layout	34
Figure 3-9: Ensuring formwork is square	35
Figure 3-10: Assembling formwork.....	35
Figure 3-11: Completed formwork	36
Figure 3-12: Casting concrete	37
Figure 3-13: Internal vibration.....	37
Figure 3-14: Specimen preparation before CFRP installation (continued)	39
Figure 3-15: Typical prepared specimen	40
Figure 3-16: Premanufactured anchor	41
Figure 3-17: Pulling fibers apart from mat	41
Figure 3-18: Finished CFRP anchor bundle	42
Figure 3-19: Prepared CFRP material.....	42
Figure 3-20: Proportioning and mixing the epoxy components	43
Figure 3-21: Saturating anchor holes and surfaces	43
Figure 3-22: Saturating anchors, patches, and strips	43
Figure 3-23: Applying CFRP strips on the tension face and sides of the beam	44
Figure 3-24: Fanning out the anchor.....	45
Figure 3-25: Applying patches (first one perpendicular to strip and second one parallel to strip).....	45
Figure 3-26: Finished specimens with CFRP installed.....	46
Figure 3-27: Alternative anchor layouts	47
Figure 3-28: Anchor made from longitudinal strip.....	52
Figure 3-29: Specimen nomenclature	54
Figure 3-30: Test setup	56

Figure 3-31: Specimen with targets	57
Figure 3-32: Setup of optical measurement system	58
Figure 3-33: Statics of beam specimen	60
Figure 3-34: Beam Equilibrium (adapted from Sun, 2014)	61
Figure 3-35: LVDT locations on the underside of the beams	61
Figure 3-36: Load deflection plots illustrating total and net deflection at mid-span	62
Figure 3-37: Contour plot of strain in the longitudinal x-direction	63
Figure 3-38: Elements used to determine average strain and max strain	63
Figure 4-1: Loading diagram	64
Figure 4-2: Test setup	64
Figure 4-3: Load-deflection response for specimen D-10-2-L-6 illustrating a typical test response	65
Figure 4-4: Longitudinal strain contours (ϵ_x) on the surface of the anchored CFRP strip for specimen D-10-2-L-12	66
Figure 4-5: Load vs deflection of nominally identical test specimens (Sun 2014)	67
Figure 4-6: Failure modes, (continued)	70
Figure 4-7: Failures modes versus strength of test specimens	71
Figure 4-8: Experimental bond stress between CFRP anchors and strip at ultimate load	73
Figure 4-9: Location of strain gauges	75
Figure 4-10: Comparison of strains for different chamfer radii for specimens D-10-1- M-12 and D-10-1-M-12-c	75
Figure 4-11: Strains across a 10" strip with a small anchor-hole chamfer radius (Specimen D-10-2-M-12-c)	76

Figure 4-12: Strains across 10" strip with large chamfer radius (Specimen D-10-2-M-12)	76
Figure 4-13: Strains for a 10-in. wide strip with one anchor from strain gauges (Specimen D-10-1-L-12)	79
Figure 4-14: Strains for a 10-in. wide strip with two anchors from strain gauges (Specimen D-10-2-L-12)	79
Figure 4-15: Strain rows used in analysis	80
Figure 4-16: Longitudinal strain distributions across strip width for specimens D-5-1-L-12, D-10-1-L-12, and D-10-2-L-12	82
Figure 4-17: Longitudinal strain distributions across strip width at an applied load of 40 and 46 kips	84
Figure 4-18: Strip fracture stress versus the normalized strip area parameter (α_s)	86
Figure 4-19: Strip fracture stress versus the normalized strip area parameter (α_s) including data from Sun et al. (2016)	88
Figure 5-1: Plan view of anchor system; left: anchor prior to adding patches, right: patches over anchor	89
Figure 5-2: Isometric view of anchor system	90
Figure 5-3: Anchor fan details	96
Figure 5-4: Anchor hole details	97
Figure 5-5: Example layout	103

Chapter 1: Introduction

1.1 MOTIVATION

As our infrastructure ages and loadings continue to increase, the structural engineering community needs retrofit and strengthening techniques that are cost-effective and can be applied with minimal disruption to the use of the existing structures. Carbon fiber reinforced polymer (CFRP) materials are increasingly being used as externally bonded reinforcement to retrofit or strengthen existing structures. One of the major benefits of CFRP materials is their versatility. They can be used for flexural and shear strengthening, as well as axial confinement. Qualities of CFRP materials, such as resistance to corrosion, a high strength to weight ratio, and ease of application are increasing their popularity in strengthening applications. The external applications of CFRP materials can also be accomplished with relatively little architectural impact and disruption to the users of a structure.

To be effective in strengthening concrete structures, however, CFRP materials must be adequately anchored to develop their full capacity. CFRP materials are typically bonded to the concrete surface through the epoxy resin forming the laminate system. If not anchored, CFRP laminates debond from the concrete substrate typically prior to reaching 50% of the CFRP tensile strength. The limiting factor in the debonding process is the low tensile strength of the concrete which fails and initiates debonding. In applications where concrete members cannot be fully wrapped with CFRP materials, some type of anchorage is recommended to prevent a debonding failure, and to fully develop the tensile strength of the CFRP materials.

Many anchorage materials and systems have been proposed to anchor CFRP strips and laminates to concrete members. CFRP spike anchors installed in pre-drilled holes and

fanned over CFRP strips have been proven effective in developing the full tensile strength of the strips. CFRP anchors are flexible, which allows them to overcome numerous geometric complications. In addition, such anchors require low maintenance as they are made from CFRP materials that are resilient to environmental and corrosive factors.

Only a limited number of studies have been conducted to investigate the behavior of CFRP strips anchored using CFRP anchors. These studies identified clear size effects that influence the strength of the anchors and strips. However, past research was conducted on relatively small anchor and strip systems that are on the low end of practical sizes for use in infrastructure retrofit and repair applications.

1.2 OBJECTIVES AND SCOPE

The behavior and strength of CFRP strips anchored using CFRP anchors is investigated experimentally in this study. Twelve tests were conducted on 12-in. x 12-in. x 68-in. concrete beams that were strengthened in flexure using anchored CFRP strips up to 10-in. wide. The main objective of this study was to explore and quantify size effects that govern CFRP anchor and strip strength. Design guidelines for achieving CFRP anchors capable of developing CFRP strips are proposed as well. This study is part of a larger project, in which shear strengthening of various reinforced bridge members was investigated (Jirsa et al., 2016).

1.3 ORGANIZATION

This thesis is organized as follows:

- Background material is presented in Chapter 2, where the history of CFRP as a repair and rehabilitation material is presented, with emphasis on anchorage developments. In the background material, CFRP spike anchors

and the important parameters that govern their design are discussed. Gaps in knowledge for CFRP anchors are highlighted.

- In chapter 3, the test program including specimen design, material properties, test matrix, and instrumentation are detailed.
- Test results are presented in Chapter 4, with emphasis on size effects. The influence of size effects on anchor performance are presented at the end of Chapter 4.
- Based on the results from this study as well as prior studies, which are presented in the background chapter, CFRP spike anchor design guidelines are presented in Chapter 5.
- Summary and conclusions are presented in Chapter 6.

Chapter 2: Background Information

2.1 FRP MATERIALS

Fiber Reinforced polymers (FRP) are used in a variety of industries, but have become increasingly used as externally bonded reinforcement in concrete structures. FRP is a composite material made up of fibers that carry the load and a polymer resin that binds them together. There are three primary types of fibers used in FRP composites: Carbon, Glass, and Aramid. Table 2-1 and Table 2-2 show typical tensile properties for each FRP material.

Table 2-1: Typical tensile properties of fibers used in FRP systems (ACI 440.2R)

Fiber type	Elastic modulus (ksi)	Ultimate Strength (ksi)	Rupture strain minimum (%)
Carbon (high-strength)	32,000 - 34,000	550 - 700	1.4
Glass (E-glass)	10,000 – 10,500	270 - 390	4.5
Aramid (High-performance)	16,000 – 18,000	500 - 600	1.6

Table 2-2: Tensile properties of FRP laminates with fiber volumes of 40 to 60% (ACI 440.2R)

FRP system	Young's modulus (ksi)	Ultimate Strength (ksi)	Rupture strain (%)
Carbon (high-strength)	15,000 - 21,000	150 - 350	1.0 – 1.5
Glass (E-glass)	3,000 – 6,000	75 – 200	1.5 – 3.0
Aramid (High-performance)	7,000 – 10,000	100 - 250	2.0 – 3.0

The individual FRP fibers have tensile properties that are greater than those of the laminates. However, the laminate system is needed to protect the fibers, distribute the stresses between fibers, and bond the fibers to the concrete substrate. Out of the three types, carbon fiber is most widely used for strengthening. It is considered the most durable, an

important consideration for external applications. As indicated in ACI 440.2R (2008), carbon fiber has the highest environmental reduction factor (closest to 1), meaning it has the smallest strength reduction due to environmental conditions. It also has the largest elastic modulus and ultimate strength.

CFRP has a lower elastic modulus than steel, but is brittle with a linear stress-strain relation up to fracture (Figure 2-1). Steel, on the other hand, is a ductile material. The difference in stiffness and ductility between the two materials creates complex interactions, which add complexity to analyzing a CFRP strengthening system applied to a reinforced concrete section.

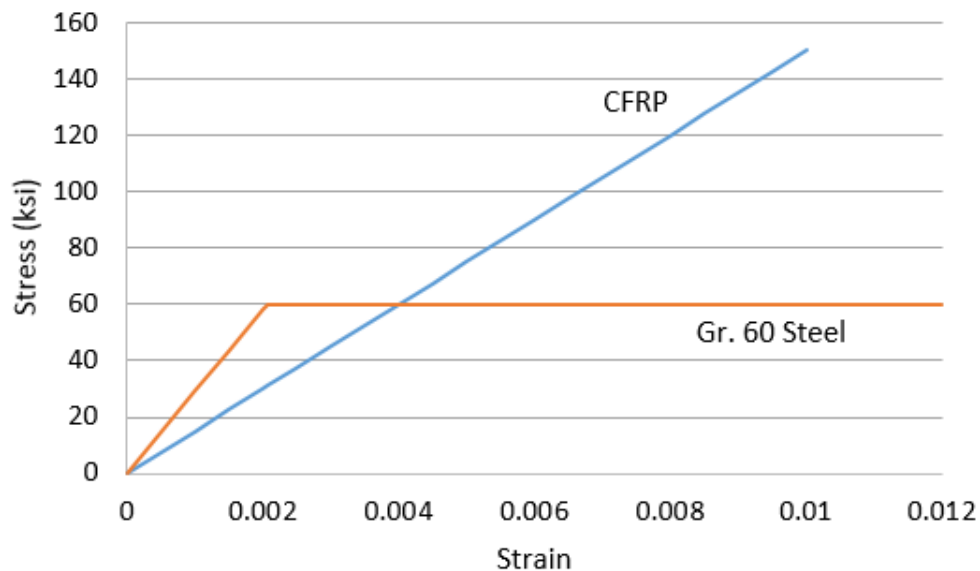


Figure 2-1: Typical material properties of grade 60 steel and CFRP

2.2 FRP IN RETROFIT AND STRENGTHENING

As our infrastructure ages and loading on it continues to increase, the structural engineering community needs retrofit and strengthening techniques that are cost-effective and can be applied with minimal disruption to use of the existing structures. FRP materials

are increasingly being used as externally bonded reinforcement to retrofit or strengthen existing structures. One of the major benefits of CFRP materials is their versatility. They can be used for flexural and shear strengthening, as well as axial confinement (Khalifa et al., 1999; Kim, 2011; Kobayashi et al., 2001; Kim and Smith, 2009; Neimitz, 2008; Ortega et al., 2009; Triantafillou and Antonopoulos, 2000). Qualities of CFRP materials, such as resistance to corrosion, a high strength to weight ratio, and ease of application are increasing their popularity in strengthening applications. The external applications of CFRP materials can also be accomplished with relatively little architectural impact and disruption to the users of a structure. In fact, strengthening of bridge sections using externally applied CFRP can be accomplished in as little as one night (Garcia et al., 2014).

To be effective in strengthening concrete structures, however, CFRP materials must be adequately anchored to develop their full capacity. CFRP materials are typically bonded to the concrete surface through the epoxy resin forming the laminate system. If not anchored, CFRP laminates debond from the concrete substrate typically prior to reaching 50% of the CFRP tensile strength. The limiting factor in the debonding process is the low tensile strength of the concrete, which fails and initiates debonding (Ceroni et al., 2008). Currently, ACI 440.2R (2008) states that the effective strain of FRP laminates should not exceed 0.004 in any case. This is a reduction of over 50% in capacity for most FRP materials. For shear applications in which concrete members are not fully wrapped with FRP materials, some type of anchorage is recommended in ACI 440.2R to prevent failure due to debonding, but little guidance is given as to the means for anchoring.

Khalifa et al. (1999) demonstrated the need for anchorage through concrete beam tests strengthened in shear with U-wrapped CFRP strips. When beams cracked beneath an unanchored CFRP strip, depending on the location of the crack from the strip end, the strip could suddenly debond. This situation is even more critical when a beam is in reverse

curvature because cracks will form from the top of the beam (Khalifa et al., 1999). However, when U-anchors were installed, the location of the cracks became immaterial, and the CFRP strips were utilized to their full strength. U-anchors are further discussed in section 2.3.5.

Teng et al. (2003) further explain this mechanism of localized debonding at a crack. Intermediate crack debonding occurs when a crack is formed in the concrete under the FRP strip. The stress the crack releases is transferred into the FRP strip, which therefore creates a localization of stresses. As the stress in the FRP continue to grow, the subsequent bond stress also increase. This stress increases until debonding is initiated. As the crack continues to grow, the debonding propagates towards the end of the strip (Teng et al., 2003). If anchorage is present, the strip transfers stress to the anchors and debonding failure is prevented. However if anchorage is not present, the debonding will propagate over the entire strip until it is completely debonded and failure ensues.

Anchorage plays a primary role as the mechanism for transferring forces from the strips to the concrete member (Grelle and Sneed, 2013). Whenever a crack forms in the concrete below a FRP strip, debonding will take place around the crack and continue to propagate towards the end of the strip until it is arrested (Teng et al., 2003; Kim et al., 2015; Kim et al., 2014; Kim et al., 2012). Ortega et al. (2009) noted that while localized debonding still occurred, the final failure mode was FRP rupture. The FRP may still debond but at some point the anchors will engage and allow for higher strains in the CFRP strip to be reached. This permits for the full strength of the strip or the anchor to be developed, which is critical to increasing the efficiency of FRP materials in strengthening applications.

2.3 PAST STUDIES ON FRP ANCHORAGE SYSTEMS

2.3.1 Overview

Many anchorage materials and systems have been proposed to anchor FRP strips and laminates to concrete members and prevent strip-debonding as a failure mode. Anchorage systems can be categorized through two characteristics. The first is the load transfer mechanism (mechanical interlock, friction, or chemical bond), the second is the anchor installation method (cast in place or post installed) (Kim and Smith, 2009). In strengthening applications, most anchors are post installed by drilling. The following is an overview of various drilled-in anchorage systems, as these relate more closely to this study where spiked CFRP anchors were placed in relatively shallow drilled holes.

2.3.2 Deformable Anchorage

Hall et al. (2002) studied GFRP strips anchored at the base of a Concrete Masonry Unit (CMU) wall using various types of structural steel plates and angles (Figure 2-2). Because of the brittle nature of FRP laminates, the authors attempted to create an anchorage system that would introduce some ductility into the system. A single CMU block was placed on a 3/8in. mortar joint over a concrete footing. A GFRP strip with unidirectionally oriented fibers was then applied and the anchors were installed. In early specimens, it was found that the structural steel angles caused high stress concentrations at the sharp exterior corner (Hall et al., 2002). This was remedied by using a rounded steel angle in addition to a structural steel plate (Figure 2-3).

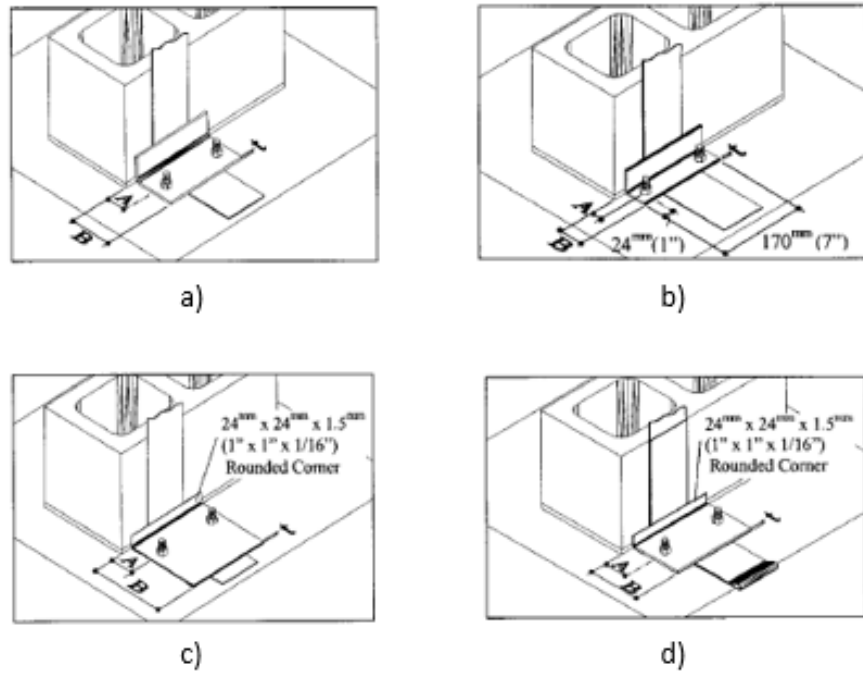


Figure 2-2: Anchoring GFRP against CMU wall (adapted from Hall et al., 2002)

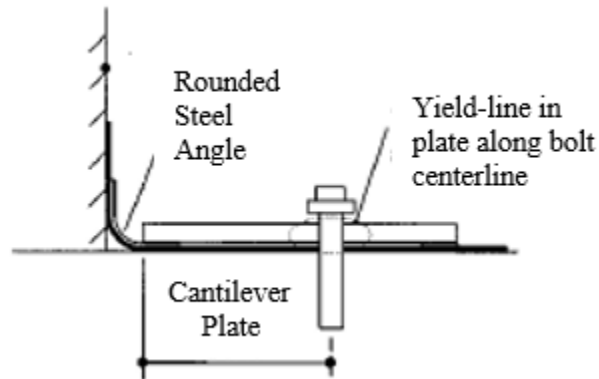


Figure 2-3: Detailed drawing of anchorage system (Hall et al., 2002)

After some iterations, the design of the connection increased in both strength and deformability. However, the anchoring method was never able to develop more than half the tensile strength of the GFRP strips. The authors postulated that as the radius of the rounded angle increases, the efficiency of the connection will approach 100% with respect to developing the full strength of the strips. However, as is common with steel anchorage systems, that may not be possible due to inevitable stress concentrations at the connection

between steel and FRP. Another disadvantage of steel-based systems is that exposed steel will corrode over time, which will offset the benefit of FRP materials as environmentally resilient, particularly CFRP.

2.3.3 U-jackets with Full-Depth Threaded Anchor Rods

Deifalla and Ghobarah (2006) developed a method of anchorage where threaded rods are inserted in a concrete section and used to clamp CFRP strips. This method requires holes to be drilled through a beam or slab section (Figure 2-4). However, in all cases the reported mode of failure was “FRP intermediate debonding,” which unloaded the CFRP strips. Because this method requires drilling through the web or flange of beams, it is time consuming and limited to cases where the top flange is accessible and will not be impacted by protruding steel hardware. Similarly to the deformable anchorage system, galvanic corrosion due to steel-carbon fiber contact can once again be problematic for durability (Khalifa et al., 1999).

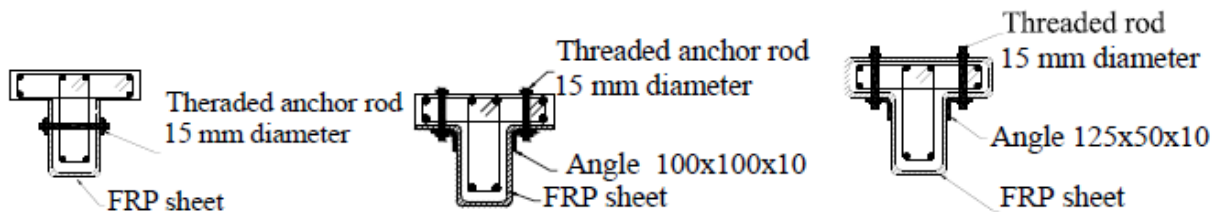


Figure 2-4: Types of U-jackets (adapted from Deifalla and Ghobarah, 2006)

2.3.4 CFRP Anchor Bolts

Ortega et al. (2009) proposed a FRP anchorage system comprised of wedge anchors, steel anchor bolts, and FRP plates (Figure 2-5). This method, termed the Discontinuous Mechanical Anchorage (DMA), relies primarily on friction to keep FRP strips from debonding. Experimental testing, however, indicated that this method could

not provide sufficient anchorage (Ortega et al., 2009). The FRP strips slipped at the sheet-plate interface and resulted in the strips debonding prior to developing their ultimate strength.

A second system was developed by Ortega et al. (2009) to remedy issues with the DMA system. The Sandwich Panel Mechanical Anchorage (SDMA) is similar to the DMA system, but utilized two FRP plates to sandwich the FRP strip being developed. The two systems are compared in (Figure 2-5).

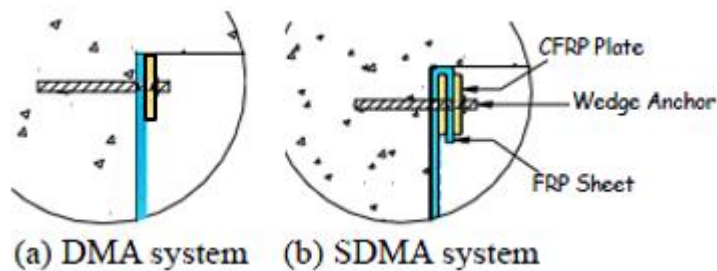


Figure 2-5: Details of DMA and SDMA systems (adapted from Ortega et al., 2009)

The SDMA system performed as desired and ruptured the FRP strips. While there is more work involved in the installation of the SDMA system, it allowed for the development of higher FRP strip stresses. Shear strength gain was used as the criteria to evaluate each system's effectiveness. The average normalized results provided a shear strength increase of 39% with no anchors, 65% with the DMA system, and 73% with the SDMA system. These increases are with respect to the control specimen, which had no CFRP. While the SDMA method did result in fracture of the strips, it is a time-consuming and difficult installation process. As before, the use of steel may cause corrosion and durability issues.

2.3.5 U-Anchors

Khalifa et al. (1999) developed a U-anchor system that only uses FRP materials. For this anchorage system, a groove is cut into the concrete near the end of the FRP sheet wherever anchorage is desired. The FRP sheet is saturated and placed in the groove and allowed to set. Then an epoxy paste is pressed into the groove. Finally an FRP reinforcing bar is pressed into the paste, and the paste is smoothed out to match the existing concrete surface. Figure 2-6 and Figure 2-7 show the finished product.

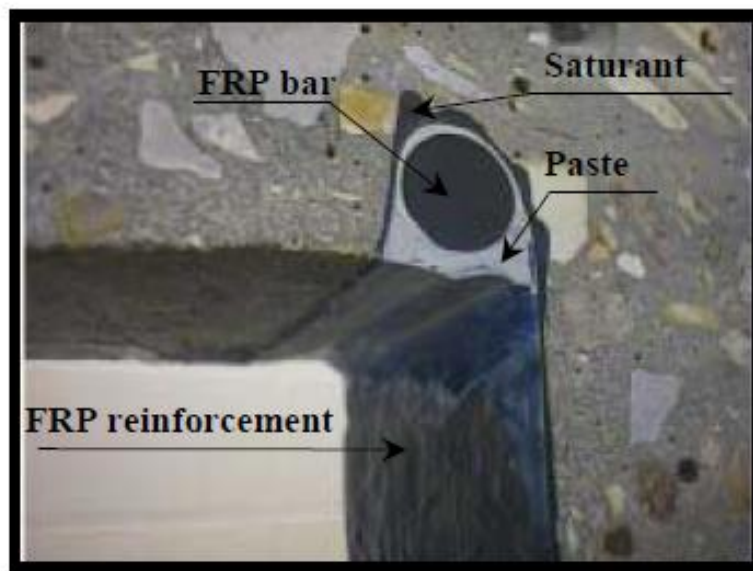


Figure 2-6: Cut-away section of U-Anchor installed at web flange junction (Khalifa et al., 1999)

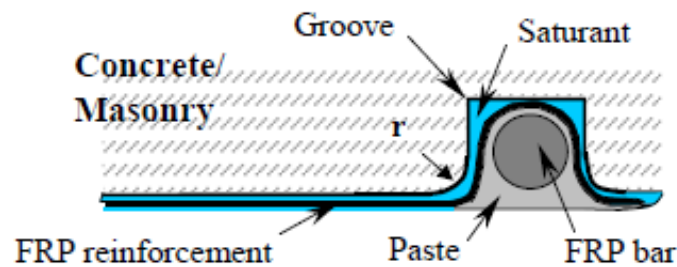


Figure 2-7: Drawing of U-Anchor (Khalifa et al., 1999)

The system was beneficial in several respects that were verified experimentally. Because the whole system was made of FRP materials, there is no concern for corrosion. There was also no concern for drilling into the beam, which can be problematic if reinforcement is intercepted. The system only needs a small groove in the concrete cover. Khalifa et al. (1999) tested three nominally identical concrete beams with no steel transverse reinforcement. One beam was not strengthened with CFRP, one was strengthened only with bonded CFRP but no anchorage, and one was strengthened with anchored CFRP with U-anchors. The third test with U-anchors produced the highest strength. No debonding was observed near the anchors. The strengthened beam with no anchors sustained 42% higher shear forces than the control specimen while the beam with U-anchors sustained 145% higher shear forces than the control beam and fractured the strip. The large strength increases could partially be attributed to the lack of steel stirrups in the test beams. This study clearly demonstrated the effectiveness of end region anchorage in developing the full potential of FRP as a strengthening method (Khalifa et al., 1999). While only having to notch out the cover is an advantage for not intercepting any steel reinforcing bar in the concrete member, concrete cover can crack and deteriorate, which favors anchorage systems inserted past the concrete cover into the core of the member (Orton et al., 2008). Cutting a notch across the entire width of the strip may also be more difficult than other methods such as drilling a hole.

2.3.6 CFRP Rope

El-Saikaly et al. (2015) tested a method of anchorage where a CFRP rope is used to connect both sides of the CFRP u-wrap (Figure 2-8). In order to use this anchorage scheme, a hole is drilled through the web just below the flange. The CFRP U-wrap is installed first, followed by the installation of the CFRP rope. The rope is pulled through

the hole in the web and fanned out over the U-wrap on either side of the beam (Figure 2-8). For this experiment, both pre-cured CFRP L-strips and CFRP fabric strips were used to make a U-wrap (Figure 2-8).

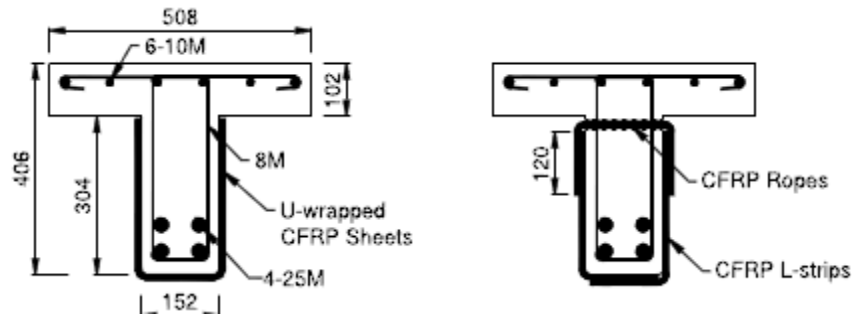


Figure 2-8: CFRP rope test specimens (El-Saikaly et al., 2015)

It was concluded that CFRP rope can be effective in preventing debonding failures and rendering the behavior of U-wrapped members akin to that of fully-wrapped members. Minor strength gains were witnessed and debonding was the primary failure mode when no anchorage was used. However, when CFRP rope was used, significant shear strength was gained, and debonding was prevented as a failure mode. While this anchorage system is similar to spiked FRP anchors, it is more difficult to implement because drilling through-web holes is more difficult than drilling spike anchors, particularly in thick webbed members. It is also difficult to pull epoxy saturated rope through the holes in the web.

2.4 SPIKE FIBER REINFORCED ANCHORS

2.4.1 Overview

Post installed CFRP anchors use chemical bond as the primary force transfer mechanism between anchors and concrete and anchors and CFRP strips (Kim and Smith, 2009). The first CFRP anchors were developed by the Shimizu Corporation and were studied by Kobayashi et al. (2001). The primary goal of the research was to provide continuity for

CFRP wrapped around thickened wall boundary regions where wall webs prevented full wrapping around the sections. Kobayashi et al. (2001) demonstrated that CFRP anchors could provide the needed continuity to axially confine the boundary regions. Since then, through-thickness or partially inserted (spike) FRP anchors have been used to develop the full strength of FRP strips in shear and flexural applications (Grelle and Sneed, 2013; Huaco, 2009; Kalfat et al., 2013; Kim, 2011; Kobayashi et al., 2001; Niemitz, 2008; Orton et al., 2008; Pham, 2009; Quinn, 2009; Sun et al., 2016).

Kalfat et al. (2013) reviewed available FRP anchorage system and found that “FRP anchors have the highest flexibility and potential for application to both slab and beam members, and their effectiveness and ease of installation make them a highly recommended form of anchorage”. In addition, such anchors require low maintenance. All of these attributes make them a promising choice for a wide variety of projects. Grelle and Sneed (2013) state that FRP anchors can be manufactured to overcome numerous geometric complications. Another advantage is that anchors can be fabricated from the same material as the FRP strip. This ensures the materials are compatible and will not cause problems such as corrosion (Grelle and Sneed, 2013). Research has also shown that spike CFRP anchors perform well and allow for the full development of the CFRP strips when designed properly. Spike CFRP anchors have been shown to be effective in flexural applications through small scale and full-scale beam tests (Kim et al., 2015; Sun et al., 2016). Such anchors were also shown to be effective in confinement applications (Kim, 2008), as well as shear strengthening of full-scale bridge girders (Huaco, 2009; Kim, 2008; Kim, 2011; Kim et al., 2012; Kim et al., 2014; Kim et al., 2015; Orton et al., 2008; Pham, 2009; Quinn, 2009; Sun, 2014; Sun et al., 2016). Even though various parameters that are important to anchor design have been studied (Sun et al. 2016; Sun, 2014; Pham, 2009; Hacuo, 2009; Quinn 2009; Orton et al., 2008)), issues related to larger spike CFRP anchors and sizes

effects have not been studied. Important parameters for FRP anchors are illustrated in Figure 2-9.

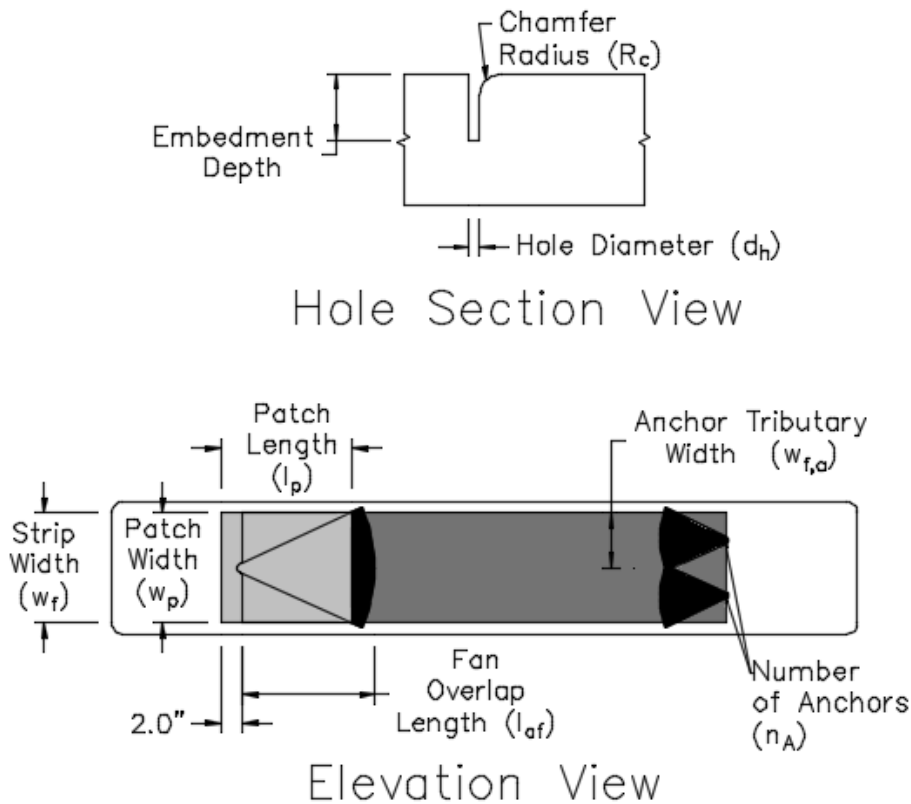


Figure 2-9: FRP anchor parameters

2.4.2 Anchor Hole Details

2.4.2.1 Hole Diameter

The anchor hole diameter needs to be drilled large enough to insert the anchor saturated with epoxy, but not so large that it generates epoxy voids. This is particularly a problem with horizontally drilled holes where epoxy can seep out if the hole is too large. A hole diameter 1 to 2 mm larger than the anchor diameter was recommended by Akyuz

and Ozdemir (2004). Others have recommended a hole area that is 40% larger than the equivalent laminate cross-sectional area of the anchor (Kim, 2008; Kim et al. 2015; Kim et al. 2014; Kim et al. 2012). This recommendation was shown to work reliably in numerous applications, from small-scale beams strengthened in flexure to full-scale bridge girders strengthen in shear (Kim et al. 2015; Kim et al. 2014; Kim et al. 2012; Pham, 2009; Hacuio, 2009; Sun et al., 2016).

2.4.2.2 *Embedment Depth*

Embedment depth is critical to ensure that an anchor fully transfers loads to a concrete section without pulling out. Akyuz and Ozdemir (2004) studied the effect of embedment depth on CFRP anchor strength when pulled in tension perpendicular to the concert surface (Figure 2-10). Anchor strength appeared to increase linearly up to a depth at which the failure mode shifted from anchor pullout to anchor rupture. This critical depth was about found to be 4-in. (100 mm) and was considered the minimum embedment depth for an anchor loaded in direct tension (Akyuz and Ozdemir, 2004).

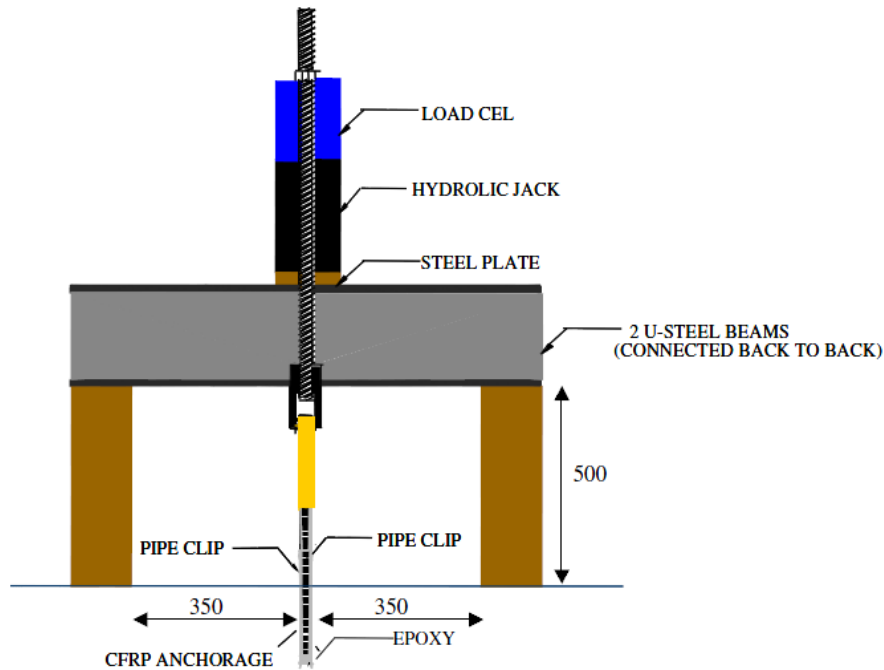


Figure 2-10: Test Setup for direct pullout tests (Akyuz and Ozdemir, 2004)

Ozbakkaloglu and Saatcioglu, (2009) investigated the performance of spiked CFRP anchors inserted at various angles from the perpendicular to the concrete surface (0, 15, 30 and 45 degrees) and pulled in tension in a direction perpendicular to the surface (Figure 2-11). The stress distribution in the anchors was found not be uniform throughout the depth of the hole (Ozbakkaloglu and Saatcioglu, 2009). Anchors appeared to sustain shear forces at the edge the hole, and transitioned to a tension pull out force as the depth of the anchor increased (Figure 2-12). This effect allows for a shorter embedment depth than in straight pullout application. Niemitz (2008) used a 2-in. embedment length for shear tests on anchors. Of all the tests, only one failed by anchor pull out. For these tests, anchors were embedded into large blocks of concrete that had no visible damage or cracking. In a field beam, however, the outer concrete layer may be cracked or become cracked under loading, therefore requiring a larger embedment depth for post-installed spike anchors. Ozbakkaloglu and Saatcioglu (2009) also determined that as the anchor diameter increases,

bond strength decreases. Therefore more embedment depth is needed with larger diameter anchors to develop their full strength. It is speculated that this may be due to a Poisson's effect that causes the diameter of the anchor to decrease and pull away from the concrete surface.

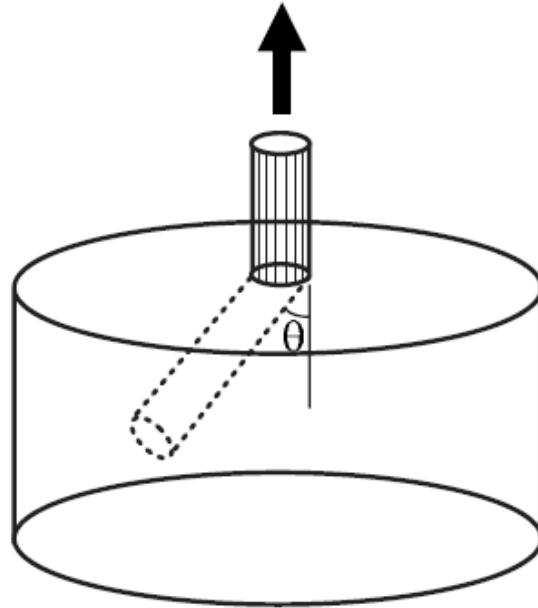


Figure 2-11: Inclined anchor pull-out (Ozbakkaloglu and Saatcioglu, 2009).

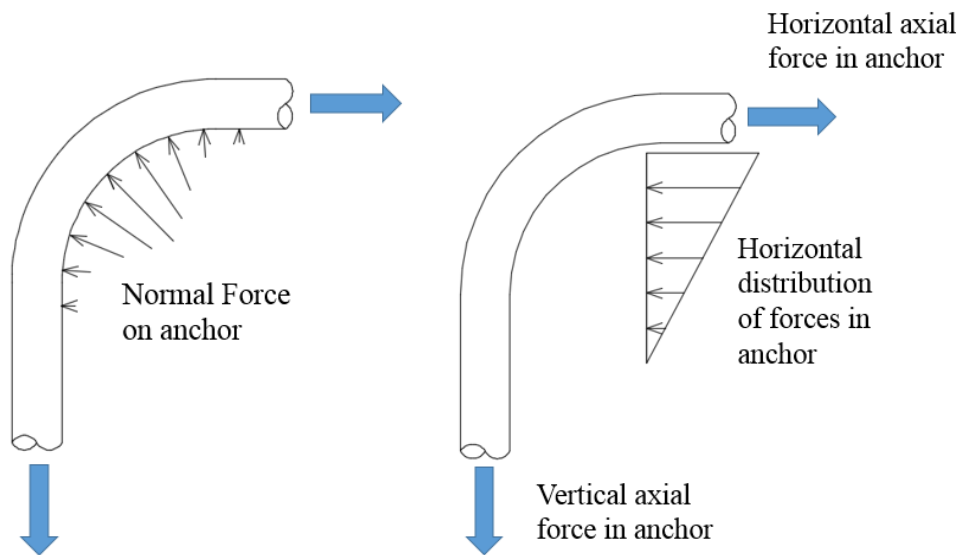


Figure 2-12: Stress distributions around the anchor bend

Research by Orton et al. (2008) concurs that spike FRP anchors must be inserted deeper than the concrete clear cover to reinforcement to avoid premature anchor failures due to cover deterioration. Inserting anchors past the clear cover of an element also provides a load path for the tensile forces in the anchors to be transferred to the reinforcing steel, which minimizes the likelihood of a concrete cone pull out failure around the anchors.

2.4.2.3 Hole Chamfer Radius

The chamfer radius at the edge of the anchor hole is an important parameter with respect to stress concentrations at the anchor bend. As previously discussed, Ozbakkaloglu and Saatcioglu (2009) investigated the performance of spiked CFRP anchors with no hole chamfer and varying insertion angles from the perpendicular to the concrete surface (0, 15, 30 and 45 degrees) (Figure 2-11). Test results indicated that the strength difference between anchors inserted at 0° and 15° was minimal. However, the anchor apparent strength dropped rapidly when insertion angles increased beyond 15°. This can be attributed to stress concentrations at the entry point of the anchor. The greater the angle, the higher the stress concentrations in the anchor at the edge of the concrete, and therefore the lower the anchor tensile capacity.

It is important to note that no chamfer radius was given to the entry holes, therefore as the angle of inclination increased, so did the sharpness of the hole entry point. A 45° inclination decreased capacity by over 50% (Ozbakkaloglu and Saatcioglu, 2009). Anchors attached to CFRP strips applied on concrete surfaces have an equivalent angle of inclination of 90°, therefore it can be expected that anchor strength would continue to decrease as the angle of inclination goes from 45° to 90°.

Chamfering the edge of the anchor hole to smooth the anchor bend can alleviate the stress concentrations that occur at that location. Early studies based chamfer radii on

relations developed for bent FRP bars (Orton, 2007). The Japanese Society of Civil Engineers (JSCE) research committee (1997) published an equation for estimating the reduction in capacity of FRP bars due to bend radius (Equation 2-1).

$$\frac{f_a}{f_u} = 0.09 \frac{r}{d} + 0.3 \quad \text{Equation 2-1}$$

Where:

f_a : reduced capacity of bent FRP bar

f_u : ultimate capacity of FRP bar

r : bend radius

d : diameter of CFRP

Using an anchor size of 3/8-in. and a bend radius of 1/2-in. only 40% of the ultimate capacity of FRP bars can be utilized. This equation results in a linear increase of strength with an increase in bend radius. Based on Equation 2-1, a CFRP anchor size of 3/8-in. diameter would require a bend radius, or chamfer radius, of almost 3 in. to achieve its full tensile capacity (Orton, 2007). A 3-in. chamfer radius is impractical in field applications where hole edges must be mechanically ground.

Kobayashi et al. (2001) suggested a 3/4-in. chamfer radius and compensated for loss of anchor strength by oversizing anchors. Other researcher concluded that a minimum chamfer radius of 1/4-in. should be used for CFRP anchors (Pham, 2009). Pham (2009) studied anchors with a chamfer radius of 0-in., 0.25-in. and 0.5-in. It was reported that anchor strength did increase with increased bend radius but only a 20-30% difference in capacities was reported when comparing no chamfer to a 0.5-in. radius. Because of this, the middle value of at least 1/4 inch radius was recommended. Previous projects conducted at the University of Texas at Austin have used a variety of chamfer radii, however the latest

research recommended the use of a ½-in. radius for anchor applications (Sun et al., 2016). This agrees with the current specifications in ACI 440.2R-08 which recommends a ½-in. radius at any corners to reduce stress concentrations in FRP materials.

Previous studies have found different chamfer radii to be acceptable. Based on the JSCE Equation presented earlier, (Equation 2-1) a larger amount of material will need a larger bend radius to transfer the same percent of load.

2.4.3 Geometry of Anchor Fan

2.4.3.1 *Overlap Length*

Fan overlap length is an important parameter for ensuring the force in a strip can be fully transferred to the CFRP anchor developing it. An insufficient length leads to delamination between the strip and anchor, not allowing the full capacity of either to be developed. On the other hand, too long a fan length is impractical and wasteful. Kobayashi et al. (2001) recommended an overlap length of 6-in. (15cm) and a 0.4-in. (10mm) overlap between adjacent fans (Figure 2-13). It is important to note that in this study, only one layer of FRP 0.00657-in. thick (0.167 mm) was used. If a stronger strip per unit width was used, either by using more layers or a thicker strip, the anchor fan would likely need to be extended (Kobayashi et al., 2001). Theoretically if the bond strength between strip and anchor-fan is known and the strength of the strip is known, the overlap length can be determined. The overlap length should be a constant for a constant strip strength per unit width.

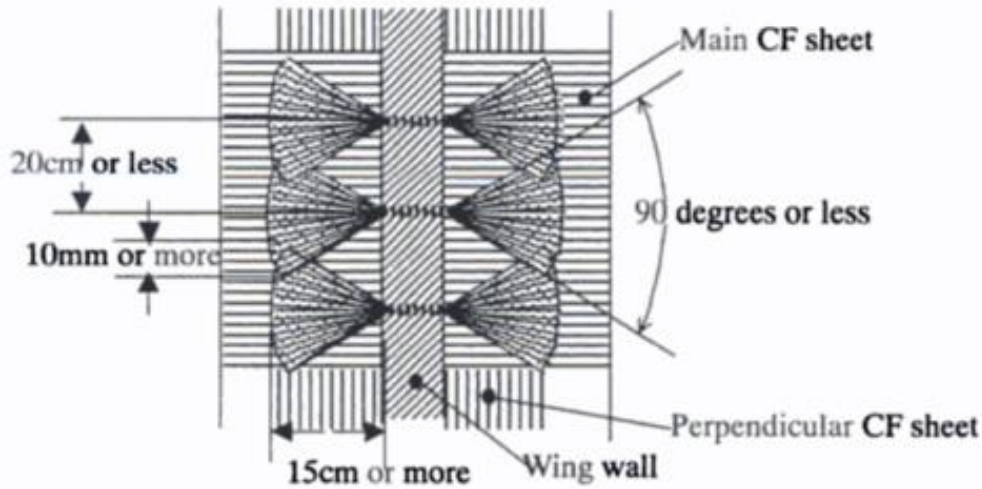


Figure 2-13: Anchor fan details (Kobayashi et al., 2001)

2.4.3.2 Fan Angle

Fan angle is important for distributing the stress from the strip into the anchor hole (Figure 2-14). A wide fan angle reduces the effectiveness of force transfers from the outer edges of the strip into the anchor hole. Small fan angles, on the other hand, require long anchor fans to cover the width of a strip. Kobayashi et al. (2001) recommended that fan angles should not exceed 90 degrees. This value was also reported in other test programs as the largest value that should be used (Pham, 2009; Kim, 2008; Orton, 2007). Since then, more research has suggested that smaller anchor fans provide a better distribution of stresses (Kim, 2011; Sun et al., 2016). Kim (2011) used anchor fans with angles of 60 degrees that proved reliable in developing strip tensile strength. It was suggested that smaller fan angles improve the force transfer efficiency at the outer edges of a FRP strip (Kim, 2011). Sun et al. (2016) investigated various CFRP anchor fan angles. Angles ranging from 37° to 64° were tested and it was concluded that there was little difference in the strain distributions and ultimate strengths within that range of angles. A fan angle of 60° was also recommended by Sun et al. (2016) for practical reasons and to ensure

sufficient fan overlap length. The maximum fan angle in a particular application may be determined by the required fan overlap length due to limitations on the bond stress between fan and strip.

A 0.4-in. (10mm) overlap of fans was recommended by Kobayashi et al., (2001) for adjacent anchors developing the same strip (Figure 2-13). Kim (2008) recommended an overlap of 0.5-in. and an anchor fan 0.5-in. wider than the strip to ensure adequate load transfer from strip to anchors.

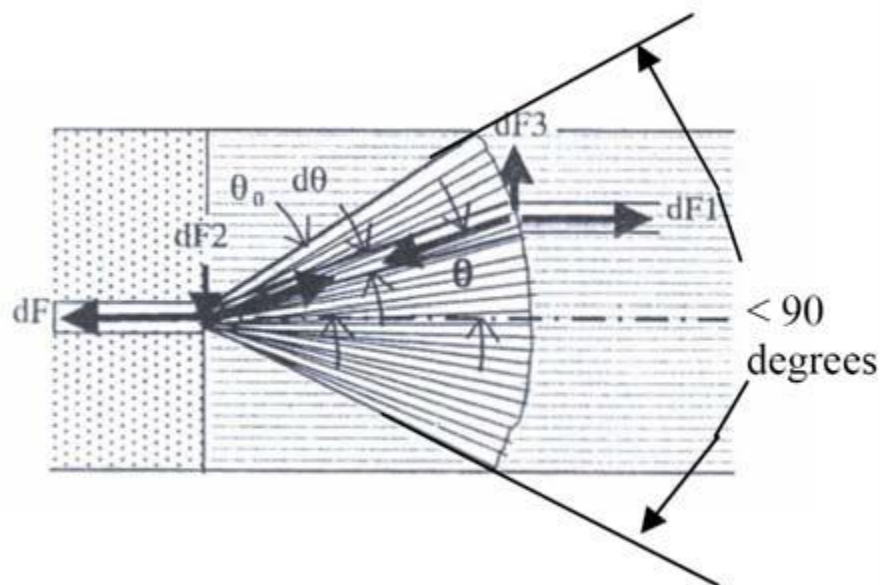


Figure 2-14: Anchor fan stresses (Kobayashi et al., 2001)

2.4.4 Width of Strip per Anchor (Anchor Tributary Width)

The width of strip developed by one anchor (effective anchor width or anchor tributary width) determines the anchor size needed to develop a strip, and influences the efficiency of the force transferred between anchor and strip (Sun et al., 2016). Kobayashi et al. (2001) proposed a fixed spacing of 7.9-in. (20 cm) between anchors (Figure 2-13). Orton et al. (2008) concluded that a larger number of smaller anchors were more effective at developing the full capacity of strips than fewer larger anchors. Anchors with a spacing

more than 7.9-in. could not be found in the literature and therefore that value constitutes the current upper limit on anchor effective width prior to this study.

2.4.5 Anchor Material Ratio

Recent reports on CFRP anchorage design have specified a ratio of anchor cross-sectional fiber material to that of the strip being developed of 2.0 to avoid anchor failures (Quinn, 2009; Sun et al., 2016). Quinn (2009) tested anchors with material ratios of 1.5 and 2 and found that anchors with a material ratio of 2 allowed reliable development of the full strength of CFRP strips without the anchors prematurely rupturing. The lower anchor material ratio of 1.5 resulted in several anchor ruptures prior to strip fracture. Such high anchor material ratios are needed to compensate for the stress concentration at anchor-hole edges. It is important to note that Quinn (2009) used 5-in. wide CFRP strips. Sun et al. (2016) revisited the anchor material ratio by testing ratios of 1.06, 1.41, and 2, and strip widths of 3 and 5 inches. A ratio of 1.41 was able to fracture all 3-in. wide strips. However 5-in wide strips required a ratio of 2 to ensure strip failure. The ratio of 2 for a 5-in. wide strip agrees with the results of Quinn (2009), however the difference in required ratios based on strip size identified a size effect. The amount of anchor material needed cannot always be obtained by multiplying the strip cross-sectional material by the same constant factor. As the amount of CFRP material increases, it appears the anchor material ratio needs to be increased as well. It is noteworthy that Sun et al. (2016) only used a 0.5-in. chamfer radius at the hole edge. Increasing chamfer radius as strip width and anchor size increase may help alleviate the observed size effect in anchor strength.

2.4.6 FRP Patch Details

Patches placed over anchors have been shown to increase anchor strength (Kalfat et al., 2013; Kim et al., 2012). Kobayashi et al. (2001) suggested the application of one

CFRP patch over anchors, with patch fibers running perpendicular to the fibers of the strip. The patch thickness was recommended to be at least 50% that of the CFRP strip. Huaco (2009) suggested adding two patches with orthogonal fiber directions over CFRP anchors. Patches were added from the same material as the strip. Quinn (2009) reported that when no patches were used, the outer edges of the strip debonded from the anchors prematurely, but when patches were added, the strip edge debonding mechanism was eliminated. Later research has shown that using FRP patches with bi-directional fibers can increase the elongation and strength of a single anchor (Kalfat et al., 2013). Sun et al. (2016) successfully used two patches, with fibers running perpendicular and parallel to the strip fibers (Figure 2-15). Because the two patches were made from the same material as the main strip, the patches had a combined thickness twice that of the strip.

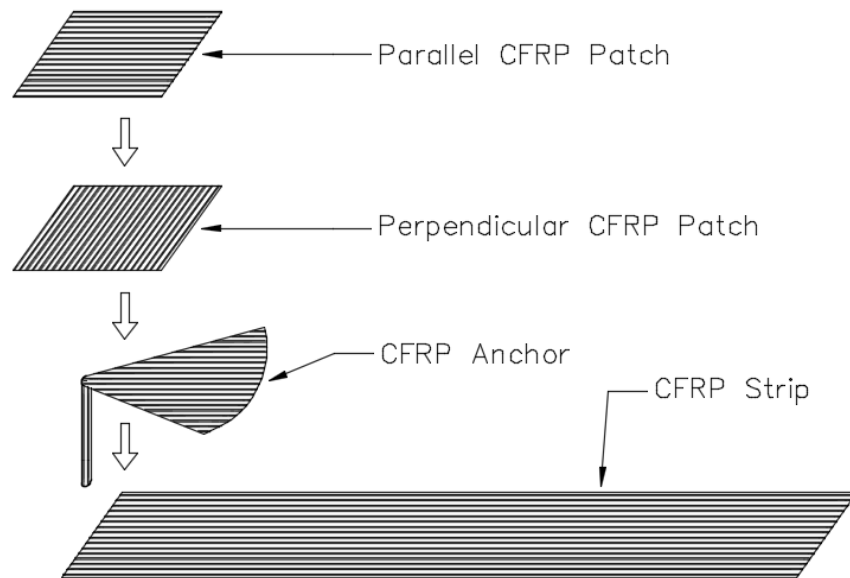


Figure 2-15: Bi-directional CFRP patches

2.5 SIZE EFFECTS IN CFRP STRIPS AND ANCHORS

While experimental evidence on FRP anchors is expanding, the behavior of anchored CFRP systems has not been fully determined. Few studies have specifically focused on anchor behavior with even fewer studies providing design guidelines or recommendations (Grelle and Sneed, 2013). Moreover, prior to this study, the largest identified CFRP anchors to be tested developed 7.9-in. (20cm) strips (Kobayahsi, 2001).

2.5.1 Size Effects on Anchor Strength

The anchor strength appears to be influenced by a variety of parameters. Some of these parameters create an apparent size effect in the strength of the anchor. Sun et al. (2016) concluded that an anchor material ratio of 2 is needed to fracture a 5-in. wide strip, while an anchor material ratio of only 1.41 was needed to fracture a 3-in. wide strip. This suggests that the anchor material ratio is related to strip width. It is possible that this effect is due to the brittle nature of the CFRP materials. The strength of brittle materials is governed by the weakest point in the materials. The larger strips and anchors become, the higher the likelihood of imperfections that lower the stress at fracture. Another possible explanation is that the size effect is related to the anchor-hole edge chamfer radius. As stated by the JSCE equation reported previously (Equation 2-1), a larger amount of FRP material requires a larger bend radius to transfer the same percentage of ultimate stress (Equation 2-1). Sun et al. (2016) used the same chamfer radius for 3 and 5 inch wide strips.

2.5.2 Size Effects on Strip Strength

Prior test results have indicated that strips with larger widths fracture at lower average stresses due to increased unevenness in strain distributions and higher peak strains at any given load (Sun et al., 2016). It appears that anchors are less effective in distributing

stresses evenly as strip widths increase. This effect is more dependent on the tributary strip width per anchor (or anchor spacing) compared to the overall strip width. The influence of strip thickness on strip stress at fracture is not documented in the literature (e.g., for strips with multiple layers of fabric).

Chapter 3: Experimental Program

3.1 OVERVIEW OF EXPERIMENTAL PROGRAM

Twelve beams were tested under three-point loading to evaluate the behavior and strength of larger anchored CFRP systems. This program was undertaken based on findings from Sun (2014), in which significant size effects were observed in CFRP strips and CFRP anchors. The beams were 12-in. deep by 12-in. wide by 68-in. long. These dimensions were selected to test CFRP strips up to 10-in. wide, which is considered to be the largest practical field installation width. A notch was cut at mid-span of the tension face to control the location of flexural cracking. Holes were drilled on the tension face of the beam for installing CFRP anchors (Figure 3-1). A CFRP strip anchored at the holes was applied to the tension face of beam specimens.

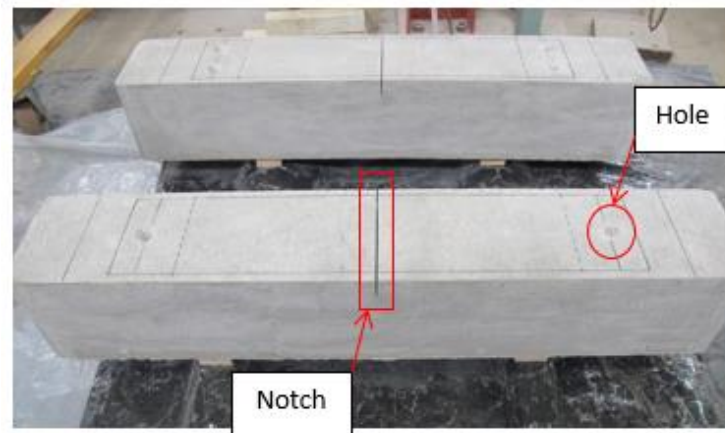


Figure 3-1: Large beam specimens before CFRP installation

The loading method induced tension forces in the CFRP strip and anchors as seen in Figure 3-2. When CFRP is used for strengthening and rehabilitation, the primary tension force in the strip is caused by widening of cracks in a concrete member (Figure 3-2). This is true for both shear and flexure cases of strengthening. Loading similar to that is observed

in the field was generated on the CFRP system in the small-scale beam specimens (Figure 3-3).

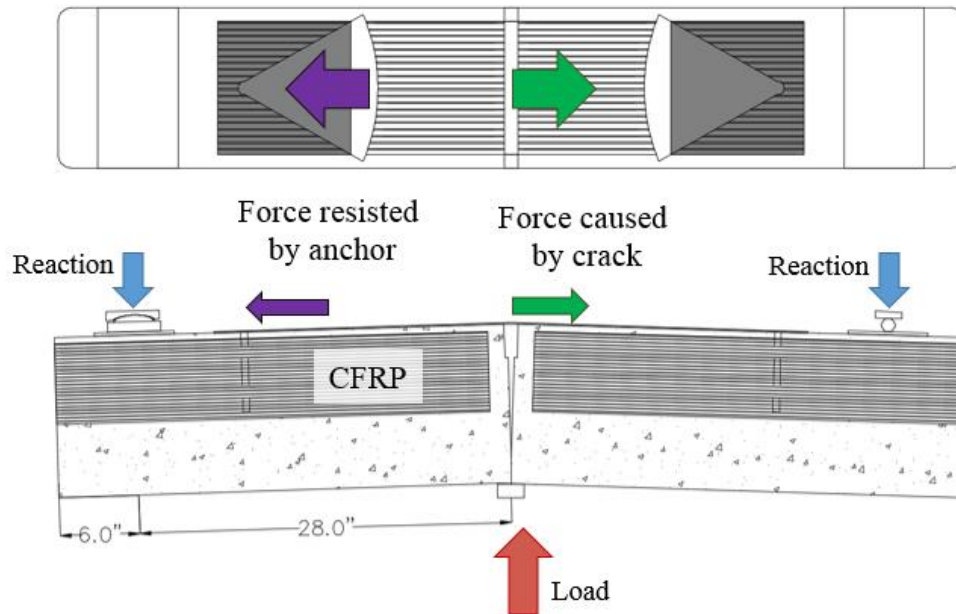


Figure 3-2: CFRP system loading in a three point load beam test

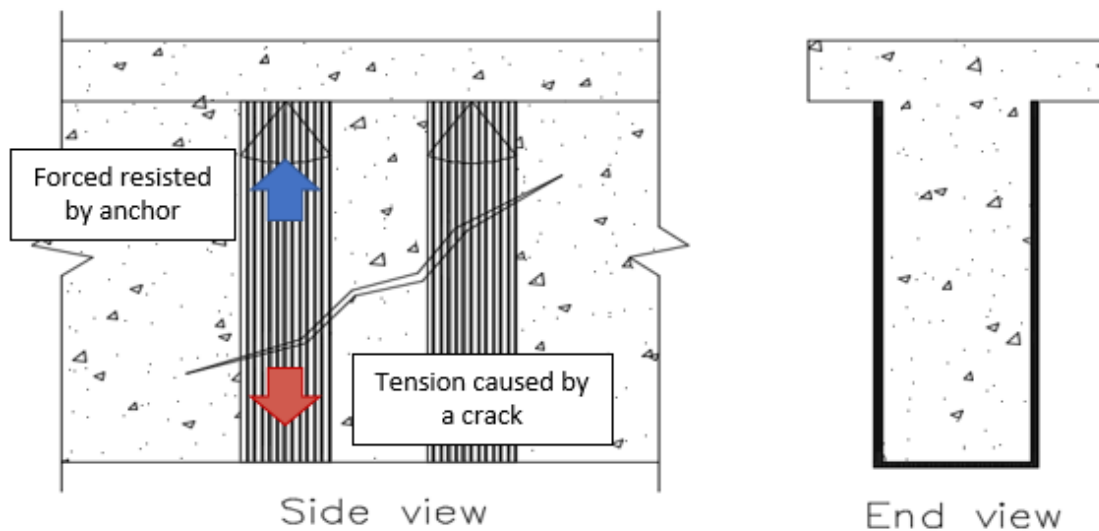


Figure 3-3: CFRP system loading in a shear strengthened concrete beam with inclined cracking

3.2 SPECIMEN DESIGN, DETAILS, AND CONSTRUCTION

The drawings in Figure 3-4 and Figure 3-5 provide the dimensions and details of the beam specimens. The dimensions were selected such that CFRP strips up to 10-in. wide could be tested.

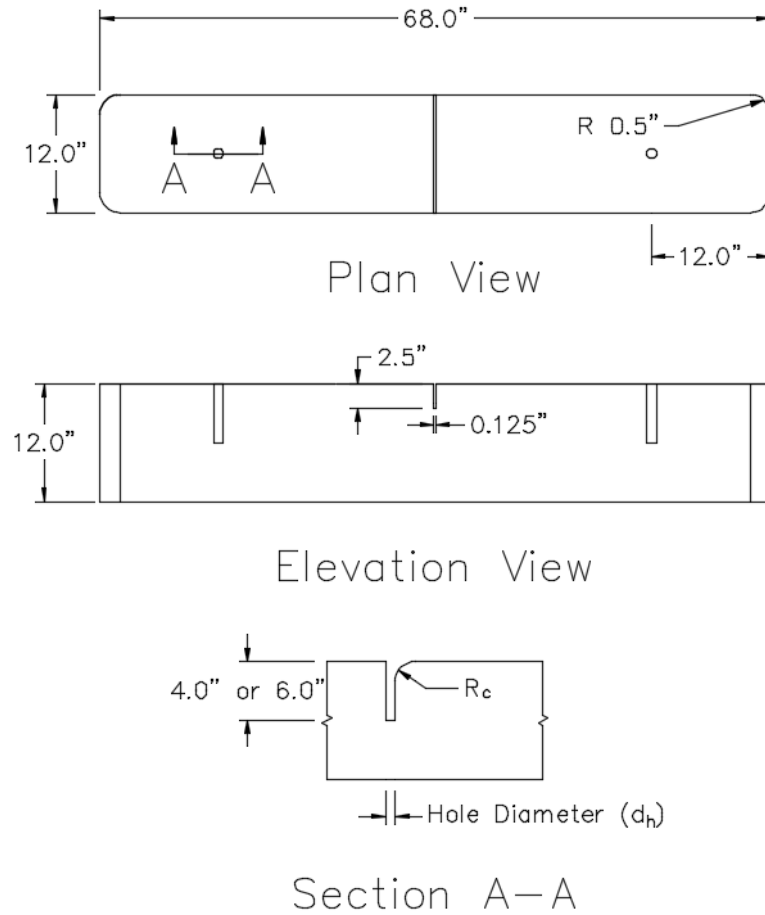


Figure 3-4: Detailed drawings of concrete specimen

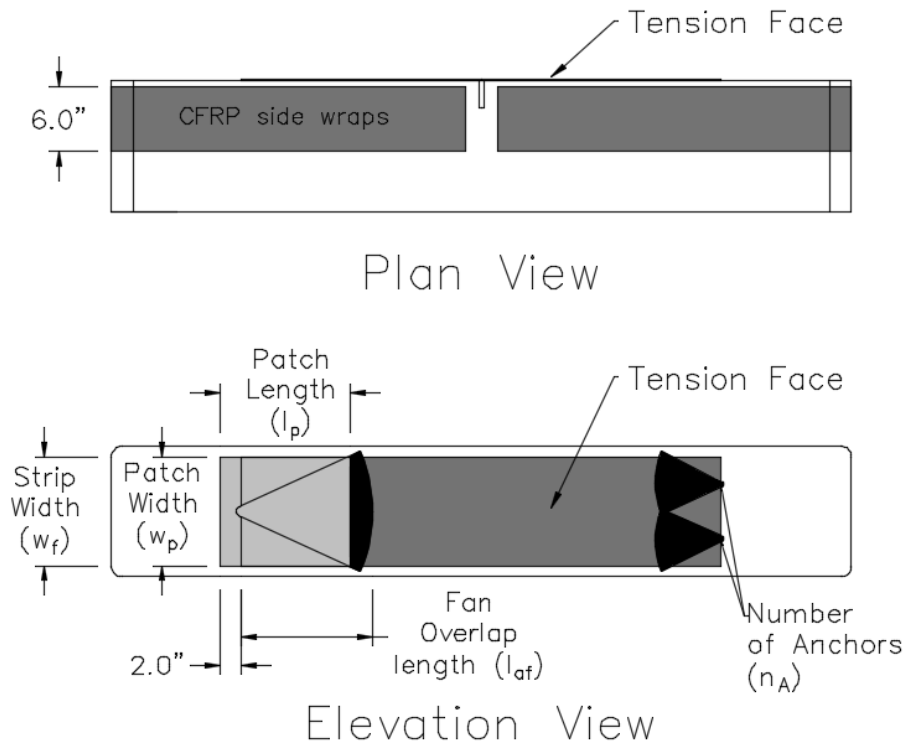


Figure 3-5: Detailed drawings of concrete specimen with CFRP

At first, no steel reinforcement was in the beams. However, after one specimen sustained an undesirable concrete failure (Figure 3-6), steel reinforcing cages were added to the specimens (Figure 3-7). The steel cages did not cross the mid-span of the beams and therefore did not affect the flexural strength at mid-span. Without steel reinforcing, the specimen sustained a concrete failure at a shear stress of $1.38\sqrt{f'_c}$, which is much lower than the ACI 318-14 (2014) design value of $2\sqrt{f'_c}$ for concrete in shear (in psi units). This indicated that the concrete failure may not have been a pure shear failure but rather governed by tension forces in the concrete at the anchor edge (Figure 3-8). Therefore the steel reinforcement was designed to resist the maximum tensile strength of the strip to avoid a concrete failure. The maximum force expected was 60 kips for a test specimen with two layers of 10-in. wide strips having a laminate thickness of 0.02-in. and a fracture stress of 143 ksi. Six - #4 bars with a specified yield stress of 60 ksi were introduced as U

bars (Figure 3-7) to provide sufficient strength to prevent the tension failure at the anchor edge. Side CFRP U-wraps were also used to help control failures in the concrete. Figure 3-8 shows the layout of reinforcing bars used in most of the test specimens.



Figure 3-6: Beam Specimen Failure

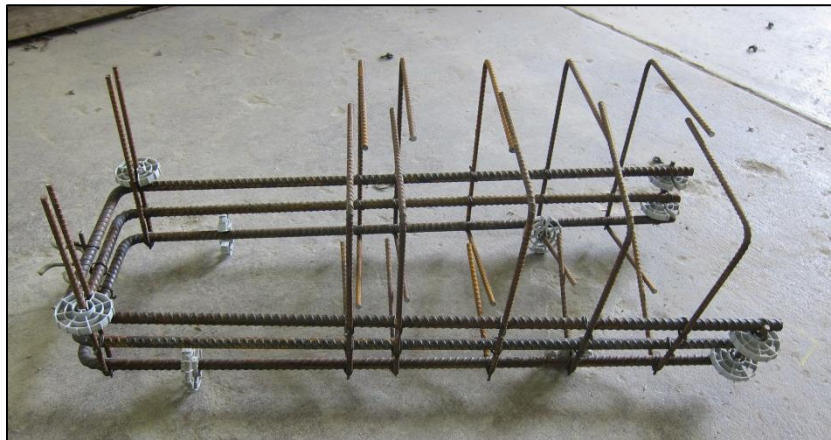


Figure 3-7: Typical steel reinforcing cage

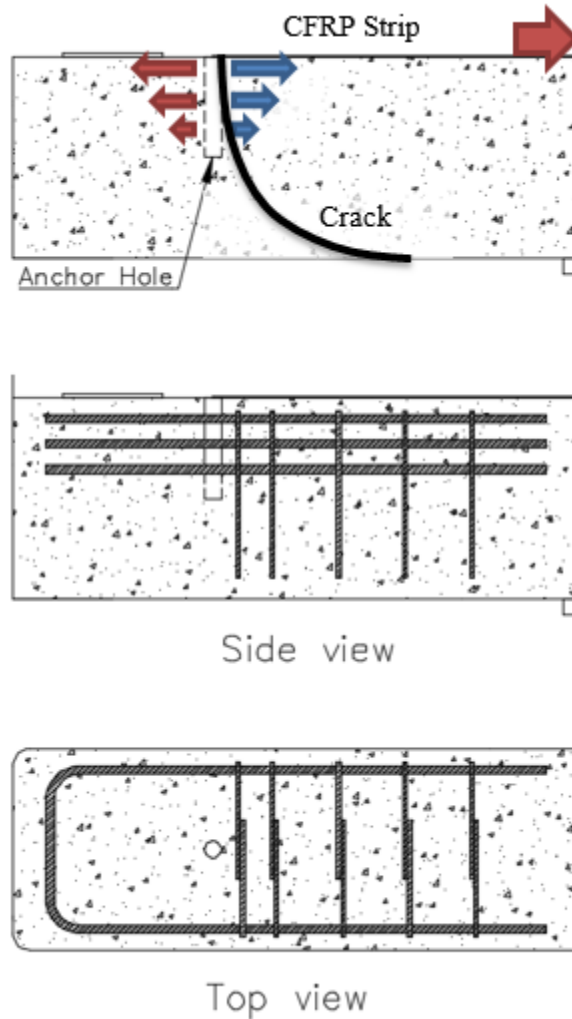


Figure 3-8: Diagram of forces and reinforcing bar layout

3.2.1 Construction

All specimens were built using wooden formwork. Shims were added to ensure the walls were perpendicular to the base. (Figure 3-9). One end piece was first attached to the base, then each of the four wall segments were attached one at a time, starting with the inner two, and then attaching the outer two (Figure 3-10). Lastly the other end piece was attached and sandwiched the walls. After all wood pieces were attached, screw holes were

taped over to allow for disassembly, and inserts were put in the corners to round the edges of the concrete specimens (Figure 3-11).



Figure 3-9: Ensuring formwork is square



Figure 3-10: Assembling formwork

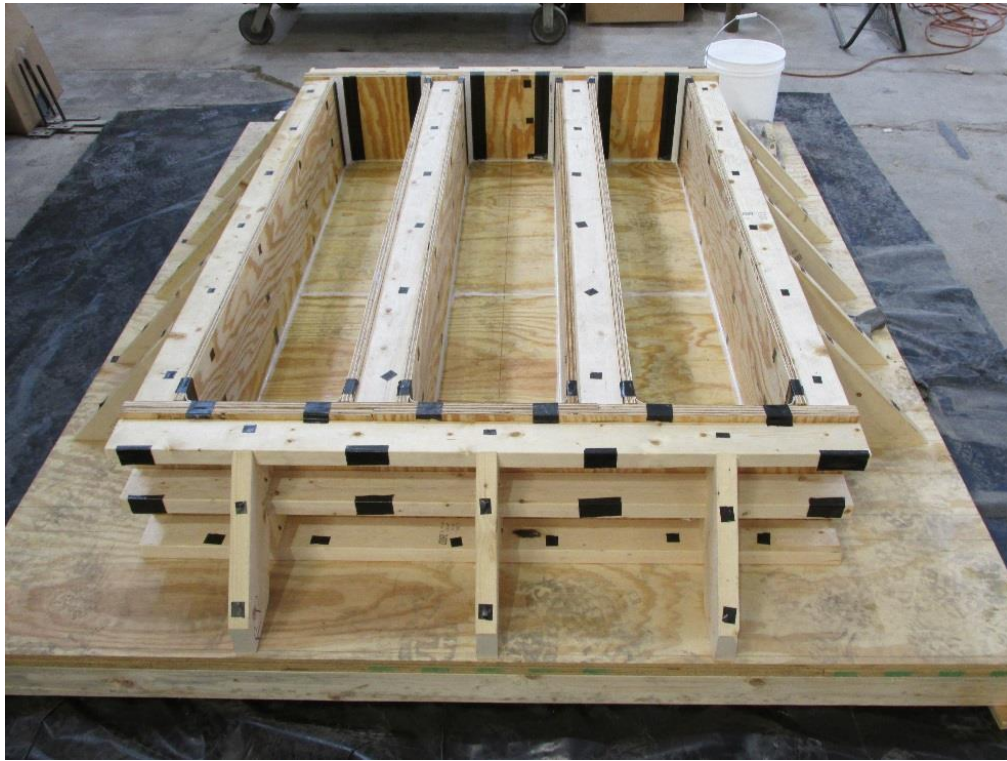


Figure 3-11: Completed formwork

Concrete for this project was taken from batches of concrete used in other projects in the lab. This was primarily due to the small specimen size, (17 cu. ft. or 0.63 cu. yd.) and the minimum order limit of 3 cu. yd. for a concrete truck. While concrete strength was not intended to be a variable for the experimental program, it did vary throughout the different batches. The relatively small size of the specimens allowed for ease of casting, and only two people were needed, one person operated the bucket (Figure 3-12), and one the vibrator (Figure 3-13). Both people screeded the concrete to the desired level and troweled the surface.



Figure 3-12: Casting concrete



Figure 3-13: Internal vibration

3.3 TYPICAL SPECIMEN PREPARATION AND STRENGTHENING

3.3.1 Specimen Preparation

The concrete surfaces, anchor holes, specimen corners and mid-span notch were prepared before installation of CFRP U-wraps, CFRP strip, and CFRP anchors. To improve bond between concrete and CFRP, the concrete surfaces that contacted CFRP were prepared by grinding off laitance and removing all dust and residue (Figure 3-14 (a)). Two holes were drilled on both ends of the beam tension face for anchor installation (Figure 3-14 (b)). The anchor holes were rounded to avoid premature CFRP anchor failure at the hole edge (Figure 3-14 (c)). Compressed air or a vacuum cleaner were used to remove the dust from the anchor holes (Figure 3-14 (d)). Finally, a 2.5 in. notch was cut at mid-span to control the location of concrete flexural cracking (Figure 3-14 (e)). Compressed air was then used again to remove all dust from the surfaces of the specimen.

Figure 3-15 shows a fully prepared beam specimen in which the corners of the beams are rounded to a radius of 0.5 in. so that U-wrapped CFRP strips would not fail at sharp corners. Beam corners were rounded by using form inserts and therefore did not require any grinding.



(a) Grinding a concrete surface



(b) Drilling holes

Figure 3-14: Specimen preparation before CFRP installation



(c) Rounding hole edge



*(d) Cleaning holes with compressed air
and vacuum cleaner*



(e) Cutting a notch at the center

Figure 3-14: Specimen preparation before CFRP installation (continued)

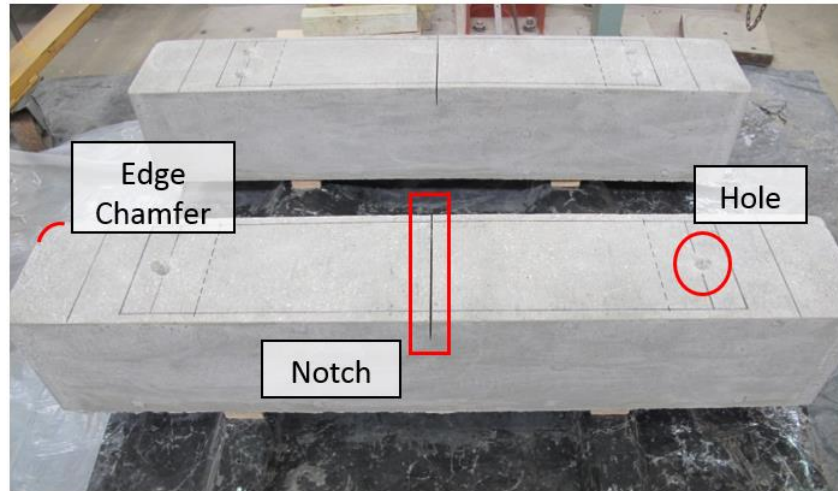


Figure 3-15: Typical prepared specimen

3.3.2 Preparation of CFRP Anchors

For this experimental program, both premanufactured anchors and anchors made from CFRP fabric were used. Premanufactured anchors ordered directly from the manufacturer consisted of a carbon fiber bundle tied at mid length using steel wire (Figure 3-16). In order to make an anchor from fabric, CFRP fabric was cut to the desired dimensions that provided the needed length and amount of fiber material. The fiber mesh of the fabric was first pulled apart so it acted more like independent fibers than a woven mat (Figure 3-17). Cross fibers were cut periodically to help ease the process of pulling apart the mesh. Pulling apart the mesh was needed in order to evenly fan the anchor out over the strip. The anchor was then tied with a steel wire tie to hold it together at mid length (Figure 3-18).



Figure 3-16: Premanufactured anchor



Figure 3-17: Pulling fibers apart from mat

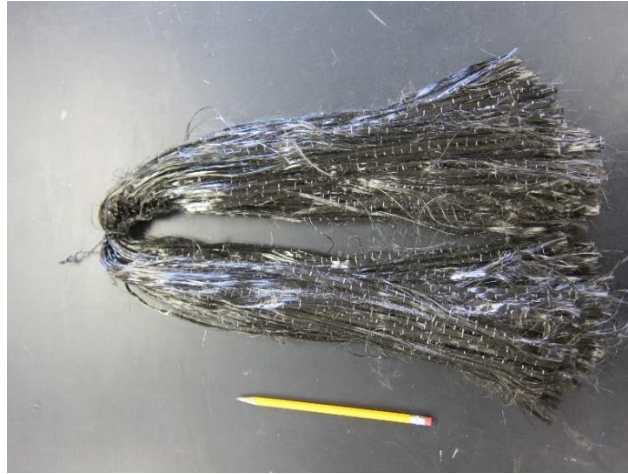


Figure 3-18: Finished CFRP anchor bundle

3.3.3 Installation of CFRP Strips and Anchors

CFRP strips were cut to desired dimensions from a larger roll of CFRP fabric. After all CFRP elements and installation supplies were prepared (Figure 3-19), epoxy was mixed according to the supplier's instructions (Figure 3-20). Anchor holes were saturated with epoxy using an extra anchor while beam surfaces were saturated using rollers (Figure 3-21). CFRP strips were then saturated with epoxy and applied to the beam side and tension surfaces as shown in Figure 3-22 and Figure 3-23. Putty knives and rollers were used to remove air bubbles and excess epoxy.



Figure 3-19: Prepared CFRP material



Figure 3-20: Proportioning and mixing the epoxy components



Figure 3-21: Saturating anchor holes and surfaces



Figure 3-22: Saturating anchors, patches, and strips



Figure 3-23: Applying CFRP strips on the tension face and sides of the beam

After strips were placed, saturated anchors were inserted into the holes and fanned out over the width of the strip to engage the full strip width (Figure 3-24). Two patches of CFRP were then applied over each anchor to reduce stress concentrations and achieve better load transfer between the strip and the anchors. The fiber direction of the first patch fibers was perpendicular with the CFRP strip fibers, while the fibers of the second patch were parallel to the strip fibers (Figure 3-25). A completed installation is shown Figure 3-26.



Figure 3-24: Fanning out the anchor



Figure 3-25: Applying patches (first one perpendicular to strip and second one parallel to strip)

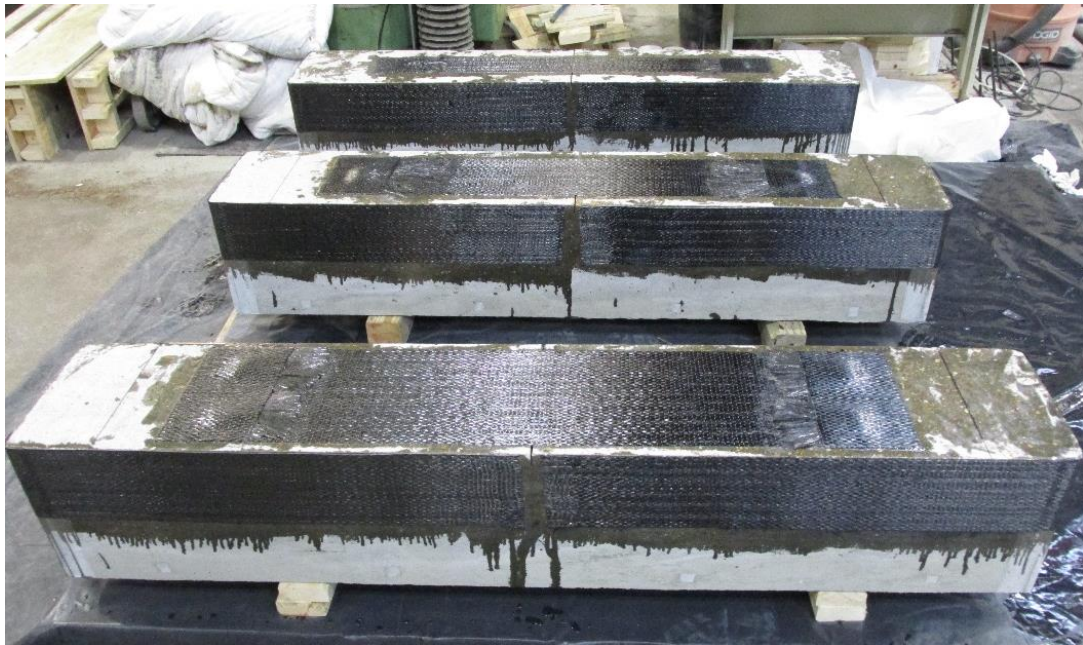
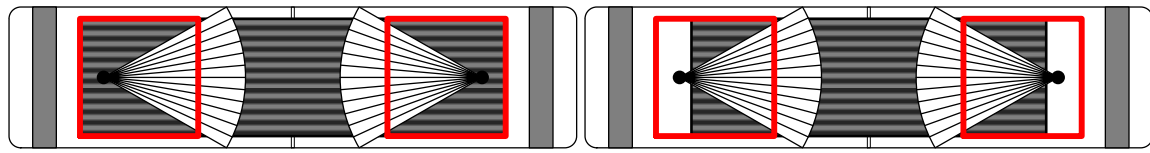


Figure 3-26: Finished specimens with CFRP installed

This method of anchor installation is different from previous research conducted at the University of Texas at Austin (Sun et al., 2016; Sun, 2014; Kim et al., 2012; Kim et al., 2014; Quinn, 2009) and stems from a recommendation by Garcia et al. (2014). In the previous studies, strips extended over the anchor holes and the anchors were threaded through the CFRP strips (Figure 3-27(a)). However, Garcia et al. (2014) found that it was difficult to find the anchor hole after it was covered by the strip in order to insert the anchors through the strips. On this experimental program, a new anchorage detail described above was used. The strip stopped just short of the anchor hole, making it much easier to install the anchor (Figure 3-27 (b)). Anchor patch placement is illustrated by red rectangles in Figure 3-27. The modified anchorage detail was shown to reliably develop the full strength of CFRP strips by Jirsa et al. (2016).



(a) Anchor through strip (previous studies) (b) Anchor adjacent to strip (this study)

Figure 3-27: Alternative anchor layouts

3.4 MATERIAL PROPERTIES

3.4.1 CFRP

All tests used the same CFRP fabric materials (Table 3-1) and the same epoxy material as binder (Table 3-2). The material properties of the premanufactured composite CFRP anchors are given in Table 3-1.

Table 3-1: Fiber material properties

Property	CFRP Laminate (Typical test values)	CFRP Laminate (Design values)	Composite Anchors (CFRP)
Dry fiber			
Tensile Strength	550,000 psi	-	550,000 psi
Tensile Modulus	33.4×10^6 psi	-	33.4×10^6 psi
Ultimate Elongation	1.7%	-	1.7%
Minimum weight per sq. yd.	9.3 oz	-	-
Laminate			
Expected Tensile Strength	143,000 psi	121,000 psi	143,000 psi
Expected Tensile Modulus	13.9×10^6 psi	11.9×10^6 psi	13.9×10^6 psi
Expected Ultimate Elongation at Fracture	1%	0.85%	1.2%
Thickness	0.02 in.	0.02 in.	-

Table 3-2: Epoxy material properties

Property	Epoxy
Tensile Strength	10,500 psi
Tensile Modulus	461,000 psi
Elongation	5%

3.4.2 Concrete

For each group of three specimens, 18 cylinders were prepared for testing at 7, 14, and 28 day as well as test day, following the procedures in the ASTM C39/C39M (2015) standard. Cylinders were removed from molds the same day the specimens were demolded, typically 7 days. Because three specimens were cast with each placement, the test day cylinders were tested the same day as the second beam test. Beams were normally tested within two or three days of each other. The test day strength from sampled cylinders is reported in this study. The only exception to this is the last set of beams (D-10-1-M-12, D-10-1-M-12-c, and T-5-1-M-18) when cores were taken from the specimens. The cast cylinder strength was much lower than expected, which might have been caused by premature demolding of the cylinders. This was the only set of cylinders that were demolded on a different day than the specimens themselves.

3.5 TEST MATRIX DETAILS

3.5.1 Primary Test Parameters

The following primary parameters, illustrated in Figure 3-4 and Figure 3-5 , were varied in this study:

1. Width of CFRP strip

Sun et al. (2016) observed that increasing the strip width from 3-in. to 5-in. resulted in a lower ultimate tensile stress at strip fracture. This trend was further investigated in

this study using strip widths of 5-in., 8-in., and 10-in. The widest strip width recommended for one anchor was reported by Kobayashi et al. (2001) to be 7.9-in.

2. Number of layers of CFRP strips

Multiple layers of CFRP strips can be used in applications where a large CFRP tensile strength is required. Single, double, and triple CFRP strip layers were used in this series to evaluate the strength of multi-layer layouts. Multiple layers can also be useful when geometry does not allow for wide strips.

3. Number of anchors per strip width

The number of anchors per strip width or the effective width of CFRP strip developed by an anchor can affect anchor and strip strength (Sun et al., 2016). Orton et al. (2008) concluded that a higher number of smaller anchors was more effective over a lower number of larger anchors. One or two anchors were used across the width of 10-in. wide strips.

4. Anchor fan overlap length

A 6-in. anchor fan overlap with the CFRP strip was used in previous research (Sun et al., 2016). While this length worked well for a single 0.02-in. thick layer of CFRP laminate, it did not for multiple layers. The anchor fan length was increased when developing multiple CFRP layers to maintain the interface bond stress between anchors and strips below the manufacturer recommended bond strength of 500 psi. The length of the anchor fan and width of CFRP strip developed determined the angle of the anchor fan. Because load transfer at the outer fibers of a fan with a large angle is less effective than at the center fibers, a reduction of anchor capacity may occur with a large fan angle. In all cases, the anchor fan angle did not exceed 60° as was suggested by Kim (2011).

5. Chamfer radius of anchor hole

Chamfers of one half inch radius were recommended by Kim et al. 2012. This was acceptable for the size of anchors used in that previous test program. Sun et al. (2016) also demonstrated that one half inch was an acceptable chamfer radius for the anchors used in that study. However, Sun et al. (2016) found that as anchors increased in size, their strength increased at a less than linear trend. Therefore, for this study where larger anchors were used, chamfers were adjusted based on the radius of the hole and taken as 1.4 times the radius of the hole.

6. Anchor material ratio (AMR)

The ratio of anchor to strip cross-sectional material, or anchor material ratio (AMR), is calculated as the ratio of the anchor equivalent laminate cross-sectional area divided by the strip laminate cross-section area. Because both strips and anchors are of the same material, the ratio of dry fiber weight per unit length of an anchor to that of the strip is equal to the AMR. Manufacturers typically provide the dry fiber weight per square surface area of a CFRP fabric ($\gamma_{s,Exp}$). While for prefabricated anchors, typically the dry fiber weight per unit length is provided (total anchor weight / total anchor length) (λ_A). The AMR can therefore be calculated as:

$$AMR = \frac{\lambda_A}{w_{f,A} \gamma_{s,Exp} n_l} \quad \text{Equation 3-1}$$

With:

$w_{f,A}$: anchor tributary width of the laminate strip

n_l : number of fabric layers in the strip

t_f : individual strip fiber thickness

t_l : total laminate strip thickness = $n_l t_f$

The equivalent laminate area of anchor can be evaluated using the following equation:

$$A_{Eqv} = \text{Eqv. laminate area of anchor} = AMR \times (w_{f,A} n_l t_f) \quad \text{Equation 3-2}$$

$$= \frac{\lambda_A}{\gamma_{s,Exp}} (t_f)$$

The effects of anchor material ratio (AMR) were investigated to determine whether anchor size affects anchor and strip performance, and to determine the required ratio to fully develop wide strips. An insufficient amount of CFRP material in the anchors will lead to rupture of the anchors before the full strength of strips is reached. On the other hand, Sun et al. (2016) demonstrated that increasing the AMR improved the strain distributions in CFRP strips and resulted in larger stresses in strips at fracture. In that previous study, larger AMR were needed to develop wider strips. Sun et al. (2016) recommended a minimum AMR of 2.0 for anchors developing 5-in. wide strips and a minimum AMR of 1.4 for anchors developing 3-in. wide strips. Three ratios were used in this series, 1.7, 2, and 2.8 with strip widths reaching 10-in.

3.5.1.1 Examples for obtaining the desired anchor material ratio (AMR)

Example 1: For anchors made from the CFRP fabric used for the longitudinal strip

This process is simple because the anchor is made from the strip fabric. Therefore simply multiplying the strip width by ½ the anchor material ratio provides the equivalent width of strip that needs to be cut and turned into an anchor. The ratio is multiplied by ½ because the strip should be cut twice as long as needed and folded in half along the fiber length, therefore doubling the area (Figure 3-28). Assuming a 5-in. wide CFRP strip with a desired material ratio of 2.4, the anchor would be made from a strip that was $5 \times (2.4/2) = 6$ in. wide and folded in half lengthwise, making its fiber area 2.4 times that of the strip.

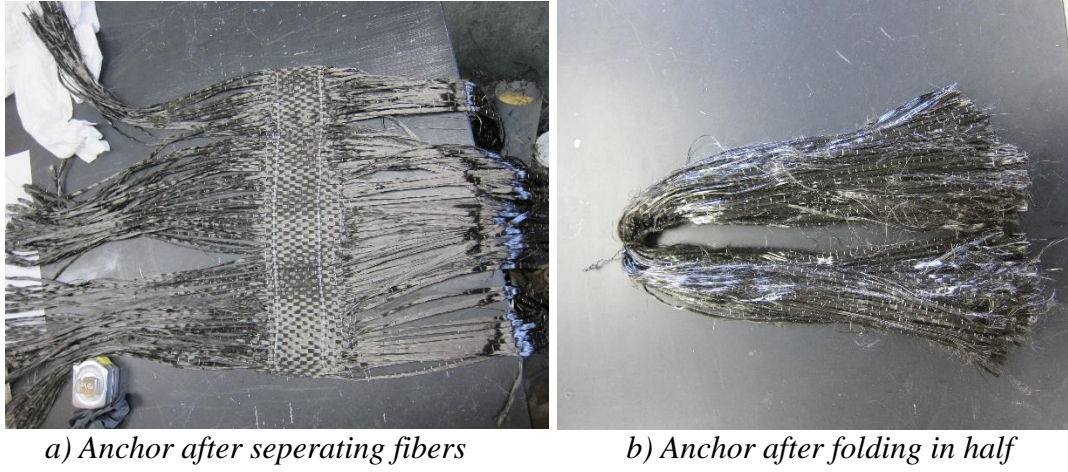


Figure 3-28: Anchor made from longitudinal strip

Example 2: For premanufactured anchors

To achieve a given AMR, the minimum anchor dry fiber weight per unit length ($\lambda_{A,min}$) can be evaluated as follows:

$$\lambda_{A,min} = \text{AMR } w_s \gamma_{s,Exp} n_l$$

For example, given the following data:

Weight of strip laminate per surface area ($\gamma_{s,Exp}$) = 0.005 oz/in²

Width of strip (w_s) = 5 in.

Number of layers (n_l) = 1

AMR = 2.0

$$\lambda_{A,min} = \text{AMR } w_s \gamma_{s,Exp} n_l = 2 \times 5 \times 0.005 \times 1 = 0.05 \text{ oz/in}^2$$

3.5.2 Other Test Parameters

The concrete compressive strength varied due to the use of different mixes based on availability of those mixes. Concrete strength ranged from 3.6 to 9.9 ksi. Sun et al. (2016) found that concrete strength had limited effect on the overall behavior and strength of anchored CFRP systems, and therefore it was not considered in analyzing the results.

The following test parameters were either held constant or varied as a function of the primary varied parameters:

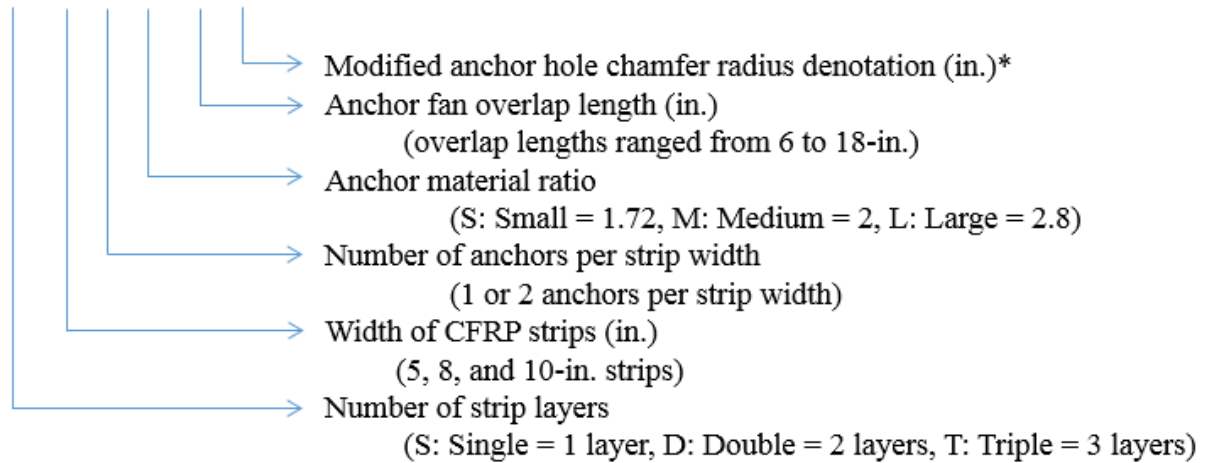
- All CFRP strips were fully bonded to the concrete beam tension face. CFRP anchors were proven to develop the tensile strength of CFRP strips even when the strips were fully debonded from the concrete surface (Sun et al., 2016; Kim et al., 2012; Kim et al., 2014). However, narrower inclined cracks were observed in beams strengthened in shear using anchored and bonded CFRP strips as compared to beams with anchored but unbonded strips (Kim et al., 2012; Kim et al., 2014).
- Anchor patch length was the same as the anchor overlap length.
- Anchor hole size was varied according to the equivalent laminate area of the anchors. Anchor hole size was selected as 1.4 times the equivalent anchor laminate area as recommended by Sun et al (2106) and Kim et al (2012). Hole diameter is important for a proper installation. Making the hole too large or too small will result in more difficult installation and lower quality. This will also affect the capacity of anchors.
- A hole depth of 4-in. was used in some tests, but when larger anchor sizes and chamfer radii were used, a longer hole depth of 6-in. was selected. In tests where anchors were developing up to 10-in. single-layer strips or 5-in. strip widths with multiple layers, a 4 in. embedment depth was used based on previous studies (Huaco, 2009; Ozbakkaloglu and Saatcioglu, 2009). However, when larger anchors were used to develop a 10-in. wide strip with two layers of fabric, the embedment depth was increased to 6 in. The embedment depth was increased to avoid a pullout failure given the larger forces in the larger anchors (Ozbakkaloglu and Saatcioglu,

2009). Tests one through six had anchors with an embedment depth of 4-in. while anchors in tests seven through twelve had a depth of 6-in.

3.5.3 Test Matrix and Specimen Nomenclature.

Specimen nomenclature is shown in Figure 3-29. The details of all 12 tests conducted in this series are shown in Table 3-3.

D-10-1-M-12-c



*All chamfer radii were 1.4 x hole radius, except for test 11 in which a smaller 0.5-in. chamfer radius was used. c = modified anchor hole chamfer radius

Figure 3-29: Specimen nomenclature

Table 3-3: Test parameters

Test #	Nomenclature	Number of CFRP strip layers (n_a)	Total laminate thickness (t_l) (in.)	Width of strip (w_f) (in.)	Number of anchors per strip width	Anchor material ratio (AMR)	Anchor fan overlap length (l_{af}) (in.)	Anchor hole edge chamfer radius (R_c) (in.)	Anchor embedment depth (in.)	Concrete Compressive Strength (ksi)
1	S-5-1-S-6	1	0.02	5	1	1.72	6	0.5	4	8.8
2	S-8-1-M-7	1	0.02	8	1	2	7	0.625	4	9.0
3	S-10-2-S-6	1	0.02	10	2	1.72	6	0.5	4	9.0
4	D-5-1-L-6	2	0.04	5	1	2.8	6	0.75	4	9.9
5	S-10-1-M-9	1	0.02	10	1	2	9	0.625	4	9.9
6	D-10-2-L-6	2	0.04	10	2	2.8	6	0.75	4	9.9
7	D-5-1-L-12	2	0.04	5	1	2.8	12	0.75	6	5.1
8	D-10-1-L-12	2	0.04	10	1	2.8	12	1.125	6	5.1
9	D-10-2-L-12	2	0.04	10	2	2.8	12	0.75	6	5.1
10	D-10-1-M-12	2	0.04	10	1	2	12	0.875	6	3.6*
11	D-10-1-M-12-c	2	0.04	10	1	2	12	0.5	6	3.6*
12	T-5-1-M-18	3	0.06	5	1	2	18	0.875	6	3.6*

*Compressive strength taken from concrete cores

3.6 DATA COLLECTION AND PROCESSING

3.6.1 Instrumentation

A three-point loading configuration was used for testing. A hydraulic ram applied a load to the beam, which was restrained by two reaction beams. The applied load was monitored using a 100 kip load cell placed adjacent to the loading ram at mid-span of each beam. Four Linear Voltage Displacement Transducers (LVDT) were used to monitor specimen deflection. Two were placed at mid-span, one on either side of the loading plate, and one at each end of the beam under the reactions beams. Strain gauges were applied to measure longitudinal fiber strains at several locations across mid-span on the surface of the CFRP strips applied to the tension face of beam specimen (Figure 3-30).

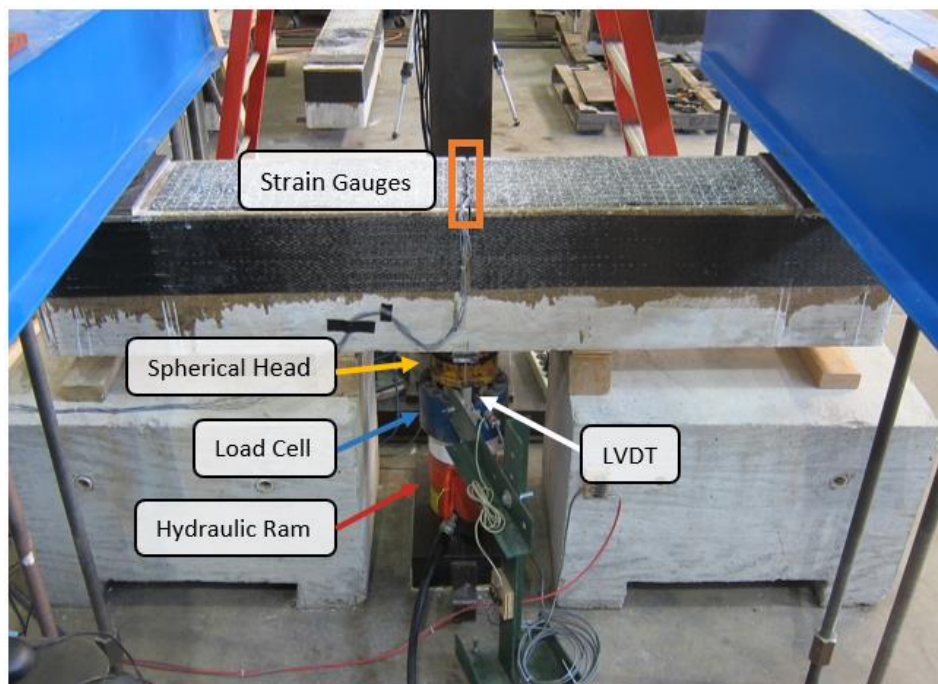
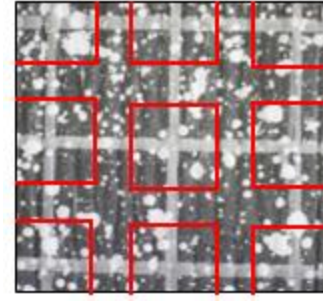
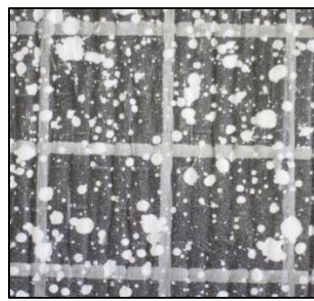


Figure 3-30: Test setup

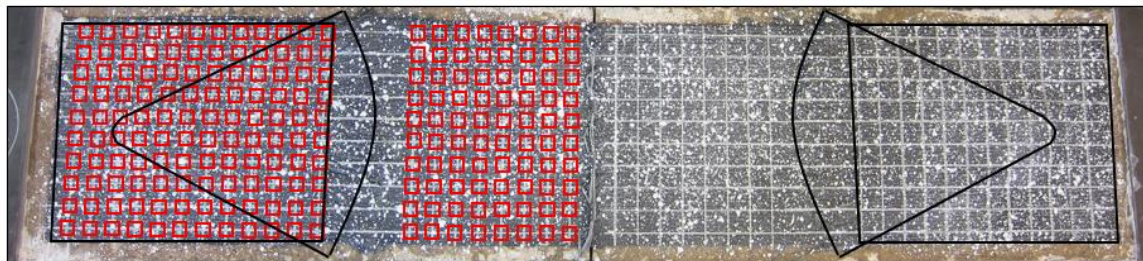
A high-resolution optical measurement system, reported by Sokoli et al. (2014), was used in some tests to study the 3-dimensional movement and surface strain profiles of the tension face of beam specimens. This system works by using digital image correlation (DIC) to track the three-dimensional movement of targets that are placed on the surface of the beams or CFRP elements. These targets can be either paper squares with high contrast patterns that are glued to the specimen, or a speckle pattern that is painted on (Figure 3-31). A speckle pattern was used in this test program. Both have been proven to produce reliable measurements, with paper targets providing higher deformation resolution at the expense of longer installation time. The optical measurement system consisted of two high-resolution cameras (Figure 3-32). The system was able to resolve surface strains on the order of 10^{-4} over a gauge length of less than 1 in. in this study.



(a) Paper targets



(b) Speckle paint targets (right showing target placement)



(c) Speckle paint pattern with target grid on specimen (target locations shown on left half)

Figure 3-31: Specimen with targets

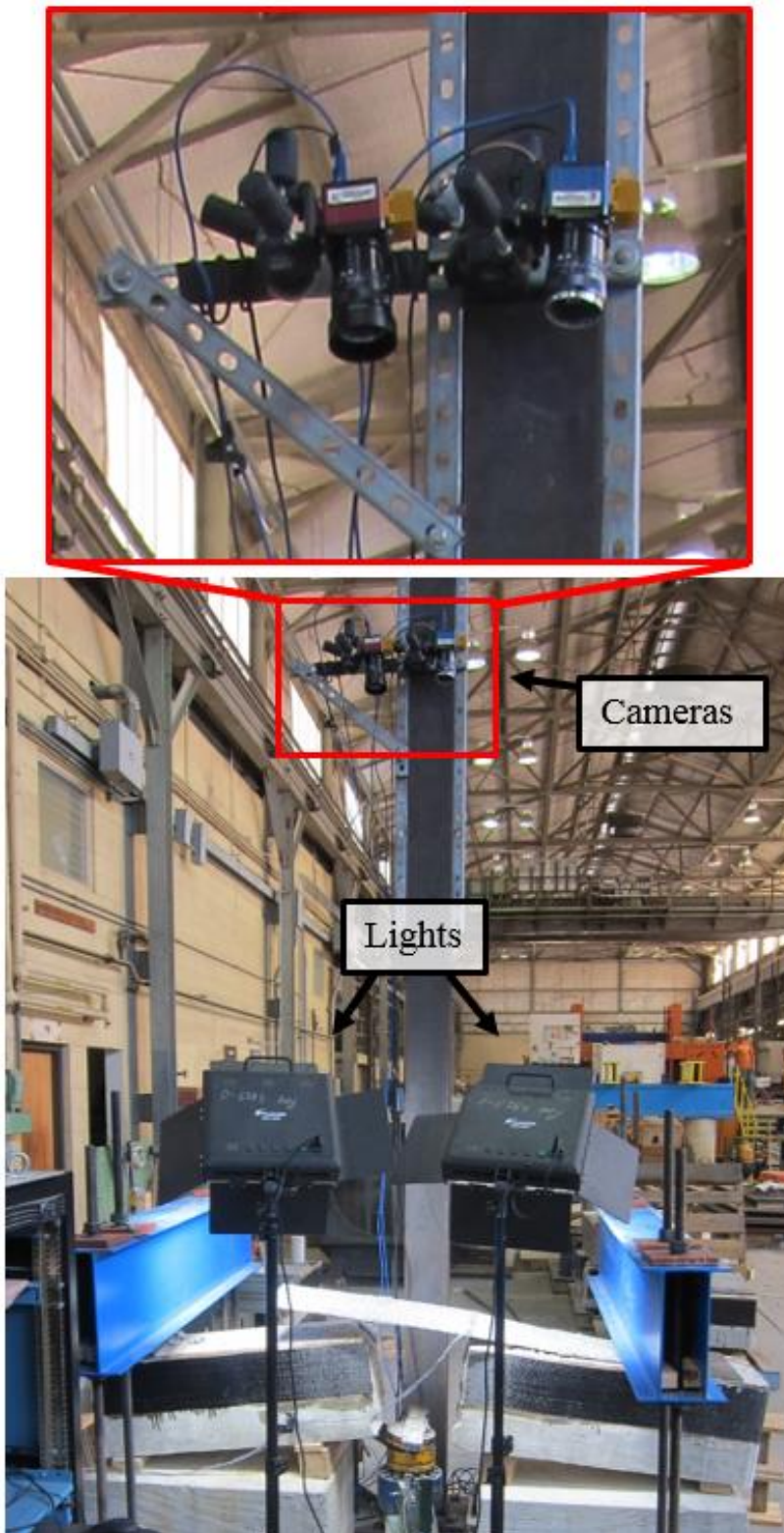


Figure 3-32: Setup of optical measurement system

3.6.2 Data Processing

3.6.2.1 Forces

The CFRP strips at the tension face of the beams acted in a similar fashion to flexural steel reinforcement in a concrete beam. The loading setup produced a moment on the beam specimen, which was resisted by a tension force in the strip and a compression force in the concrete (Figure 3-33 and Figure 3-34). Based on the moment applied at mid-span, the force carried by the CFRP in tension was calculated. Equation 3-3 through Equation 3-7 were used to find the tensile stress in the strip at failure. These equations can be rearranged into Equation 3-8 where the stress in the strip is the only unknown.

$$M_a = P * l / 4 \quad \text{Equation 3-3}$$

$$M_{int} = j_d * T_f \quad \text{Equation 3-4}$$

$$j_d = h - a / 2 \quad \text{Equation 3-5}$$

$$a = \frac{T_f}{0.85 * f'_c * b} \quad \text{Equation 3-6}$$

$$T_f = \sigma_{CFRP} * A_{CFRP} \quad \text{Equation 3-7}$$

$$\frac{P * l}{4} = \left[h - \frac{\sigma_{CFRP} * A_{CFRP}}{2 * 0.85 * f'_c * b} \right] * (\sigma_{CFRP} * A_{CFRP}) \quad \text{Equation 3-8}$$

Where:

M_a : Applied moment calculated based on statics of test setup, kip-in

P : Applied force, kips

l : Span length, in.

M_{int} : Internal moment caused by concrete compression block and CFRP strip tension, kip-in

j_d : Lever arm between concrete and strip forces, in.

T_f : Tension in CFRP strip, kips

a : Depth of compression block, in.

α : Stress block factor, assumed to be 0.85

f'_c : Concrete strength, ksi

b : Width of specimen, in.

σ_{CFRP} : Stress in CFRP at failure, ksi

A_{CFRP} : Cross sectional area of CFRP, in².

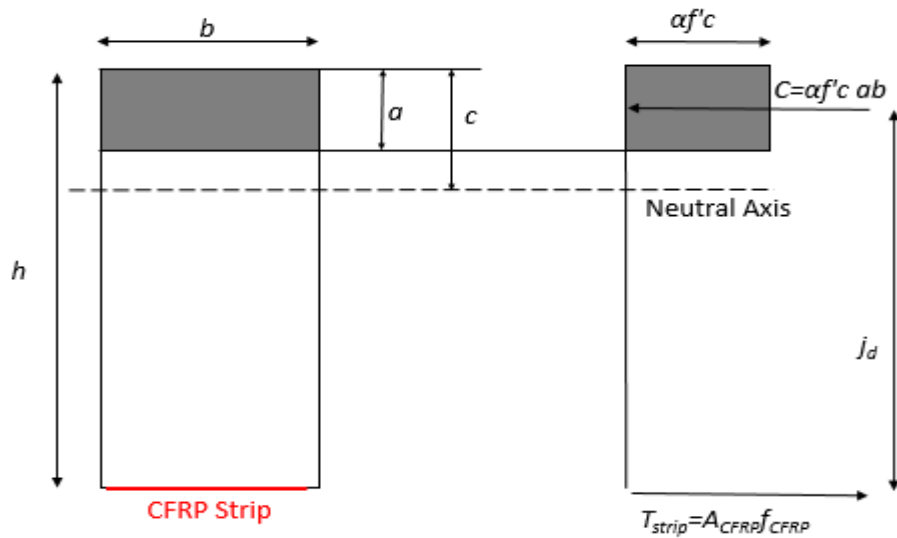


Figure 3-33: Statics of beam specimen

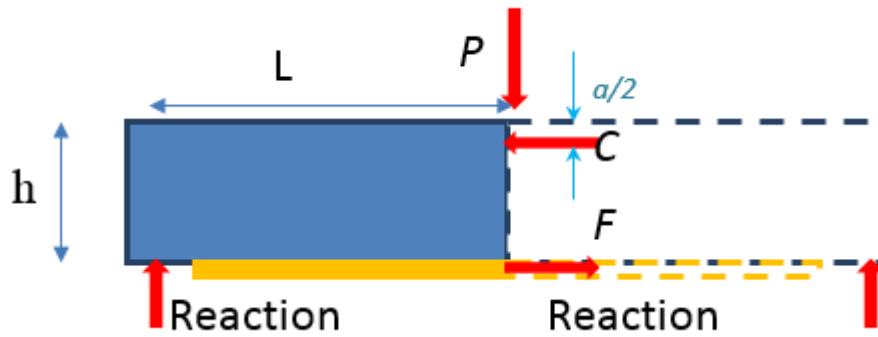


Figure 3-34: Beam Equilibrium (adapted from Sun, 2014)

3.6.2.2 Deformations

LVDTs were used to determine the deflection of specimens. Locations of the LVDTs used in the deflection calculations are shown in Figure 3-35. Readings from the LVDTs under the reaction points were averaged and subtracted from the average readings from the two LVDTs under the loading point to obtain the beam net mid-span deflection (Figure 3-36). The LVDTs under the load plate showed very consistent readings signifying that there was no torsion introduced to the specimen.

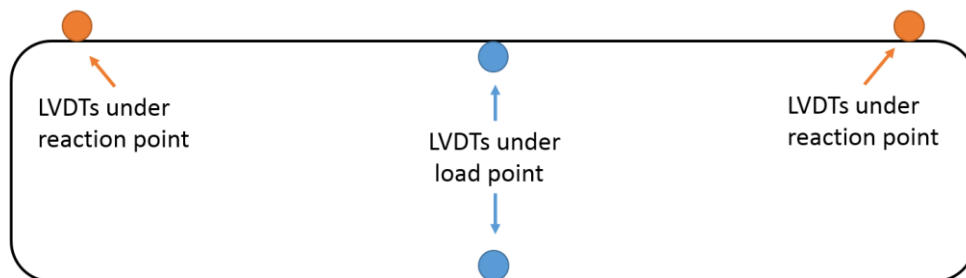


Figure 3-35: LVDT locations on the underside of the beams

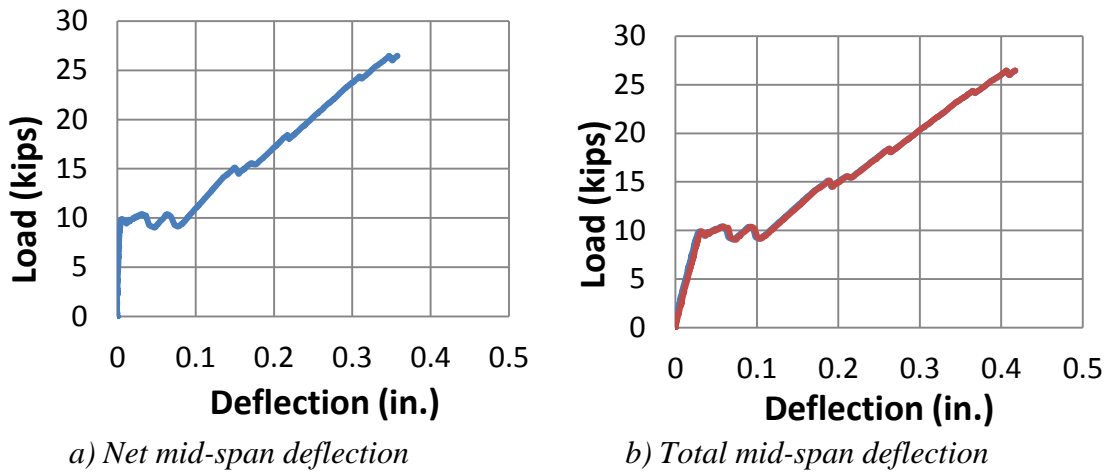


Figure 3-36: Load deflection plots illustrating total and net deflection at mid-span

3.6.2.3 Strains

Strains at mid-span were recorded from strain gauges and were used to find both average and peak strains. Average strains were calculated by taking the numerical averages of all strain gauges used, and peak strain was taken as the max strain gauge reading.

Strains at the surface of the CFRP strips were also evaluated using the three-dimensional target location data provided by the optical measurement system. Strains were used to evaluate the performance of the CFRP strips and anchors. Using optical measurements, full surface strain distributions can be plotted as contours to witness overall strip behavior, as well as strain concentrations. (Figure 3-37).

The variation in longitudinal strains (ϵ_x) across the width of the strips were used to evaluate the effectiveness of the anchors in distributing stresses. For this evaluation, longitudinal strains were calculated over a span of 11 targets at each target row along a strip width (Figure 3-38). The maximum row longitudinal strains were compared to the mean longitudinal strain across all rows to determine the effectiveness of anchors in distributing stresses across strip width.

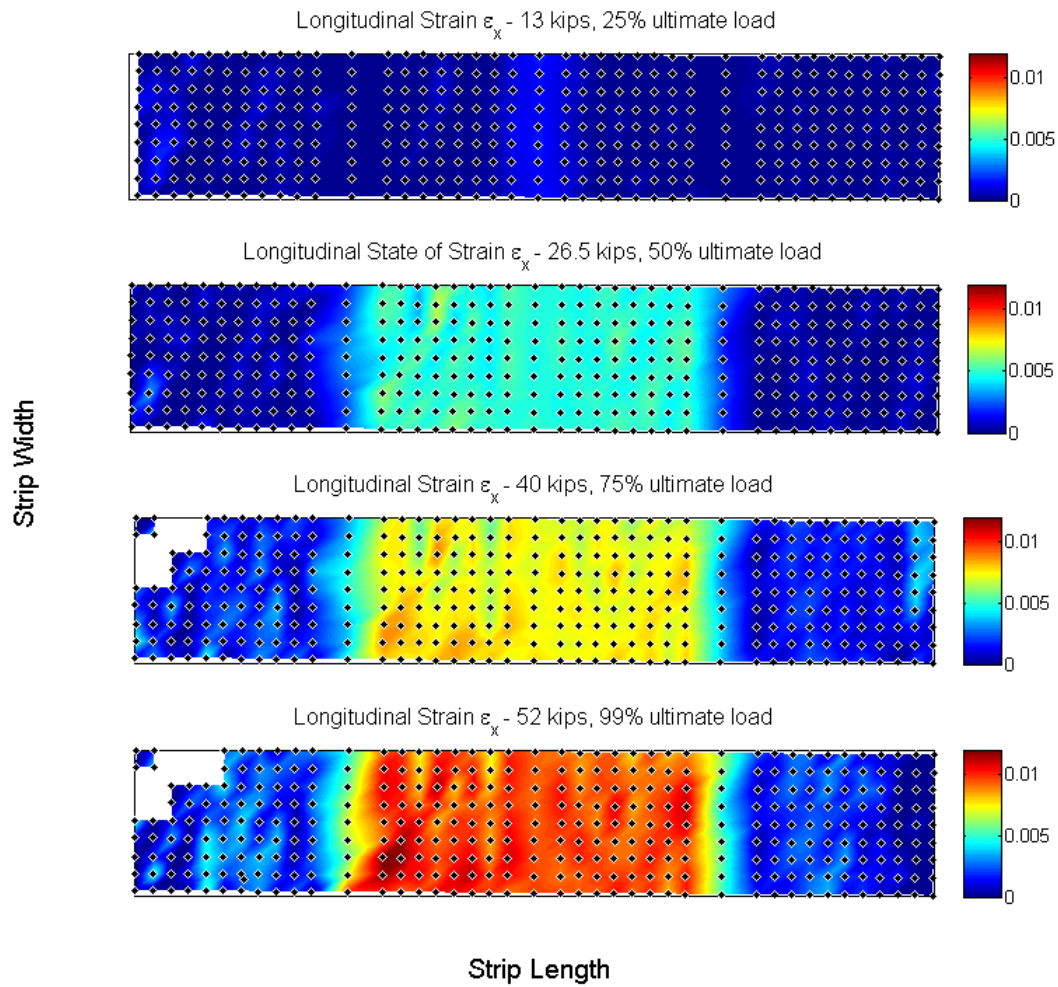


Figure 3-37: Contour plot of strain in the longitudinal x -direction

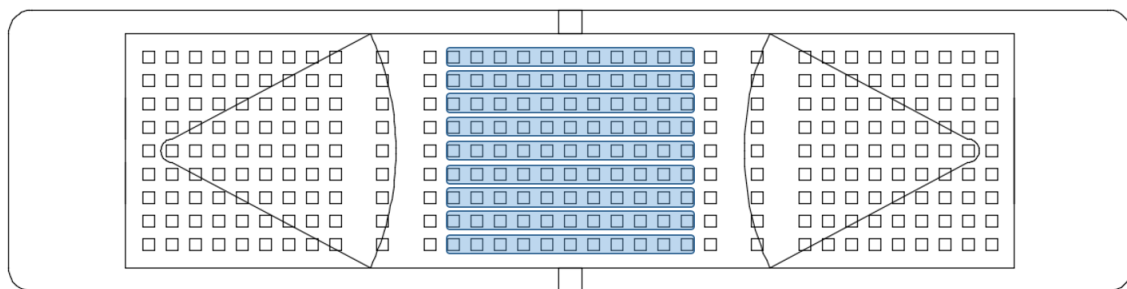


Figure 3-38: Elements used to determine average strain and max strain

Chapter 4: Test Results

4.1 TYPICAL TEST

Beam specimens were subjected to three point loading as shown in Figure 4-1. The load was placed at mid-span with the tension face up and a ram reacting against a strong floor (Figure 4-2). This loading applied tension on the anchored CFRP strip. Loading was continuous from the start of the test until failure at a rate of about 1 kip every 10 seconds.

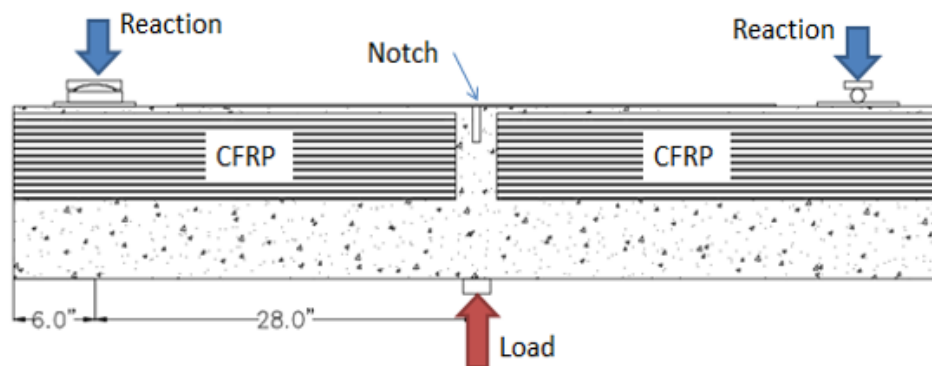


Figure 4-1: Loading diagram

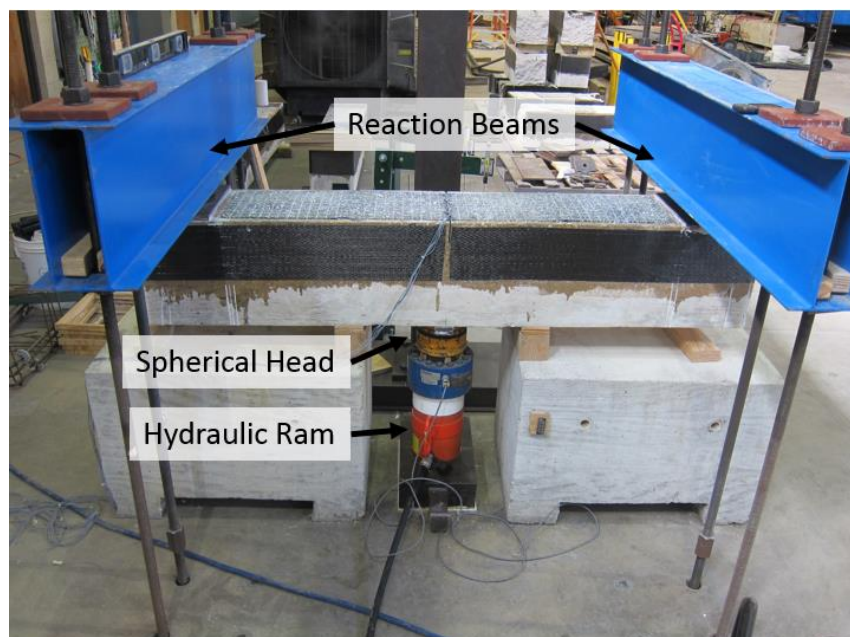


Figure 4-2: Test setup

A typical load deflection response starts with a relatively stiff linear segment up to cracking of the concrete in flexure at the mid-span notch (Figure 4-3). Immediately after cracking, the load levels off with increasing deformation as strip debonding progresses from the crack towards the anchors (Figure 4-4). After strip debonding reaches the anchors, the response becomes mostly linear again up to failure as the anchors resist most of the tensile load in the strip (Figure 4-3 and Figure 4-4).

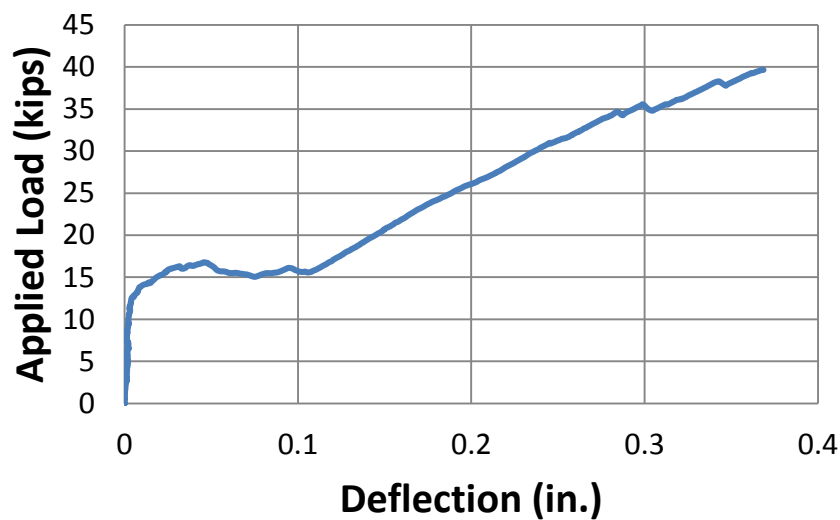


Figure 4-3: Load-deflection response for specimen D-10-2-L-6 illustrating a typical test response

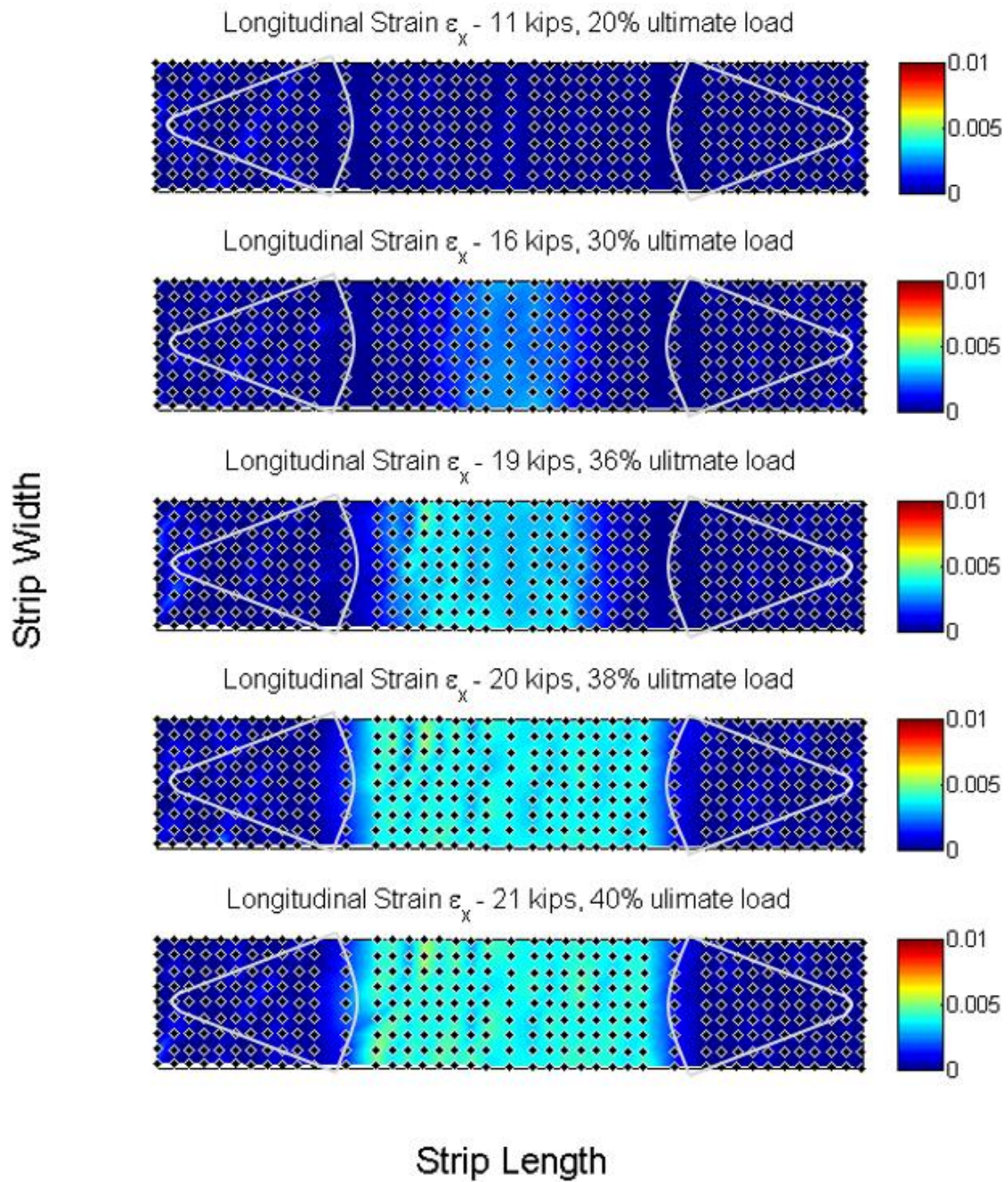


Figure 4-4: Longitudinal strain contours (ϵ_x) on the surface of the anchored CFRP strip for specimen D-10-2-L-12

To assess variability in response, Sun (2014) conducted several tests on nominally identical beam specimens similar to those in this study but of smaller dimensions. Figure 4-5, adapted from Sun (2014), illustrates how two nominally identical specimens can exhibit relatively small differences in overall responses. Because fewer large beams were tested, a similar variability study was not conducted.

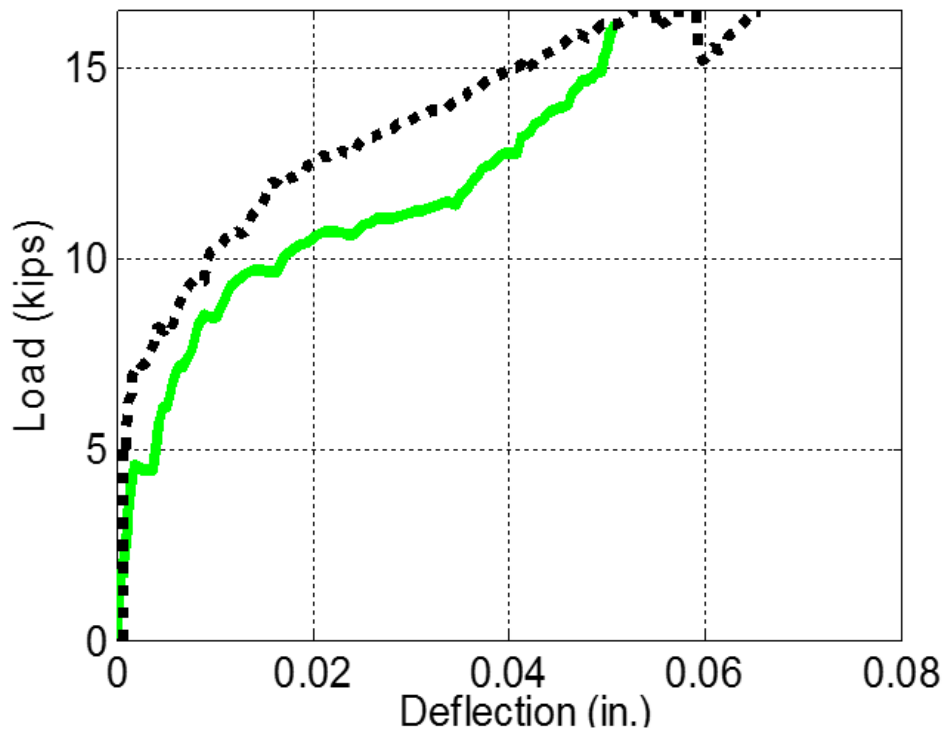
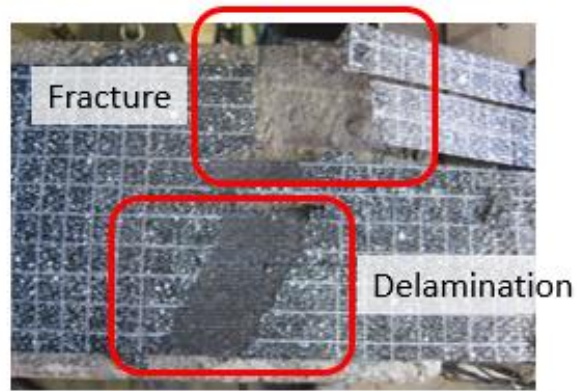


Figure 4-5: Load vs deflection of nominally identical test specimens (Sun 2014)

4.2 FAILURE MODES AND IMPLICATIONS

The observed failure modes strip fracture, anchor rupture, delamination between anchor and strip, and failure of the concrete are show in Figure 4-6. CFRP strip fracture is the most desired failure mode because it results in the highest capacity for a given CFRP strip. In retrofit projects, the CFRP system will be designed based on the strip strength,

therefore it is critical that the strip reach its designed strength. This failure mode can only occur if the anchor design and details are adequate to develop the full strength of the strip. CFRP anchor rupture implies that the anchor was not large enough or other aspects of the anchor detailing were not adequate to develop strip strength. Delamination between the CFRP strip and the CFRP anchor fans indicated that the bond strength between the anchor and strip was not sufficient to transmit the force associated with the tensile strength of the strip to the anchors. This can happen for two main reasons: 1) either the epoxy was of poor quality or 2) an insufficient overlap area was provided between the anchor and strip. Two distinct concrete failure modes were observed. One concrete failure mode consisted of the beam failing in a shear/tension manner (Figure 4-6 (c)). The other failure mode involved localized crushing at the anchor/concrete interface combined with a concrete cone detaching from the rest of the beam ahead of the anchor (Figure 4-6 (d)). In the latter failure mode, integrity of the beam was maintained by the steel reinforcement and the CFRP side strips, but generated sufficient movement at the anchor hole to cause some anchor pull out as well (Figure 4-6 (d)).



(a) Fracture and delamination

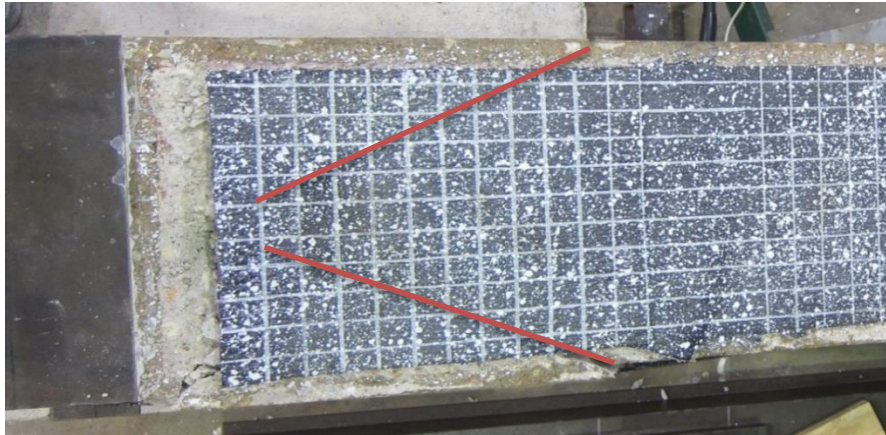


(b) Anchor rupture

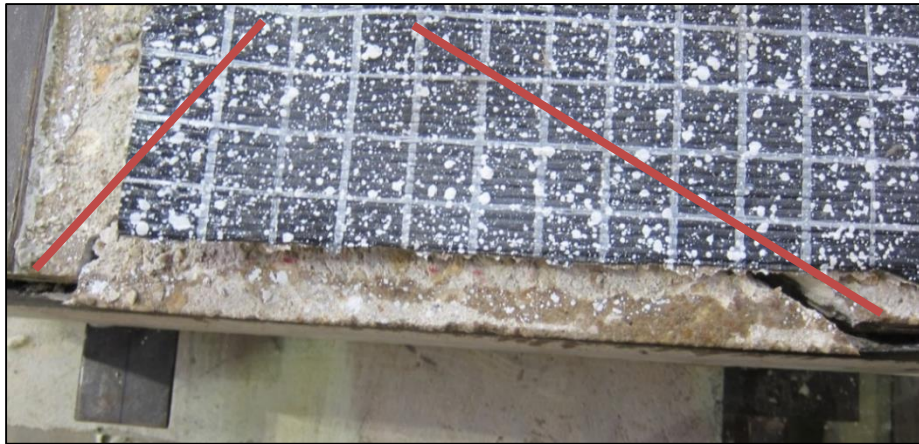


(c) Tension/Shear failure when specimen had no reinforcing bars

Figure 4-6: Failure modes



Top view



Close up of top view



End view looking at back of anchor

(d) Concrete cone/anchor pullout failure

Figure 4-6: Failure modes, (continued)

For all twelve specimens, the failure mode is plotted versus the ratio of specimen ultimate strength (P_{ult}) to specimen expected strength (P_{exp}) in Figure 4-7. The expected specimen strength was obtained as described in Section 3.6.2.1 assuming a strip fracture failure mode and using the manufacturer expected stress at fracture (Table 3-1). It is important to note that all tests that failed by strip fracture did so at loads exceeding the expected strength. This finding indicates that within the range of parameters tested, as long as strip fracture can be achieved, the expected strength will also be reached.

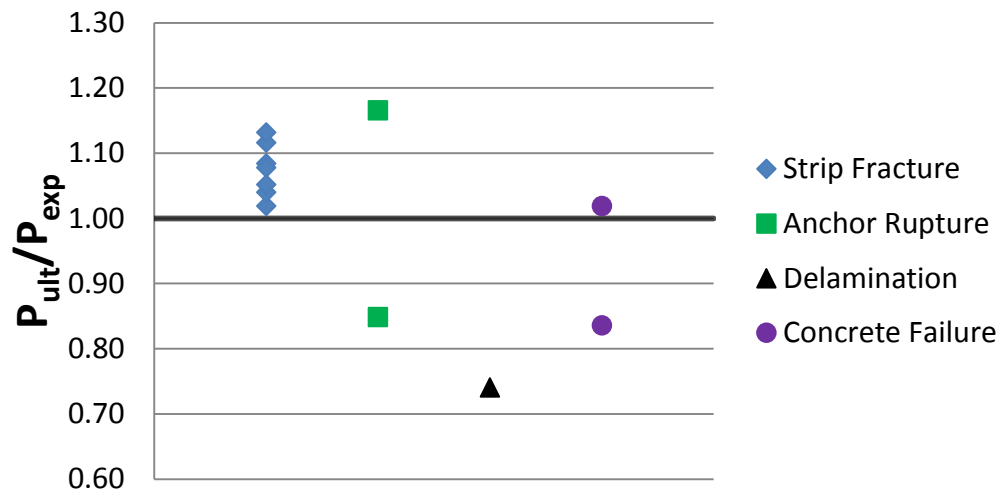


Figure 4-7: Failures modes versus strength of test specimens

4.3 TEST RESULTS

In Table 4-1, strength performance measures for the twelve tests conducted are summarized. The performance measures were used to evaluate the influence of specific parameters on strip and anchor strength. The performance measures in Table 4-1 are defined as follows:

P_{ult} The ultimate applied load at failure.

P_{exp}	The expected beam load at failure; calculated as described in Section 3.6.2.1 using the expected rupture stress for the CFRP strip provided by manufacturer (σ_{exp} = 143 ksi, Table 3-1).
F_{ult}	The anchored strip tension force at mid-span; calculated by equilibrium at ultimate load (P_{ult}) as described in Section 3.6.2.1.
σ_{ult}	The strip stress at mid-span; evaluated at ultimate load as F_{ult}/A_{CFRP} in which A_{CFRP} is the laminate cross-sectional area of the CFRP strip.

Table 4-1: Summary of strength performance measures

Test #	Test ID	P_{ult}	P_{exp}	P_{ult} / P_{exp}	F_{ult}	σ_{ult}	Failure Mode
1	S-5-1-S-6	14.1	12.1	1.17	16.7	165	Anchor Rupture
2	S-8-1-M-7	20.8	19.2	1.08	24.8	154	Strip Fracture
3	S-10-2-S-6	25.8	23.9	1.08	31.0	153	Strip Fracture
4	D-5-1-L-6	17.7	24.0	0.74	21.2	104	Delamination
5	S-10-1-M-9	24.4	24.0	1.02	29.1	144	Strip Fracture
6	D-10-2-L-6	39.6	47.4	0.84	47.8	118	Concrete
7	D-5-1-L-12	26.5	23.7	1.12	32.0	159	Strip Fracture
8	D-10-1-L-12	48.5	46.6	1.04	59.5	149	Strip Fracture
9	D-10-2-L-12	52.8	46.6	1.13	65.0	162	Strip Fracture
10	D-10-1-M-12	46.9	46.0	1.02	58.3	146	Concrete
11	D-10-1-M-12-c	39.0	46.0	0.85	48.3	120	Anchor Rupture
12	T-5-1-M-18	36.7	34.9	1.05	45.2	151	Strip Fracture

4.3.1 Effects of the Anchor Fan Overlap Length

The anchor-fan overlap length did not influence the overall behavior of the anchored CFRP system when sufficient length was provided to preclude delamination between the anchors and the strips. This minimum overlap length can be determined by dividing the strip expected tensile strength by the manufacturer provided design interface bond stress; which was 500 psi for the materials used in this study.

On Figure 4-8 the estimated anchor/strip interface bond stresses at ultimate load is plotted for all tests, conservatively assuming that the anchors resisted the full strip load. Two specimens were designed to reach an interface bond stress in excess of 500 psi at the specimen expected strength (Specimens D-5-1-L-6 and D-10-2-L-6). Specimen D-5-1-L-6 failed due to delamination, while Specimen D-10-2-L-6 failed in the concrete as highlighted in Figure 4-6(c). In Specimen D-5-1-L-6, a delamination failure occurred between the anchors and the CFRP strip at an estimated bond stress just over 700 psi. Figure 4-8 indicates that none of the specimen failed by delamination below a bond stress of 700 psi. However, given the limited number of tests conducted in this study, the manufacturer provided limit of 500 psi is deemed appropriate for designing the overlap length between anchors and strips for the material used. It is important to note that the design bond stress may be different for materials from other manufactures; therefore 500 psi should not be assumed for all CFRP and epoxy materials. The highest experimental bond stress was 800 psi in Specimen D-10-2-L-6 that did not fail by delamination.

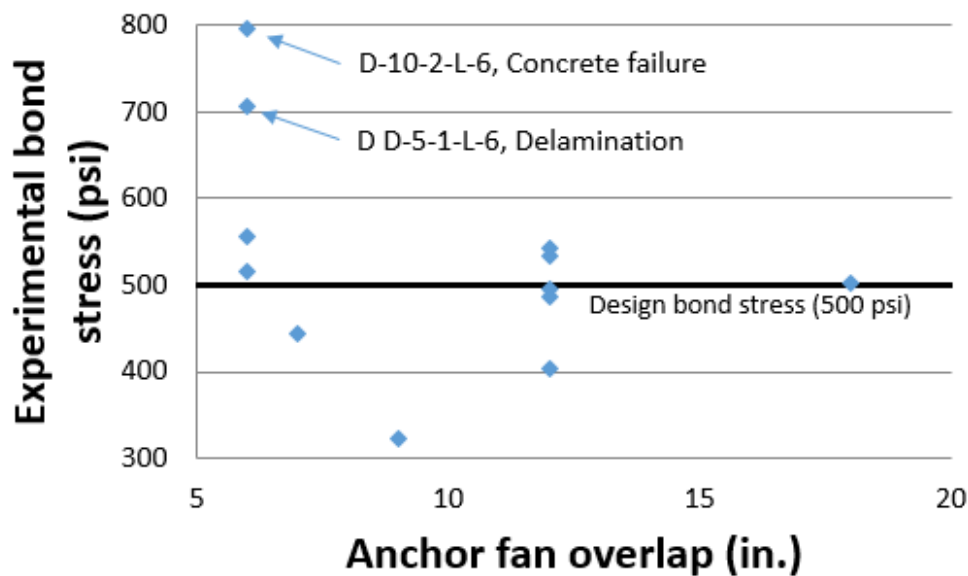


Figure 4-8: Experimental bond stress between CFRP anchors and strip at ultimate load

4.3.2 Effects of the Chamfer Radius of Anchor Hole

The chamfer radius of the anchor hole influenced the response of the anchored CFRP system in two ways: 1) it altered the strain distribution across the width of the anchored strip, and 2) it determined the strength of the anchors at the edge of the hole. An anchor-hole chamfer radius (R_c) equal to 1.4 times the hole radius was effective in all cases and allowed the anchors to develop the full strength of the strips.

Two specimens were designed to have all parameters nominally identical, except for the anchor-hole chamfer radius (D-10-1-M-12 and D-10-1-M-12-c). Both specimens used one anchor to develop a 10-in. wide strip with two layers of CFRP fabric. Both specimens had an AMR of 2. One specimen had a chamfer radius equal to 1.4 times the anchor hole radius, D-10-1-M-12, while the other, D-10-1-M-12-c, used a chamfer radius of 0.5-in. corresponding only to 0.8 times the radius of the anchor hole. The specimen with the smaller chamfer radius failed prematurely by anchor rupture at the chamfer, likely due to high strain concentrations in the anchor fibers at the chamfer. The specimen with the larger radius failed in the concrete. However, in the latter specimen the CFRP strip developed a stress larger than its expected fracture stress prior to concrete failure.

Strain gauges were placed at mid-span across the width of the strip to measure longitudinal strip strains in specimens D-10-1-M-12 and D-10-1-M-12-c (Figure 4-9). The average strain in the gauges is plotted versus the applied load in Figure 4-10 for each of the specimens. As can be seen in the figure, both specimens had almost identical average strip strains at all load levels up to the point of anchor rupture in Specimen D-10-1-M-12-c (Figure 4-10). The strains recorded by each gauge are plotted versus the applied load for both specimens in Figure 4-11 and Figure 4-12. As can be seen in the figures, the anchors with the larger chamfer radius distributed strains more evenly across the CFRP strip width than the anchor with the lower chamfer radius. The anchors with the smaller chamfer

radius generated larger differences between strains recorded close to the strip centerline and those closer to the strip edges. These strain concentrations may have contributed to the premature failure of the anchor with the small chamfer radius.

These findings therefore indicate that larger chamfer radii can not only increase anchor strength but also improve the distribution of stresses across the width of the strips they develop.

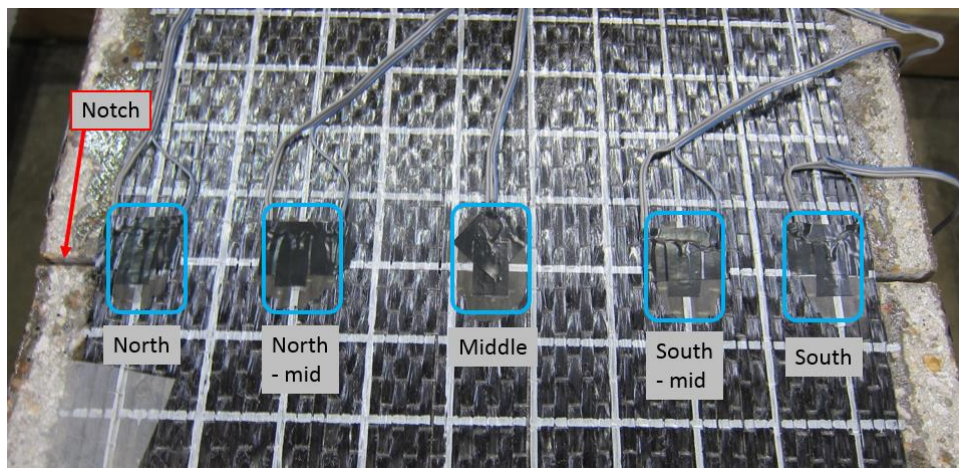


Figure 4-9: Location of strain gauges

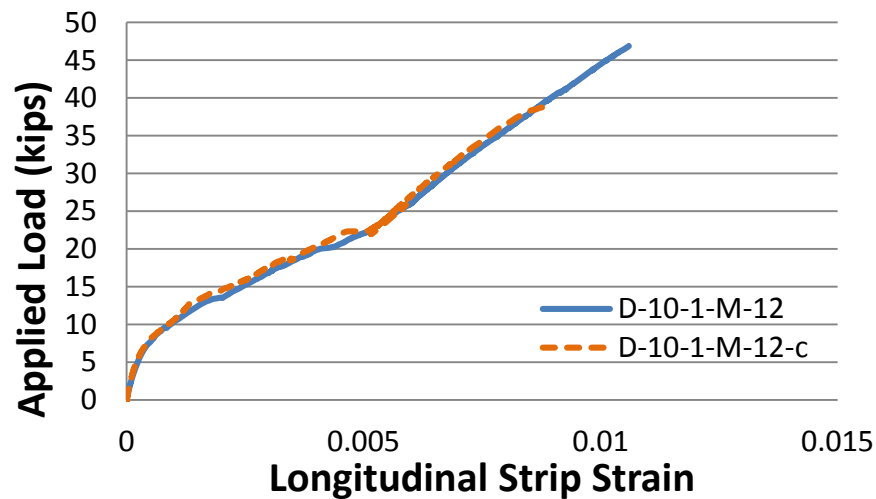


Figure 4-10: Comparison of strains for different chamfer radii for specimens D-10-1-M-12 and D-10-1-M-12-c

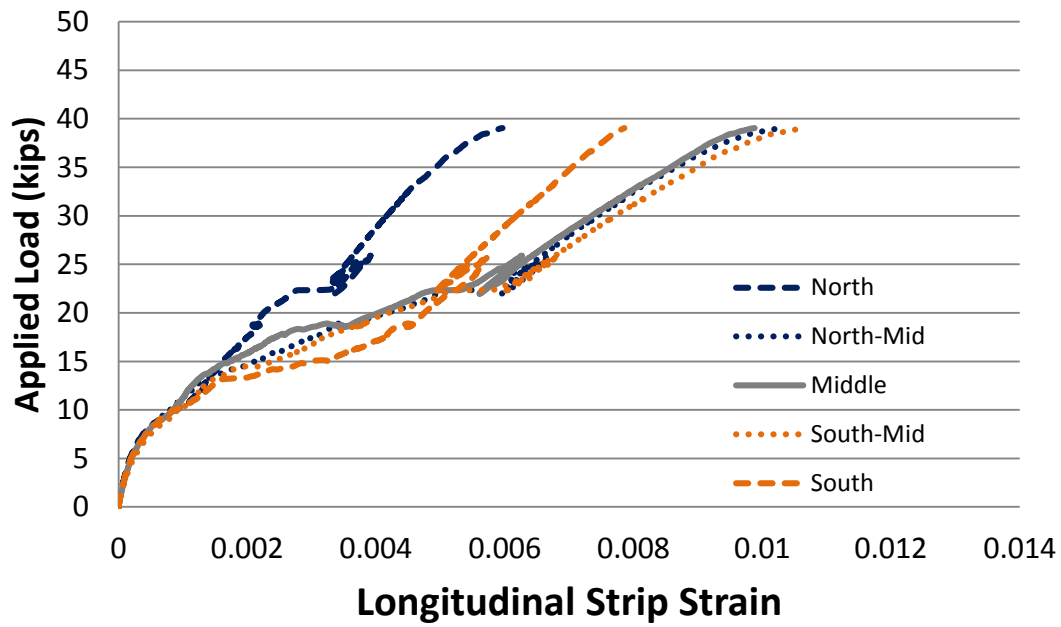


Figure 4-11: Strains across a 10" strip with a small anchor-hole chamfer radius (Specimen D-10-2-M-12-c)

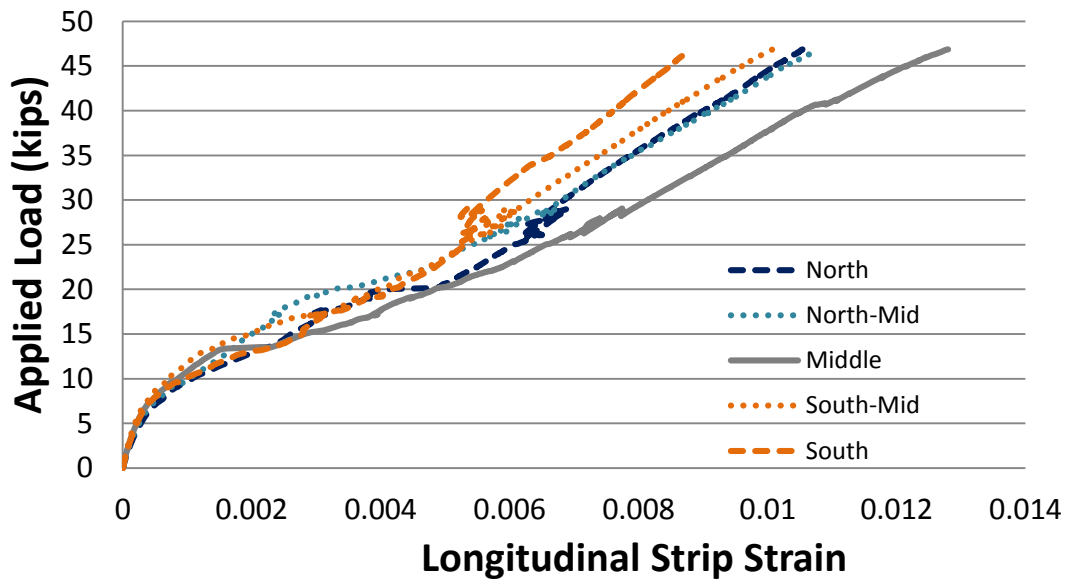


Figure 4-12: Strains across 10" strip with large chamfer radius (Specimen D-10-2-M-12)

4.3.3 Effects of CFRP Strip Thickness or Number of Fabric Layers

The effects of strip thickness or the number of layers in a strip were inconclusive with respect to strip stress at strip fracture. Up to three layers of CFRP were tested and it was found that regardless of the number of layers, the strips could be developed to fracture by CFRP anchors. However, with increasing numbers of fabric layers or strip thickness, the fan overlap length should be increased proportionally to avoid delamination failures. A practical limit on strip thickness may be governed by the length of the required anchor-fan overlap length. With three layers of CFRP fabric in this study, an overlap length of 18-in. was needed, which may be impractical in some strengthening applications.

When comparing results from tests with 5-in. wide strips, increasing the number of strip layers, or the strip thickness, resulted in lower ultimate stresses at strip fracture as shown in Table 4-2. However, all other parameters were not kept the same in the tests listed in Table 4-2. Particularly, the AMR varied between the tests. However, when observing the difference in 10-in. strips with one and two layers, the trend was reversed. Regardless of the number of anchors per strip width, the double layered 10-in. wide strips fractured at a higher stress than the strips with only one layer of fabric (Table 4-3).

Table 4-2: Effects of the number of strip layers on the ultimate stress in 5-in.wide strips

Specimen Name	Strip Width (in)	Number of layers	AMR	Ultimate Stress (ksi)	Failure mode
S-5-1-S-6	5	1	1.7	165	Anchor Rupture
D-5-1-L-12		2	2.8	159	Strip Fracture
T-5-1-M-18		3	2	151	Strip Fracture

4.3.4 Effects of Strip Width and Anchor Tributary Width

Test results have demonstrated that one CFRP anchor was able to fracture a strip having a width of 10-in. and a tensile force of about 60 kips (2 layers of CFRP fabric). However, test results also clearly indicated that wider strips fractured at lower stresses than narrower strips (Table 4-3). In fact, 10-in. strips with one anchor fractured on average at a 9.5% lower ultimate stress compared to 5-in. strips (Table 4-3). This trend also holds when multiple CFRP layers are used in the strips. On the other hand, when comparing the stress at fracture of 10-in. strips with two anchors across the width and that of 5-in. strips with one anchor across the width, the fracture stresses are much closer (2.8% difference). It appears that the strip width developed per anchor, or anchor tributary width, plays a role in determining strip stress at fracture. This trend is seen for strips with two layers of CFRP material as well (Table 4-3).

Table 4-3: Effect of strip width

Test #	Test ID	Number of layers (n_l)	Width of strip (w_f)	Number of anchors (n_a)	Width of strip per anchor ($w_{f,A}$)	Stress at failure (ksi)	Failure mode
1	S-5-1-S-6	1	5	1	5	165	Anchor rupture
3	S-10-2-S-6		10	2	5	153	Strip Fracture
5	S-10-1-M-9		10	1	10	144	Strip Fracture
7	D-5-1-L-12	2	5	1	5	159	Strip Fracture
9	D-10-2-L-12		10	2	5	162	Strip Fracture
8	D-10-1-L-12		10	1	10	149	Strip Fracture

When using one anchor to develop a 10-in. strip, the largest longitudinal strains occurred consistently along the centerline of the strip (Figure 4-13). Both edge strain gauges (north and south) recorded significantly smaller strains than the centerline strain. Using two anchors over a 10-in. strip width instead of one produced a much different strain

profile. Figure 4-14 shows how the centerline strain is no longer the largest when two anchors are used and that the strain variation at any given load is smaller for two anchors than for one anchor.

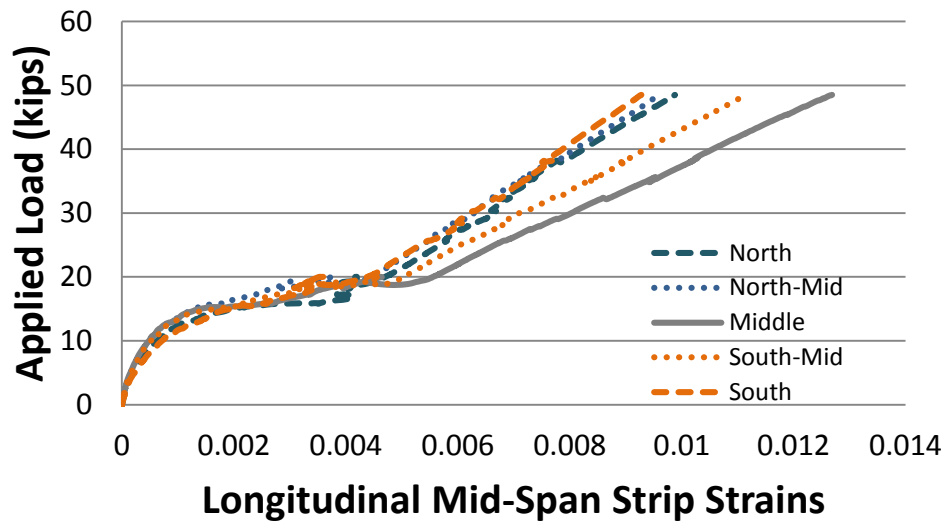


Figure 4-13: Strains for a 10-in. wide strip with one anchor from strain gauges
(Specimen D-10-1-L-12)

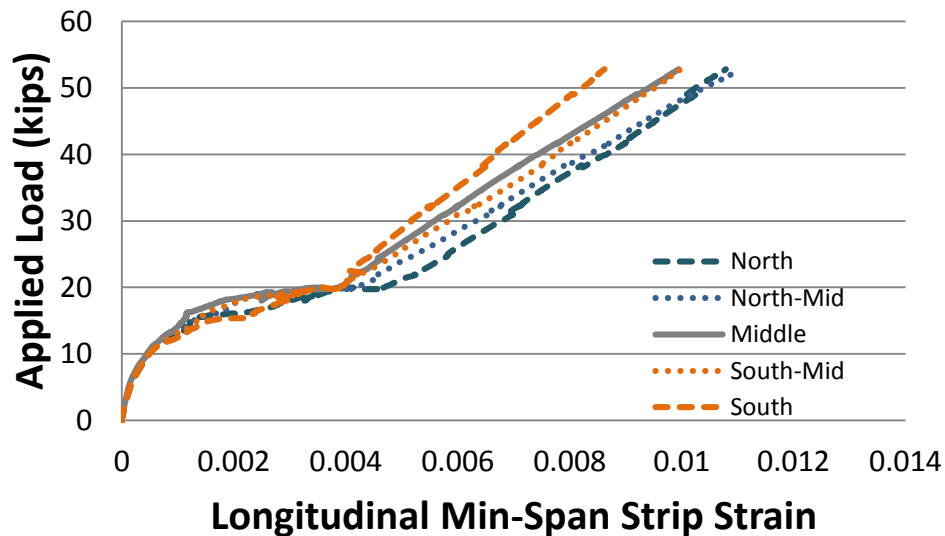


Figure 4-14: Strains for a 10-in. wide strip with two anchors from strain gauges
(Specimen D-10-2-L-12)

Surface strain data from optical measurements was also used to evaluate the effectiveness of CFRP anchors in distributing strains across the width of CFRP strips. Longitudinal strains were evaluated across the width of the CFRP strips between the anchor fans from movements of surface targets. The longitudinal strain across 13 targets was obtained for each target row to determine the strain in each row across the width of the CFRP strips (Figure 4-15).

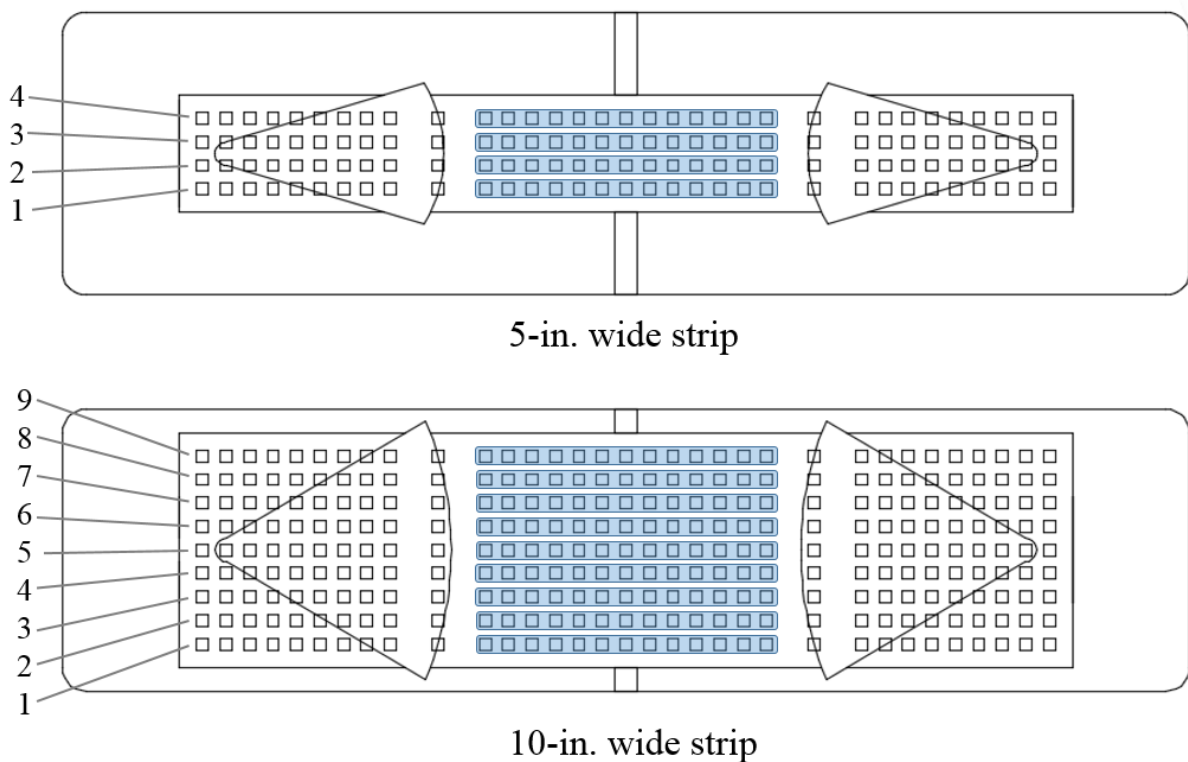
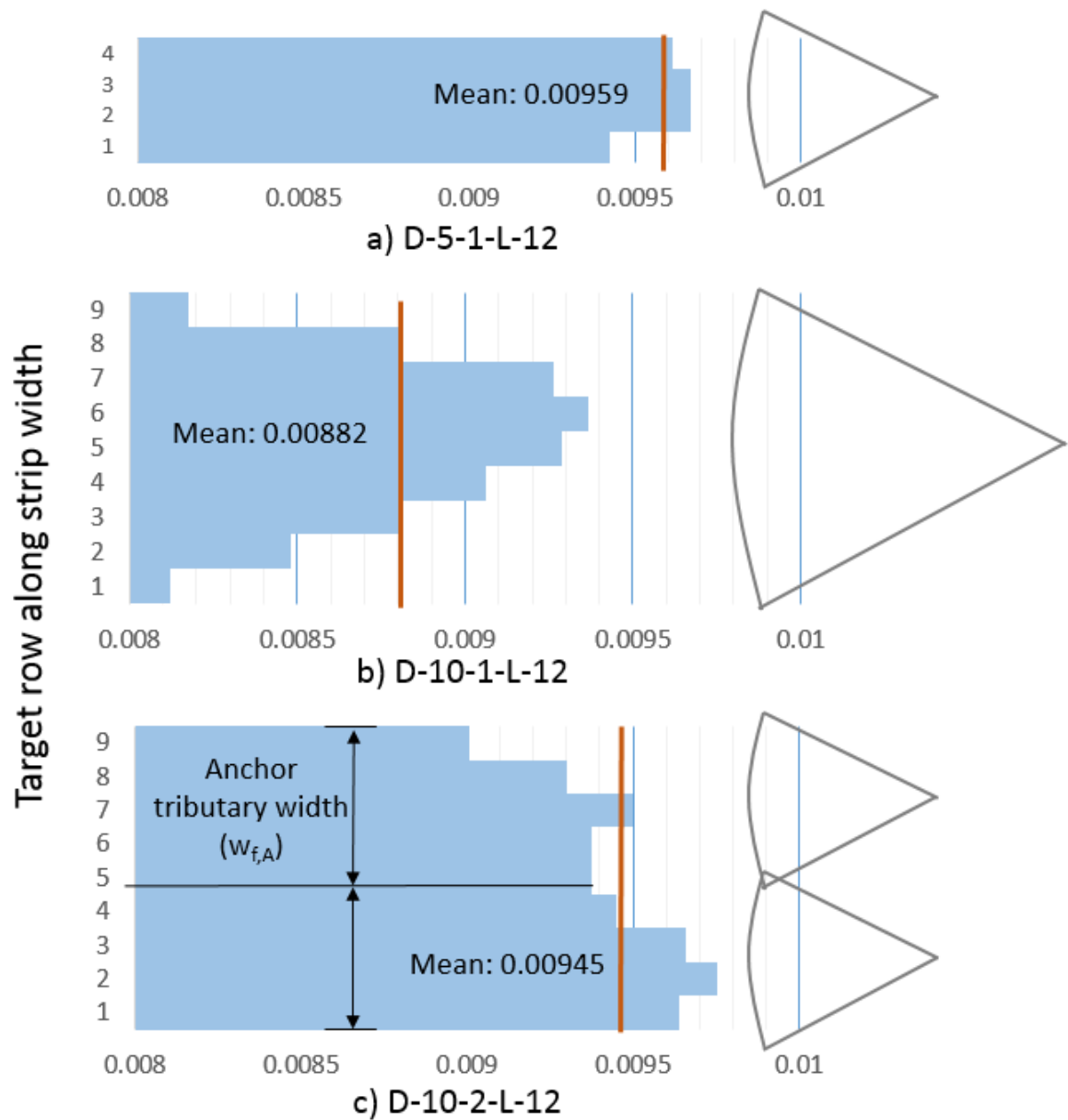


Figure 4-15: Strain rows used in analysis

One or two anchors were used per strip width in this study, which generated anchor tributary widths of 5, 8, and 10-in. Specimens D-5-1-L-12, D-10-1-L-12, and D-10-2-L-12 had two CFRP fabric layers per strip, and had anchor-material ratios (AMR) of 2.8. Specimens D-5-1-L-12 and D-10-2-L-12 had an anchor tributary width of 5-in., with Specimen D-5-1-L-12 having one anchor developing a 5-in. wide strip and Specimen D-

10-2-L-12 having two anchors developing a 10-in. wide strip. Specimen D-10-1-L-12 had an anchor tributary width of 10-in., with one anchor developing a 10-in. wide strip. The longitudinal strain profiles across strip width are plotted in Figure 4-16 for all three specimens just prior to strip fracture at ultimate load. Table 4-4 summarizes the minimum, maximum, mean, and range of these strains for the three tests. When using one anchor to develop a 10-in. strip (10-in. anchor tributary width), the largest longitudinal strains occurred consistently along the centerline of the strip just prior to strip fracture (Figure 4-16(b)). However, when an anchor tributary width of 5-in. was used (Specimen D-5-1-L-12 and D-10-2-L-12), a more even distribution of strains was achieved across the width of the strip (Figure 4-16, Table 4-4). The mean strain across the width of the strip just prior to strip fracture was also significantly higher in tests with the lower anchor tributary widths. Since CFRP is a brittle material, fracture of CFRP strips typically initiates when any region of the strip reaches its fracture strain. In strips where strains are more evenly distributed, or conversely where strain concentrations are minimized, the mean strain in the strip will be higher when the location of maximum strain reaches fracture. Therefore, strips developed by anchors with lower tributary widths, exhibited more even strain distributions, and resisted higher mean strip stresses at fracture than those with higher anchor tributary widths (Table 4-3).



Longitudinal strain across strip width

Figure 4-16: Longitudinal strain distributions across strip width for specimens D-5-1-L-12, D-10-1-L-12, and D-10-2-L-12

Table 4-4: Strip strain comparisons with respect to anchor tributary width

Test	D-5-1-L-12	D-10-2-L-12	D-10-1-L-12
Width of strip (in.)	5	10	10
Anchor tributary width (in.)	5	5	10
Maximum Strain	0.00967	0.00975	0.00937
Minimum Strain	0.00942	0.00901	0.00812
Range (Max-Min)	0.000245	0.000746	0.001247
Mean Strain	0.00959	0.00945	0.00882
% Difference Mean Strain	0	1.5	8.2

4.3.5 Effects of the Anchor Material Ratio (AMR)

Anchor material ratios of 1.72, 2, and 2.8 were tested in this study. Only one specimen in this series failed below its expected value by anchor rupture. The specimen that suffered anchor failure, however, had a relatively small anchor-hole chamfer radius (R_c) given the size of the anchor used, indicating that a material ratio of 2 can adequately develop the strength of CFRP strips up to 10-in. wide and having two layers of material.

Sun et al. (2016) demonstrated a positive trend between the AMR and strip stress at fracture, and demonstrated more even strain distributions in CFRP strips when larger anchor material ratios were used. These findings are corroborated in this study for wider strips, as Sun et al. (2016) only tested strips up to 5-in. wide. Specimens D-10-1-L-12 and D-10-1-M-12 were two comparable tests that used one anchor to develop a 10-in wide strip made of two layers of CFRP fabric. Specimen D-10-1-L-12 had an AMR of 2.8, while Specimen D-10-1-M-12 had an AMR of 2. In both tests, failure occurred after the strip stress exceeded the expected fracture stress of the material. However, the specimen with an AMR of 2.8 failed by strip fracture, while the specimen with an AMR of 2.0 failed in the concrete. Therefore, the strip strains could not be compared just prior to fracture, but

instead, strain distributions in the strips, measured as detailed in the previous section, were compared at two load levels in Figure 4-17 and Table 4-5. The two load levels corresponded to the load in Specimen D-10-1-M-12 just before the failure of the concrete, and the other load level was selected slightly less (46 and 40 kips, respectively).

As shown in Figure 4-17 and Table 4-5 and for both load levels, the difference between the maximum and minimum strains (or the strain range) was about 25% larger with the AMR of 2.0 as compared to that with the AMR of 2.8. This indicates that anchors with a higher AMR distribute stresses more evenly across a CFRP strip, which can result in an increase in mean strip stress at strip fracture.

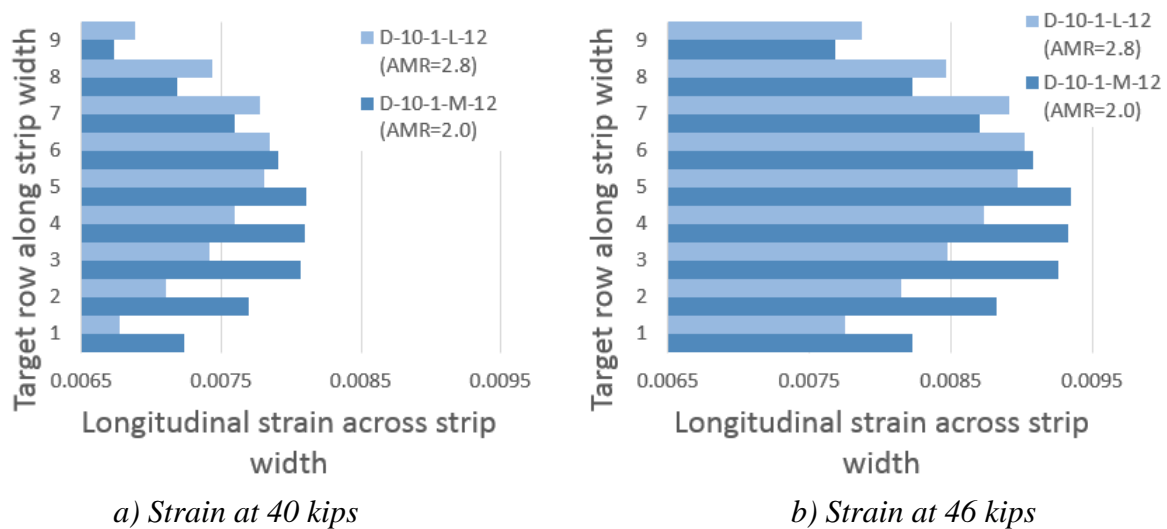


Figure 4-17: Longitudinal strain distributions across strip width at an applied load of 40 and 46 kips

Table 4-5: Strip strain comparisons with respect to AMR

Applied Load (kips)	40		46	
Test	D-10-1-L-12	D-10-1-M-12	D-10-1-L-12	D-10-1-M-12
AMR	2.8	2	2.8	2
Maximum Strain	0.00785	0.0081	0.00902	0.00935
Minimum Strain	0.00678	0.00673	0.00775	0.00768
Range (Max-Min)	0.00107	0.00137	0.00126	0.00167
Mean Strain	0.0074	0.00762	0.00848	0.00874
Difference (Max-Mean)	0.000445	0.00048	0.000533	0.000602

4.4 SIZE EFFECT RELATIONS

To investigate the effect of using wider and thicker CFRP laminate strips on the ultimate strip stress at fracture, a normalized strip area parameter is introduced. The parameter is calculated by dividing the CFRP strip laminate cross-sectional area by the number of anchors used across the strip width and the anchor material ratio.

$$\text{Normalized strip area parameter} = \alpha_s = \frac{A_{CFRP}}{n_A * AMR} \quad \text{Equation 4-1}$$

Where:

A_{CFRP} : sectional area of CFRP strip, in². = $w_s \times t_l$

w_s : width of the laminate strip

t_l : total laminate strip thickness = $n_l \times t_f$

n_l : number of fabric layers in the strip

t_f : individual strip layer laminate thickness

n_A : number of anchors across the strip width

This parameter is plotted in Figure 4-18 versus the strip stress at ultimate load for tests in this study exhibiting failure above expected fracture stress. A linear-regression

trend line is superposed on the data points and highlights a trend between size effect and strip strength. The smaller the normalized strip area parameter, the higher the strip fracture stress at ultimate load. The observed trend in Figure 4-18 indicates that the larger the CFRP strip cross sectional area developed by an anchor, the lower the stress at fracture of that strip. This size effect is attributed to the increased effectiveness of larger anchors in distributing strains evenly across CFRP strips and reducing strain concentrations. Two points in Figure 4-18 represent specimens that did not exhibit strip fracture, but had strip stresses above the expected fracture stress at failure. One specimen failed by anchor rupture at a relatively high strip stress (S-5-2-S-6), while the other exhibited concrete failure (D-10-1-M-12). The latter specimen illustrates the ability of anchored CFRP strips with a normalized strip area parameter reaching 0.2 in.² to surpass their expected strip fracture stress.

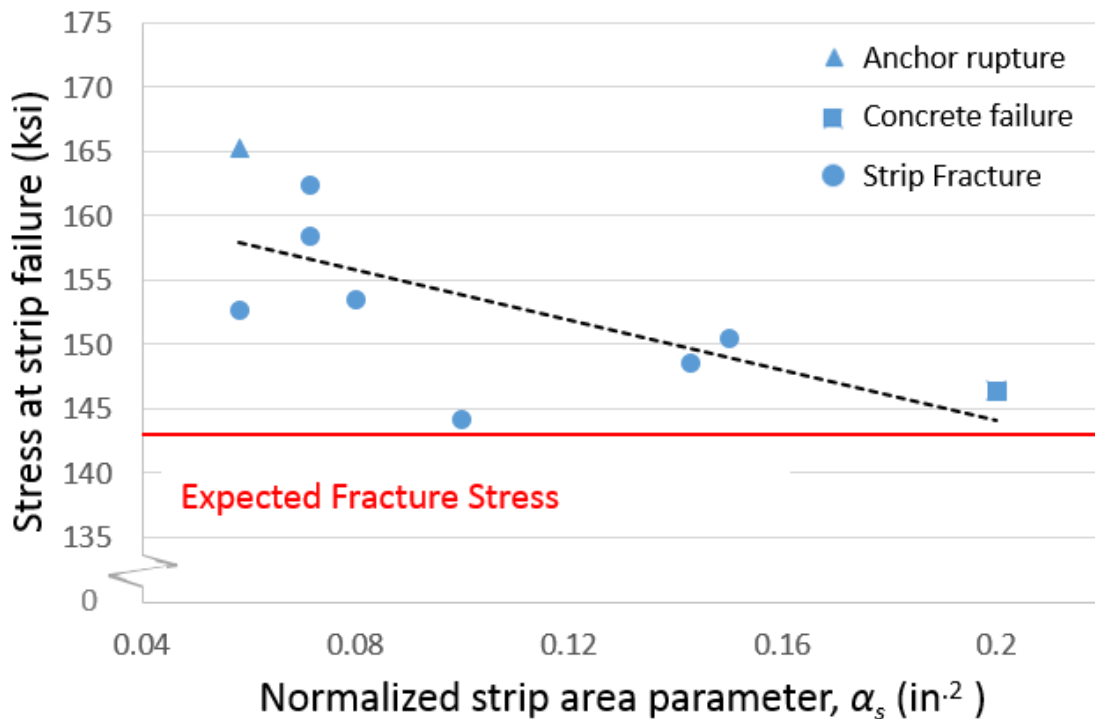


Figure 4-18: Strip fracture stress versus the normalized strip area parameter (α_s)

Data from Sun et al. (2016) for tests sustaining a strip fracture mode are added to the data from this study in Figure 4-19. Sun et al. (2016) conducted three-point loading tests much in the same fashion as was done in this study, but using smaller (6-in.x6-in.x24-in.) beams and single layered narrower CFRP strips with 3-in. or 5-in. widths. When the data from Sun et al. (2016) is introduced, the trend remains the same between strip fracture stress and the normalized strip area parameter, as seen in Figure 4-19.

The observed trend line in Figure 4-19 indicates that there may be a limit on the normalized strip area parameter beyond which the stress at fracture of CFRP strips may become lower than the expected stress at fracture. A value of $\alpha_s = 0.2 \text{ in.}^2$, corresponded to a 10-in. wide double-layer strip developed by a single anchor across its width having an AMR of 2 in this study. More testing with normalized strip area parameter greater than 0.2 in.^2 is needed to further investigate this trend.

While three tests sustained strip fracture at a strip stress slightly below the manufacture specified rupture stress of 143 ksi (Figure 4-19), no tests failed with strip stresses below the design stress value of 121 ksi. These results therefore confirm that adequately anchored CFRP strips fracture above their design stress value. For all the tests reported in Figure 4-18 all of which failed by strip fracture, the mean strip stress at fracture was 153 ksi (1.27 times the design stress and 1.07 times the expected fracture stress), with a coefficient of variation of 0.039. In addition, since test results are in agreement with manufacturer specified tensile strength values derived from coupon testing in accordance with ASTM D3039 (2014), it appears that reliable tensile strength values for anchored CFRP strips can be obtained either by testing coupons or flexurally strengthened concrete beams.

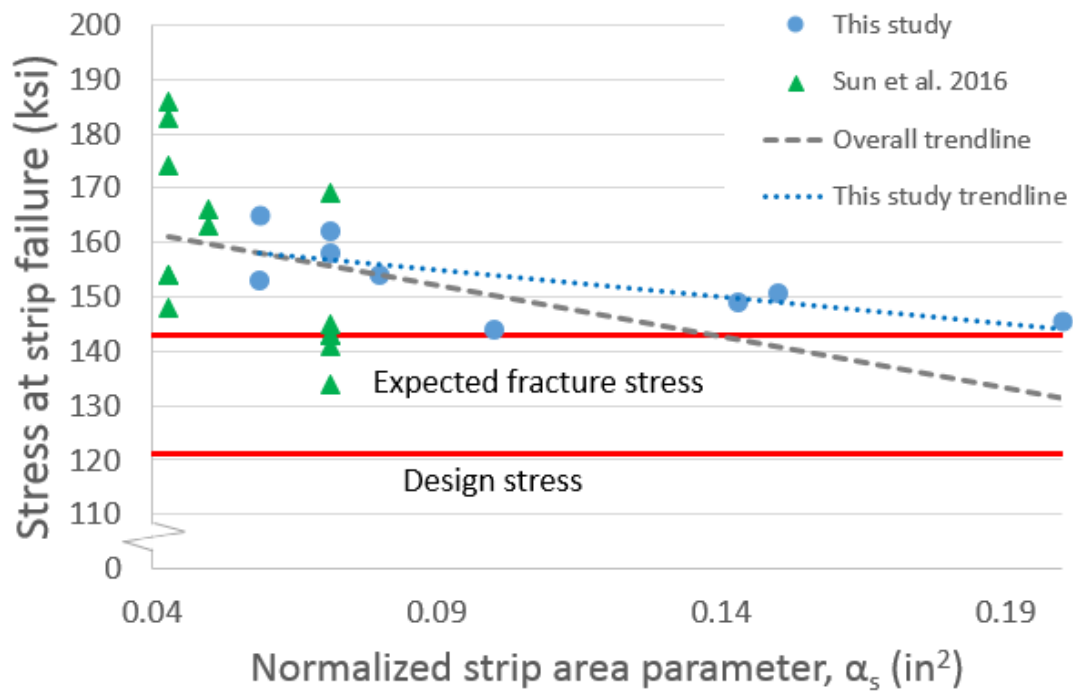


Figure 4-19: Strip fracture stress versus the normalized strip area parameter (α_s) including data from Sun et al. (2016)

Chapter 5: Design of Anchored Carbon Fiber Reinforced Polymer (CFRP) Systems

5.1 DESIGN APPROACH

Anchored CFRP strengthening systems consist of CFRP strips bonded to the surface of a concrete member where they are needed to resist tensile forces, with CFRP anchors that connect the CFRP strips to the concrete section. The overall layout of the CFRP anchored system developed in this study is shown below in both plan and isometric views in Figure 5-1 and Figure 5-2 respectively.

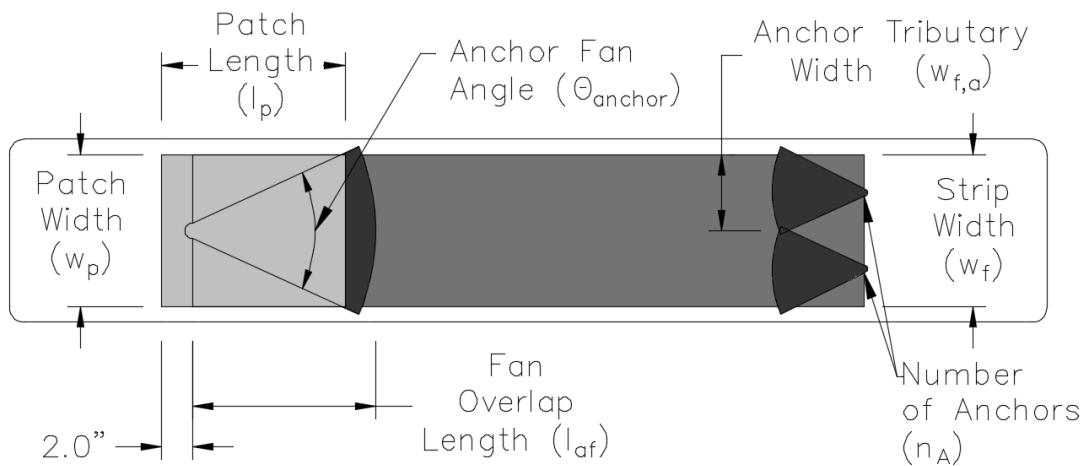


Figure 5-1: Plan view of anchor system; left: anchor prior to adding patches, right: patches over anchor

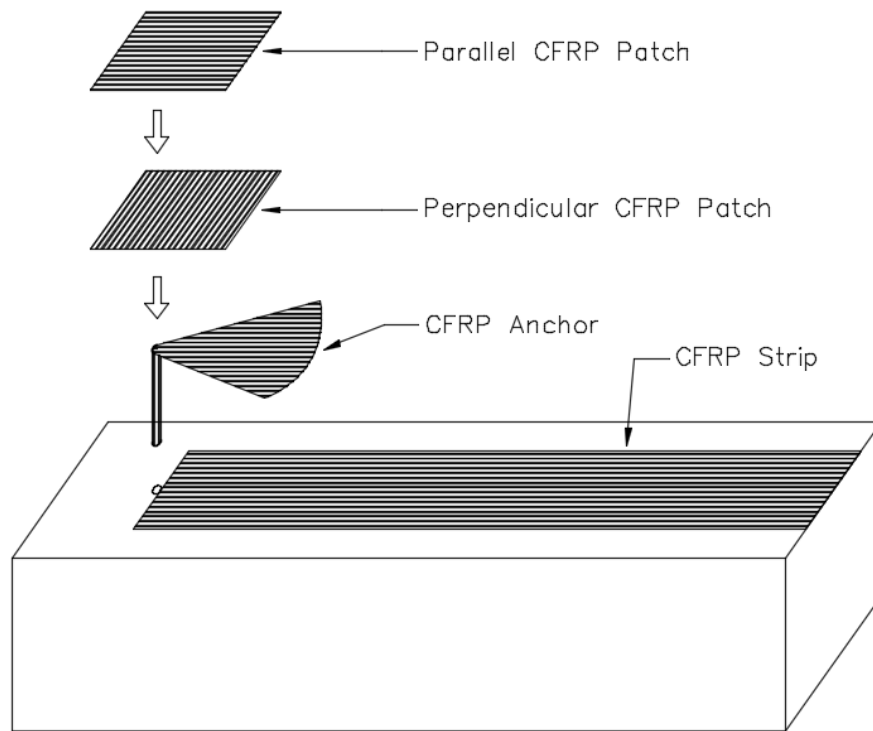


Figure 5-2: Isometric view of anchor system

CFRP strips are made of CFRP fibers embedded in an epoxy matrix to create a hardened laminate. CFRP strips are a brittle material having a modulus of elasticity that is less than half that of reinforcing steel and an expected fracture stress in the range of 140 ksi. Due to the brittle nature of CFRP materials, they are highly sensitive to stress concentrations that can be generated from changes in direction (e.g., at bends), poor installation procedures (e.g., when ripples are introduced in attaching the strips), or uneven distributions of stresses generated by the anchorage systems. CFRP strip systems fail when the first strip reaches its fracture stress, while other strips sharing load across the critical crack will have lower strains. Therefore the average strains in all loaded strips is normally lower than ultimate. For this reason, only a fraction of the CFRP strips ultimate strain is used in design. However, CFRP anchors should always be designed to develop the full tensile strength of the CFRP strips to ensure strip fracture occurs before the anchor

ruptures. This is because it is not possible to predict which strip will reach fracture strains first and which strips will not.

CFRP anchors are designed based on the cross-sectional fiber area, or tensile strength, of the strip they are developing. Due to stress concentrations that occur at the anchor-hole edge where the anchor material is bent, a significantly larger cross-sectional area of CFRP fibers is required in the anchor compared with the area of CFRP strip. In this study, this ratio of anchor to strip CFRP fiber area is recommended to be at least 2.0 to reliably achieve a strip fracture mode. This material ratio was matched to a specific anchor-hole geometry- especially the anchor-hole edge chamfer radius, to limit stress concentrations in the anchor material.

In the following sections, guidelines for designing CFRP anchors and detailing embedment holes are provided. These guidelines assume the strip and anchor materials are the same and have the same properties. The guidelines are only applicable to carbon fiber anchors. The anchor details developed in this study were shown to develop the full strength of CFRP strips. Due to the beneficial effects of adequate bonding of strips to concrete, such as reducing stress concentrations in anchors and reducing crack widths in concrete members, it is recommended to always prepare the concrete surface for bonding the strips to the concrete.

5.2 DESIGN GUIDELINES

5.2.1 Notations and Definitions

AMR_D = design anchor material ratio = the ratio of anchor fiber material to that of the strip it is developing. This ratio is recommended to be at least equal to 2.0.

AMR_A	=	actual anchor material ratio = the ratio of anchor fiber material to that of the strip it is developing. This ratio is calculated after anchors have been chosen and is the true AMR for the specified anchors.
A_{Eqv}	=	anchor equivalent laminate cross-sectional area, in. ² ; this area is needed to determine the required fiber area in anchors as well as determine the diameter of the anchor hole.
d_h	=	diameter of the anchor hole, in.
d_e	=	embedment depth, in.
$f_{u,Exp}$	=	manufacturer specified expected tensile stress at fracture of the CFRP laminate material, psi
l_a	=	total anchor length
l_{af}	=	CFRP anchor fan overlap length, in.
l_{af-min}	=	minimum permitted anchor fan length based on the specified design values for the inter-laminate bond stress capacity (σ_b), in.
n_a	=	number of manufactured anchor per anchor hole
n_A	=	number of anchors per strip width
n_l	=	number of laminate layers in the CFRP strip
R_c	=	anchor edge chamfer radius, in.
T_f	=	$(w_f n_l t_l f_{u,Exp})$ = strip tensile capacity based on the manufacturer specified expected tensile stress at fracture, lbs.
t_f	=	specified thickness of the laminate material used in the CFRP strip, in.
t_l	=	$(n_l t_f)$ = total thickness of the CFRP strip, in.
w_f	=	width of the CFRP strip, in.
$w_{f,A}$	=	the anchor tributary width, in.

$\gamma_{s,Sp}$	=	manufacturer specified fiber weight per surface area of the laminate material, oz/in. ²
$\gamma_{s,Exp}$	=	1.25 $\gamma_{s,Sp}$ = expected fiber weight per surface area of the laminate material, oz/in. ²
λ_s	=	weight of fibers in the strip per length, oz/in.
λ_A	=	specified weight of fibers in the anchor per length, oz/in.
λ_{A-Req}	=	required weight of fibers in the anchor per length, oz/in.
σ_b	=	specified design value for the inter-laminate bond stress capacity, psi.
θ_{anchor}	=	CFRP anchor fan angle, degrees (recommended not to exceed 60°)
l_p	=	length of CFRP patch, in.
w_p	=	width of CFRP patch, in.

5.2.2 Sizing CFRP Anchors

The cross-sectional area ($w_f n_l t_f$) of a CFRP strip can be determined based on the force it is required to resist in a particular strengthening project. The width of a CFRP strip (w_f) as well as the number of laminate layers (n_l) are determined according to the required strip tensile strength (T_f). Equation 5-1 can be rearranged to solve for either the width of strip or number of laminate layers required.

$$T_f = w_f n_l t_f f_{u,Exp} \quad \text{Equation 5-1}$$

Anchor design is based on the tributary strip width the anchor is engaging ($w_{f,A}$). For instance, in a 10 in. wide strip developed by two anchors, the anchors have the same tributary width as a single anchor developing a 5 in. strip. In both cases, the anchors will

be designed to develop the strength of a 5 in. wide strip. The anchor tributary width is determined based on the desired number of anchors per strip.

$$w_{f,A} = w_f / n_A \quad \text{Equation 5-2}$$

In this study, CFRP anchors were found to effectively develop the strength of CFRP strips with tributary widths ranging from 5 to 10 in. Anchors were, however, more effective in developing narrower tributary widths, resulting in higher strip stresses at fracture. This size effect is attributed to anchors generating more even stress distributions in narrower strips, or conversely smaller stress concentrations in narrower strips. Selecting smaller anchor tributary widths is therefore recommended for improved performance. A balance should be struck between improved performance and increasing the number of anchors and the associated increased construction time and cost. It is not recommended to use an anchor tributary width greater than 10 in.

The minimum required weight of anchor fibers per unit length ($\lambda_{m,A-Req}$) can then be evaluated. $\lambda_{m,A-Req}$ is equal to the weight per unit length of dry fiber in the strip width developed by the anchor multiplied by the design anchor material ratio (AMR_D). As discussed previously, an anchor material ratio of at least 2.0 is recommended.

$$\lambda_{A-Req} = AMR_D \times (w_{f,A} n_l \gamma_{s,Exp}) \quad \text{Equation 5-3}$$

Anchors having a specified fiber weight per unit length (λ_A) not less than (λ_{A-Req}) should be selected.

$$\lambda_A \geq \lambda_{A-Req} \quad \text{Equation 5-4}$$

Once the anchors are selected and provided fiber weight per unit length (λ_A) is known, the actual anchor material ratio can be calculated.

$$AMR_A = \frac{\lambda_A}{w_{f,A} n_l \gamma_{s,Exp}} \quad \text{Equation 5-5}$$

It is important to note that the required fiber weight of the anchor is based on the expected dry fiber weight per surface area of the laminate ($\gamma_{s,Exp}$). When weighting laminate fiber sheets, the expected fiber weight was found to be about 25% higher than the minimum fiber weight per surface area specified by the manufacturer ($\gamma_{s,Sp}$). Since the CFRP laminate fiber weights tend to run significantly higher than the minimum weight provided by the manufacturer ($\gamma_{s,Exp} = 1.25 \gamma_{s,Sp}$), however, the expected weight should always be used in determining the fiber weight of the anchors.

The anchor equivalent laminate cross-sectional area is required for determining the anchor-hole diameter and can be evaluated as follows:

$$A_{Eqv} = AMR_A \times (w_{f,A} n_l t_f) \quad \text{Equation 5-6}$$

5.2.3 Anchor Fan Details

Anchor fan details are illustrated in Figure 5-3.

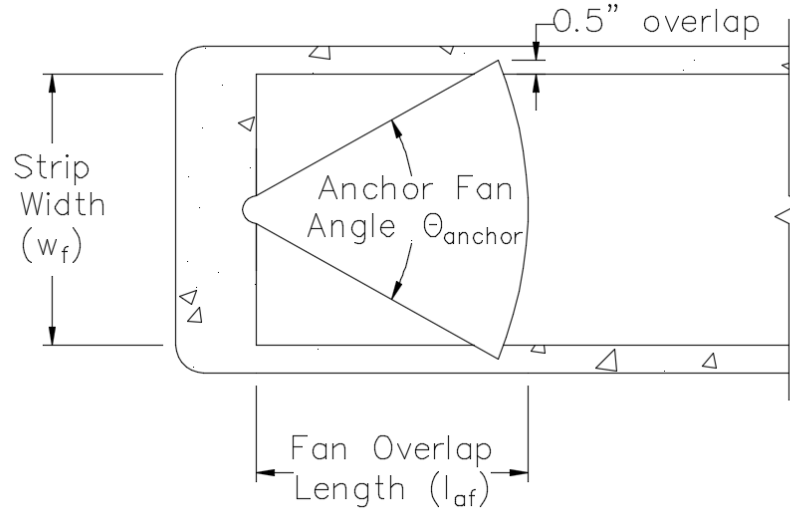


Figure 5-3: Anchor fan details

An effective anchor fan needs to extend 0.5 in. past the edges of the CFRP strip. In the case of multiple anchors per strip width, the anchor fans should overlap by at least 0.5 in. at their ends. This ensures that the entire width of the strip is engaged. The length of an anchor fan is directly related to the width it needs to span and the selected fan angle. The length of an anchor should also be sufficient to preclude an interlaminar bond failure between the anchor and the strip it is developing. The minimum anchor fan length should therefore be evaluated first based on the manufacturer specified interlaminar bond stress capacity (σ_b).

$$l_{af-min} = \frac{T_f}{w_f \times \sigma_b} \quad \text{Equation 5-7}$$

Equation 5-7 assumes that the contact area between anchors and strip is a rectangle with length equal to fan length and width equal to strip width. This is primarily because the CFRP patches placed on top of the anchors contribute to transferring stresses.

Once the minimum anchor length is determined, the actual length of the anchor can be obtained by selecting a fan angle (θ_{anchor}) smaller or equal to 60° using the following relation:

$$l_{af} = \frac{(w_f/2) + 0.5}{\tan\left(\frac{\theta_{anchor}}{2}\right)} \geq l_{af-min} \quad \text{Equation 5-8}$$

In general, a smaller fan angle produces a more gradual transfer of force to the anchor. Kim (2011) recommended a fan angle less than 60° for effective transfer of tensile loads from CFRP strips. Results from this study further support that recommendation. Considering that the tensile load transfer from the outer fibers in a strip is less efficient as the angle between the CFRP strip fiber and the anchor-fan fibers increases, a maximum anchor-fan angle of 60° is recommended for anchor design.

5.2.4 Anchor Hole Details

Parameters for anchor hole details are illustrated in Figure 5-4.

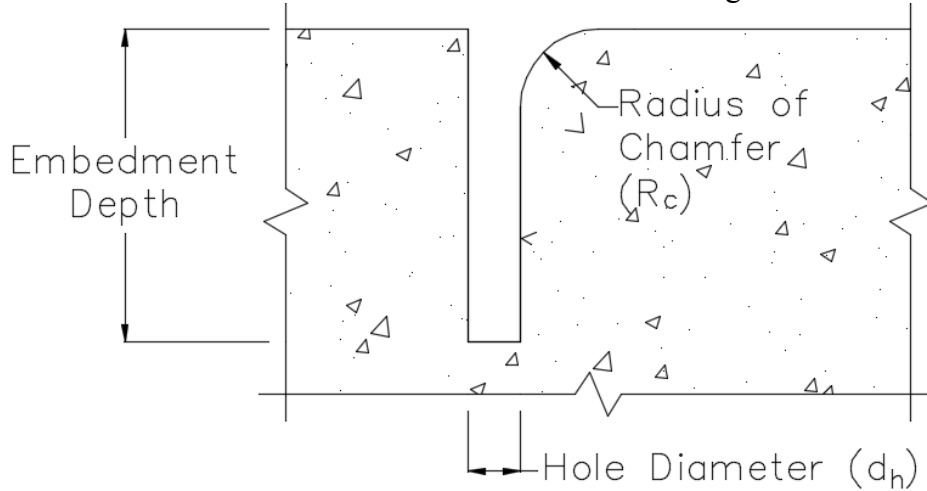


Figure 5-4: Anchor hole details

5.2.4.1 Diameter of Anchor Hole

An anchor hole area at least 1.4 times larger than the equivalent laminate area of CFRP anchors (A_{Eqv}) was previously recommended (Pham, 2009). This continues to be the recommendation and was supported throughout testing. While previous work and some work in this study tested relatively small anchors (developing a single layered 5 in. strip), tests conducted in this study on larger anchors developing a double layered 10 in. wide strip further demonstrated that the factor of 1.4 is applicable to larger anchors. To determine the required diameter of the anchor hole, Equation 5-9 can be used.

$$d_h = \sqrt{\frac{4 \times 1.4 \times A_{Eqv}}{\pi}} \quad \text{Equation 5-9}$$

5.2.4.2 Hole Edge Chamfer Radius

To reduce stress concentrations at the edge of an anchor hole, the hole edge can be rounded. A chamfer radius of 0.5 in. as recommended by Pham (2009) was used effectively in Sun et al. (2016) where anchors having an anchor material ratio (AMR) not less than 2.0 developed strips with widths not exceeding 5in. When larger anchors were tested in this study (for a double layered 10 in. wide strip), the 0.5 in. chamfer radius was found to be inadequate. A relation for increasing the chamfer radius (R_c) with increasing anchor size or hole diameter is presented below.

$$R_c = 1.4 \frac{d_h}{2} \geq 0.5 \text{ in.} \quad \text{Equation 5-10}$$

5.2.4.3 Embedment Depth

In TxDOT project 0-6306 it was recommended that a 6 in. anchor embedment depth be used. In this study, anchor embedment depths of 4 and 6 in. were successfully used. While the embedment depth was not found to be a significant factor affecting the strength of anchored CFRP systems, a 6 in. anchor embedment depth is recommended to ensure proper penetration past the concrete cover. In cases where a 6 in. embedment depth is impractical, a depth as low as 4 in. may be used. In all cases, however, the anchors need to be embedded at least 2 in. into the concrete core of a reinforced concrete member.

5.2.5 Anchor Patch Geometry

The patches over the CFRP anchor are vital for proper stress transfer from the strip to the anchor. Anchor patches should have the same width as the CFRP strip ($w_f = w_p$) and the same length as the CFRP anchor ($l_{af} = l_p$). The patches should start 2 in. behind the anchor hole (Figure 5-1). This distance helps distribute stresses around the anchor hole and prevent premature anchor rupture and delamination between anchor and strip.

5.3 DESIGN EXAMPLE

The design of an anchored CFRP system is given next for a given strengthening scenario, which requires a factored strip strength (T_f) of 28,000 lbs. The material properties of the CFRP fibers and laminate are:

Laminate expected fracture stress: $f_{u,Exp} = 143,000$ psi

CFRP laminate thickness: $t_l = 0.02$ in.

Weight of dry fibers in the laminate per unit surface area $\gamma_{s,Sp} = 9.3$ oz/yd.²

$$\gamma_{s,Exp} = 1.25\gamma_{s,Sp} = 11.6 \frac{\text{oz}}{\text{yd.}^2} = 0.00897 \frac{\text{oz}}{\text{in.}^2}$$

1/2" CFRP anchor fiber weight per unit length, $\lambda_A = 0.08$ oz/in.

5/8" CFRP anchor fiber weight per unit length, $\lambda_A = 0.125 \text{ oz/in}$.

In this design, one layer of CFRP and one anchor are selected. Other designs with a narrower multi-layered narrower strips or a multi-anchored wide strip can be performed following the same procedure outlined next.

1. The required width of CFRP strip (w_f) can be determined using Equation 5-1.

$$28,000 \text{ lbs} = (w_f \times 1 \times 0.02" \times 143,000 \text{ psi}) \quad w_f = 9.8" \cong 10"$$

2. Only one anchor will be used to develop the entire strip ($n_A = 1$), Equation 5-2 can be used to determine the tributary anchor width.

$$w_{f,A} = 10"/1 \quad \rightarrow \quad w_{f,A} = 10"$$

3. Once the tributary width is established, Equation 5-3 can be used to determine the required dry fiber weight per anchor (λ_{A-Req}) assuming a design anchor material ratio (AMR_D) of 2.0.

$$\lambda_{A-Req} = 2 \times (10" \times 1 \times 0.00897 \text{ oz/in}^2) \quad \rightarrow \quad \lambda_{A-Req} = 0.179 \text{ oz/in}$$

Since this weight is larger than either of the available 1/2" and 5/8" anchors for this project, the choice is made to combine two 5/8" anchors to make a larger anchor having a dry fiber weight $\lambda_A = 0.25 \text{ oz/in}^2$, which is larger than λ_{A-Req} (Equation 5-4). It is important to note that different fabrication plants may have different anchor sizes. It may also be possible to specify the exact length and weight and have the anchors fabricated. These options should be discussed with the fabrication plant. If specifying the required total weight of an anchor, multiply the total length of anchor by the required dry fiber weight per anchor ($(l_{af} + d_e) * \lambda_{A-Req}$).

Once the anchor is selected, the actual anchor material ratio must be calculated (Equation 5-5).

$$AMR_A = \frac{0.25 \text{ oz/in}}{10" \times 1 \times 0.00897 \text{ oz/in}^2} \quad \rightarrow \quad AMR_A = 2.8$$

4. The anchor equivalent laminate area is then calculated for use later in determining the required anchor hole diameter (Equation 5-6).

$$A_{Eqv} = 2.8 \times (10" \times 1 \times 0.02") \quad \rightarrow \quad A_{Eqv} = 0.56 \text{ in}^2$$

*it is important to note that nominal anchor diameters provided by the manufacturer (i.e., 1/2-in. and 5/8-in.) **should not** be used in calculating anchor area for prefabricated anchors. The nominal dimensions are not exact and will provide incorrect areas if used in design.

5. The anchor fan geometry is determined using Equation 5-7 and Equation 5-8

$$l_{af-min} = \frac{28000 \text{ lbs}}{10" \times 500 \text{ psi}} \quad \rightarrow \quad l_{af-min} = 5.6" \cong 6"$$

$$l_{af} = \frac{(10"/2) + 0.5"}{\tan\left(\frac{60^\circ}{2}\right)} \geq 6" \quad \rightarrow \quad l_{af} = 9.5" \cong 10"$$

Assuming an anchor fan angle of 60° provides a sufficient anchor length to satisfy interlaminar bond requirements between the strip and anchor fan. An anchor length of 10 in. is selected.

6. The diameter of the anchor hole is determined based on the equivalent anchor area and Equation 5-9.

$$d_h = \sqrt{\frac{4 \times 1.4 \times 0.56 \text{ in}^2}{\pi}} \quad \rightarrow \quad d_{hole} = 0.999" \cong 1.0"$$

Hole diameters should be rounded up to the nearest larger drill bit size.

7. The chamfer radius at the hole edge is given by Equation 5-10.

$$R_c = 1.4 \times (1"/2) \geq 0.5" \quad \rightarrow \quad R_c = 0.7" \cong 0.75"$$

Round the chamfer radius up to the nearest 8th of an inch. This is approximate because chamfer radius rounding is generally done by hand.

8. Embedment depth is chosen to be 6".

9. The total anchor length needs to be 10" + 6" = 16" ($l_{af} + d_e$).

The total anchor weight is 0.25 oz/in * 16" = 4 oz ($\lambda_A * l_a$)

10. With all other parameters determined, the dimensions of the overlapping patches are determined to be 10 in. x 10 in. ($w_f \times l_p$). Two patches are needed, one with a principal fiber direction parallel to the CFRP strip and one with the principal fiber direction perpendicular to the strip, both having the same dimensions. Both patches are placed 2 in. behind the center of the anchor hole (Figure 5-1)

Figure 5-5 shows the designed CFRP system details

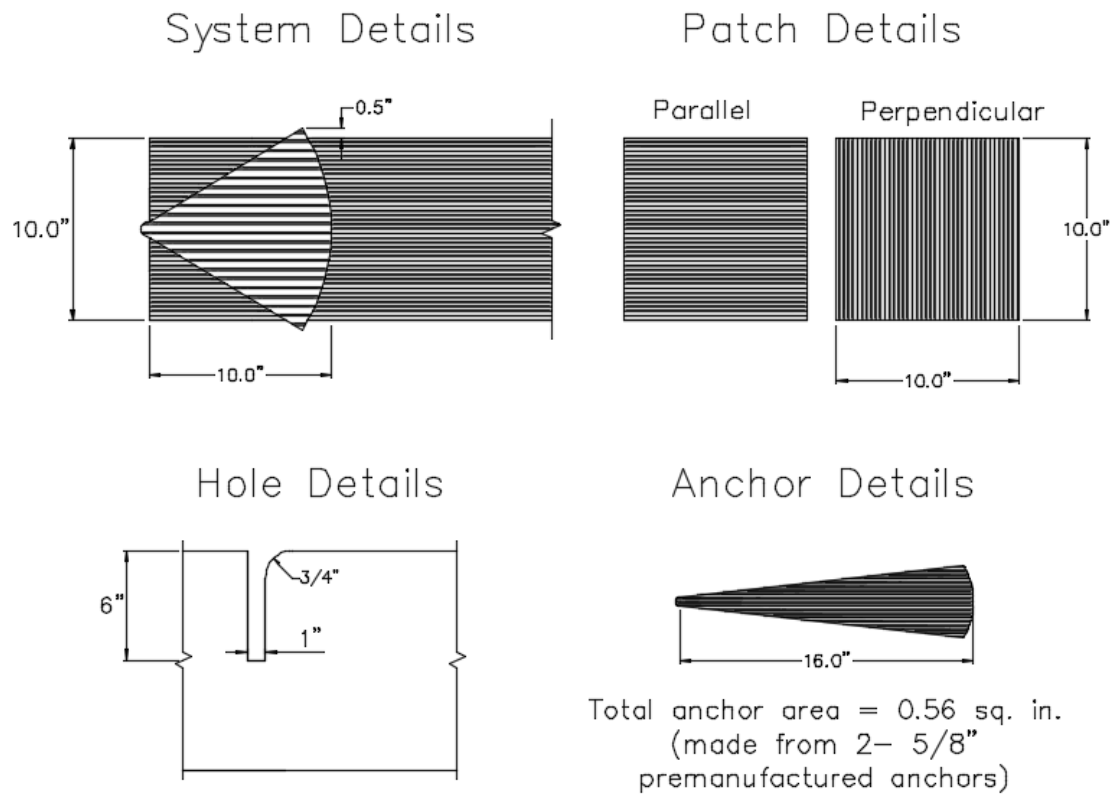


Figure 5-5: Example layout

Chapter 6: Summary and Conclusions

6.1 SUMMARY

The objectives of this project were to: 1) investigate size effects in anchored CFRP systems as CFRP anchor and strip sizes increase, and 2) provide design guidelines for CFRP anchors developing up to 10-in. wide strips with a tensile strength reaching 60 kips. Anchors of this size have not been tested or reported in the literature, but they can be convenient in retrofit applications of large concrete members (e.g., bridge girders). Using fewer, larger anchors and strips can reduce the number of anchor holes to be drilled and thereby accelerate the retrofit process.

Twelve tests were conducted on concrete beam specimens with dimensions of 12-in. by 12-in. by 68-in. to test anchored strips up to 10-in. wide. The primary parameters investigated were:

- Width of CFRP strip
- Number of layers of fabric in CFRP strips
- Number of anchors per strip width
- Ratio of anchor to strip cross-sectional materials (or anchor material ratio)
- Anchor fan overlap length
- Chamfer radius at the edge of the anchor hole

All CFRP strips were fully bonded to the concrete beam tension face. Anchor patch length and anchor hole size were each varied according to the sectional area of anchor material. Patch length was the same as the anchor overlap length, while hole diameter was selected as 1.4 times the equivalent anchor laminate area. A hole depth of 4-in. was used in some tests, but when larger anchor sizes and chamfer radii were used, a longer hole

depth of 6-in. was selected. Lastly, the concrete compressive strength varied from 3.6 to 9.9 ksi.

The full distribution of strains at the surface of the anchored CFRP strips was monitored using an optical measurement system. These measurements helped evaluate the effectiveness of various anchor details in distributing strains across strip.

Four failure modes were observed in this study, 1) strip fracture, 2) anchor rupture, 3) delamination between anchor and strip, and 4) concrete specimen failure. Strip fracture was the most desired failure mode. In such failures the anchors were sufficiently strong to develop the full strength of the strengthening strip. Anchor rupture was caused by a variety of factors including a low anchor material ratio and low hole-edge chamfer radius. One specimen failed by delamination between anchor and strip due to insufficient overlap length between the two elements. Of the 12 tests conducted, nine failed with the strip longitudinal stress above its expected fracture stress and seven of those failed by strip fracture.

Based on test results and previous work by Sun (2014), design guidelines were proposed for CFRP anchors developing strips up to 10-in. wide and with up to three layers of fabric.

6.2 CONCLUSIONS

This experimental program confirmed the size effects reported in Sun et al. (2016). Observed trends indicated that the larger the CFRP strip area developed per anchor, the lower the stress at fracture of that strip. Similarly, the smaller the anchor material area per strip area developed, the lower the stress at fracture of that strip. This size effect is attributed to the increased effectiveness of larger anchors in distributing strains more evenly across CFRP strips and reducing strain concentrations.

An individual CFRP anchor was shown to develop the expected strength of CFRP strips up to 10-in. wide; even when using two layers of fabric in the strip. However using two anchors for a 10-in. strip width (or a 5-in. anchor tributary width) resulted in an improved strip strain distribution with stresses at strip fracture that were 7.5% higher.

The normalized strip area parameter was defined as the CFRP strip laminate cross-sectional area divided by the number of anchors used across the strip width and the anchor material ratio. A clear negative correlation was observed between this parameter and the stress at fracture in anchored CFRP strips. Based on the observed correlation, strips with a normalized strip area exceeding 0.2 in.^2 could fracture below their expected fracture stress. A parameter value of 0.2 in.^2 corresponds to a 10-in. wide strip with two layers of fabric and a total thickness of 0.04-in., with a single anchor having an anchor material ratio of 2.

Debonding between anchors and strips was prevented as long as the overlap length between anchor fan and strip was increased proportionally with the number of strip layers, or strip thickness, to maintain an interface bond stress between anchors and strips below the manufacturer specified bond strength.

An anchor material ratio of 2.0 was shown to be sufficient to achieve strip fractures in all cases where it was used, as long as the edge chamfer radius of the anchor hole was taken as 1.4 times the hole radius. The chamfer radius at the edge of the anchor hole should not be taken smaller than 0.5-in. Smaller hole chamfer radii were shown not only to weaken anchors, but also resulted in a less even strain distribution across the width of anchored strips.

6.3 FUTURE WORK

This study expanded the size of tested and verified anchors and confirmed a size effect that did not level off within the parameter range tested. Testing larger anchors may

help define the size effect relation proposed in this study. Testing of anchors made of other FRP material could also be useful. Past research and this study have focused mainly on carbon fiber anchors. Exploring the behavior and strength of glass and aramid fiber anchors, which are substantially cheaper than carbon fiber anchors, may yield more cost effective anchorage solutions.

References

- American Concrete Institute, (2014). "Building Code Requirements for Structural Concrete and Commentary (ACI 318-14)." Farmington Hills, Michigan, USA.
- American Concrete Institute, (2008). "Guide for the Design and Construction of Externally Bonded FRP Systems for Strengthening Concrete Structures (ACI 440.2R-08)." Farmington Hills, Michigan, USA.
- ASTM International, (2015). "Standard Test Method for Compressive Strength of Cylindrical Concrete Specimens, (C39/C39M)," ASTM International, West Conshohocken, PA, USA, 7 pp.
- ASTM International, (2014). "Standard Test Method for Tensile Properties of Polymer Matrix Composite Materials, (D3039-14)," ASTM International, West Conshohocken, PA, USA, 13 pp.
- Akyuz, O. and Ozdemir, G. (2004). "Mechanical Properties of CFRP Anchorages", *13th World Conference on Earthquake Engineering, Vancouver, B.C., Canada*, August 1-6, 2004, Paper No. 3349.
- Ceroni, F., Pecce, M., Matthys, S., and Taerwe, L. (2008). "Debonding Strength and Anchorage Devices for Reinforced Concrete Elements Strengthened with FRP Sheets," *Composites Part B: Engineering*, Vol. 39, No. 3, pp. 429-441.

- Deifalla, A. and Ghobarah, A. (2006). "Calculating the Thickness of FRP Jacket for Shear and Torsion Strengthening of RC Girders T-Girders," *Third International Conference on FRP Composites in Civil Engineering. CICE 2006*. Miami, Florida.
- El-Saikaly, G., godat, A., and Chaallal, O. (2014). "New Anchorage Technique for FRP Shear-Strengthened RC T-Beams Using CFRP Rope." *Journal of Composites for Construction*, Vol, 19, No. 4.
- Garcia, J.; Sun, W.; Kim, C.; Ghannoum, W. M.; and Jirsa, J. O. (2014) "Procedures for the Installation and Quality Control of Anchored CFRP Sheets for Shear Strengthening of Concrete Bridge Girders," *Report 5-6306-01-1*, Center for Transportation Research (CTR), Austin, TX, 52 pp.
- Grelle, S. V., and Sneed, L. H. (2013). "Review of Anchorage Systems for Externally Bonded FRP Laminates," *International Journal of Concrete Structures and Materials*. Vol.7, No.1, pp.17–33.
- Huaco.G. (2009). "Quality Control Test for Carbon Fiber Reinforced Polymer (CFRP) Anchors for Rehabilitation." Austin, Texas, The University of Texas at Austin, *Master's Thesis*.
- Hall, J., Schuman, P., and Hamilton, H. (2002). "Ductile Anchorage for Connecting FRP Strengthening of Under-Reinforced Masonry Buildings," *Journal of Composites for Construction*, Vol. 6, No. 1, pp. 3-10.

- Hoult, N. A., and Lees, J. M. (2009). "Efficient CFRP Strap Configurations for the Shear Strengthening of Reinforced Concrete T-Beams," *Journal of Composites for Construction*, Vol, 13, No. 1, pp. 45-52.
- Japanese Society of Civil Engineers (JSCE). (1997). "Recommendations for Design and Construction of Concrete Structures Using Continuous Fiber Reinforcing Materials," *Concrete Engineering Series* , 23 . (A. Machida, Ed.), Tokyo, Japan.
- Jirsa, J. O., Ghannoum, W. M., Kim, C., Sun, W., Shekarchi, W. A., Alotaibi, N. K., Pudleiner, D. K., Zhu, J., Liu, S., Wang, H. (2016). "Use of Carbon Fiber Reinforced Polymer (CFRP) with CFRP Anchors for Shear-Strengthening and Design Recommendations/Quality Control Procedures for CFRP Anchors" FHWA/TX-16/0-6783-R1D, Center for Transportation Research (CTR), pp. 264.
- Kalfat, R. Al-Mahaidi, R., and Smith, S. T. (2013). "Anchorage Devices Used to Improve the Performance of Reinforced Concrete Beams Retrofitted with FRP Composites State-of-the-Art Review," *Journal of Composites for Construction*, Vol. 17, No. 1, pp.14-33.
- Khalifa, A., Alkhrdaji, T., Nanni, A., and Lansburg, S. (1999). "Anchorage of Surface Mounted FRP Reinforcement," *Concrete International*, Vol. 21, No. 10, pp. 49-54.
- Kim, I. (2008). "Use of CFRP to Provide Continuity in Existing Reinforced Concrete Members Subjected to Extreme Loads." Austin, Texas, The University of Texas at Austin, *PhD Dissertation*.

- Kim, S. J., & Smith, S. T. (2009.). "Strengthening of RC Slabs with Large Penetrations Using Anchored FRP Composites," *Proceedings of the 2nd Asia Pacific Conference on FRP in Structures, APFIS 2009*, Seoul, Korea. pp. 111–116.
- Kim, Y. (2011). "Shear Behavior of Reinforced Concrete T-Beams Strengthened with Carbon Fiber Reinforced Polymer (CFRP) Sheets and CFRP Anchors." Austin, Texas, The University of Texas at Austin, *PhD Dissertation*.
- Kim, Y., Ghannoum, W.M., Jirsa, J.O. (2015) "Shear Behavior of Full-Scale Reinforced Concrete T-Beams using CFRP Strips and Anchors," *Construction and Building Materials*, V. 94, pp. 1-9.
- Kim, Y., Quinn, K., Ghannoum, W.M., Jirsa, J.O. (2014.) "Strengthening of Reinforced Concrete T-Beams Using Anchored CFRP Materials," *ACI Structural Journal*, V. 111, No. 5, pp. 1027-36.
- Kim, Y., Quinn, K.T., Satrom, C.N., Garcia, J., Sun, W., Ghannoum, W.M., Jirsa, J.O. (2012) "Shear Strengthening of Reinforced and Prestressed Concrete Beams Using Carbon Fiber Reinforced Polymer (CFRP) Sheets and Anchors," FHWA/TX-12/0-6306-1, Center for Transportation Research (CTR), pp. 325.
- Kobayashi, K., Fujii, S., Yabe, Y., Tsukagoshi, H., Sugiyama, T. (2001). "Advanced Wrapping System with CF Anchor-Stress Transfer Mechanism of CF Anchor." *Proceedings of the 5th International Symposium on Fiber-Reinforced Polymer*

- (FRP) Reinforcement for Concrete Structures, FRPRCS-5. Cambridge, U.K. , pp. 379-388.
- Niemitz, C. (2008). "Anchorage of Carbon Fiber Reinforced Polymers to Reinforced Concrete in Shear Applications." University of Massachusetts Amherst, (February). *Master Thesis*.
- Ortega, C. A., Belarbi, A. and Bae, S. (2009). "End Anchorage of Externally Bonded FRP Sheets for the Case of Shear Strengthening of Concrete Girders," *The Ninth International 277 Symposium on Fiber Reinforced Polymer Reinforcement for Concrete Structures*, FRPRCS-9. Sydney, Australia.
- Orton, S. L. (2007). "Development of a CFRP System to Provide Continuity in Existing Reinforced Concrete Structures Vulnerable to Progressive Collapse. Department of Civil, Environmental and Architectural Engineering." Austin, Texas, The University of Texas at Austin. *Ph.D Dissertation*.
- Orton, S. L., Jirsa, J. O. and Bayrak, O. (2008). "Design Considerations of Carbon Fiber Anchors," *Journal of Composites for Construction*, Vol. 12, No. 6, pp. 608-616.
- Ozbakkaloglu, T., and Saatcioglu, M. (2009). "Tensile Behavior of FRP Anchors in Concrete," *Journal of Composites for Construction*, Vol. 13, No. 2, pp. 82-92.

- Pham, L. T. (2009). "Development of a Quality Control Test for Carbon Fiber Reinforced Polymer Anchors." Austin, Texas, The University of Texas at Austin, *Master's Thesis*.
- Quinn, K. (2009). "Shear Strengthening of Reinforced Concrete Beams with Carbon Fiber Reinforced Polymer (CFRP) and Improved Anchor Details." Austin, Texas, The University of Texas at Austin, *Master's Thesis*.
- Sokoli, D., Shekarchi, W., Buenrostro, E., Ghannoum, W.M., (2014). "Advancing behavioral understanding and damage evaluation of concrete members using high-resolution digital image correlation data". *Earthquakes and Structures* 7(5): 609-626
- Sun, W. (2014). "Behavior of Carbon Fiber Reinforced Polymer (CFRP) Anchors Strengthening Reinforced Concrete Structures." Austin, Texas, The University of Texas at Austin, *PhD Dissertation*.
- Sun, W., Jirsa, J. O., and Ghannoum, W. M. (2016) "Behavior of Anchored Carbon Fiber-Reinforced Polymer Strips Used for Strengthening Concrete Structures," *ACI Materials Journal*, Vol. 113, No. 2, pp. 163-172.
- Teng, J. G., Smith, S. T., Yao, J., Chen, J. F. (2003). "Intermediate Crack-Induced Debonding in RC Beams and Slabs," *Construction and Building Materials*, Vol. 17, No. 6-7, pp. 447-462.

Triantafillou, T. C., and Antonopoulos, C. P. (2000). "Design of Concrete Flexural Members Strengthened in Shear with FRP," *Journal of Composites for Construction*, Vol. 4, No. 4, pp. 198-205.

Vita

Douglas Pudleiner was born in December of 1991 in Springfield, Virginia. He graduated from Robert E. Lee High School in 2010. Then he enrolled at Virginia Polytechnic Institute and State University (Virginia Tech) in August 2010 where he earned a Bachelor's of Science in Civil Engineering, graduating May 2014. Douglas then continued his education at The University of Texas at Austin in August 2014 and earned a Master of Science in Civil Engineering and will graduate in May 2016. He has accepted a job that will allow him to peruse a career in design, primarily for public works buildings.

Email address: dpudleiner@utexas.edu

This thesis was typed by the author.